University of Kentucky
UKnowledge

Theses and Dissertations--Neuroscience | Neuroscience

2019

TGF-β, WNT, AND FGF SIGNALING PATHWAYS DURING AXOLOTL TAIL REGENERATION AND FORELIMB BUD DEVELOPMENT

Qingchao Qiu
University of Kentucky, qingchao.qiu@gmail.com
Digital Object Identifier: https://doi.org/10.13023/etd.2019.367

Right click to open a feedback form in a new tab to let us know how this document benefits you.

Recommended Citation

Qiu, Qingchao, "TGF-β, WNT, AND FGF SIGNALING PATHWAYS DURING AXOLOTL TAIL REGENERATION AND FORELIMB BUD DEVELOPMENT" (2019). *Theses and Dissertations--Neuroscience*. 24.
https://uknowledge.uky.edu/neurobio_etds/24

This Doctoral Dissertation is brought to you for free and open access by the Neuroscience at UKnowledge. It has been accepted for inclusion in Theses and Dissertations--Neuroscience by an authorized administrator of UKnowledge. For more information, please contact UKnowledge@lsv.uky.edu.

STUDENT AGREEMENT:

I represent that my thesis or dissertation and abstract are my original work. Proper attribution has been given to all outside sources. I understand that I am solely responsible for obtaining any needed copyright permissions. I have obtained needed written permission statement(s) from the owner(s) of each third-party copyrighted matter to be included in my work, allowing electronic distribution (if such use is not permitted by the fair use doctrine) which will be submitted to UKnowledge as Additional File.

I hereby grant to The University of Kentucky and its agents the irrevocable, non-exclusive, and royalty-free license to archive and make accessible my work in whole or in part in all forms of media, now or hereafter known. I agree that the document mentioned above may be made available immediately for worldwide access unless an embargo applies.

I retain all other ownership rights to the copyright of my work. I also retain the right to use in future works (such as articles or books) all or part of my work. I understand that I am free to register the copyright to my work.

REVIEW, APPROVAL AND ACCEPTANCE

The document mentioned above has been reviewed and accepted by the student's advisor, on behalf of the advisory committee, and by the Director of Graduate Studies (DGS), on behalf of the program; we verify that this is the final, approved version of the student's thesis including all changes required by the advisory committee. The undersigned agree to abide by the statements above.

Qingchao Qiu, Student

Dr. S. Randal Voss, Major Professor

Dr. Wayne Cass, Director of Graduate Studies

TGF-β, WNT, AND FGF SIGNALING PATHWAYS DURING AXOLOTL TAIL REGENERATION AND FORELIMB BUD DEVELOPMENT

DISSERTATION

A dissertation submitted in partial fulfillment of the requirements for the degree of Doctor of Philosophy in the College of Medicine at the University of Kentucky

By

Qingchao Qiu

Lexington, Kentucky

Director: Dr. S. Randal Voss, Professor of Neuroscience

Lexington, Kentucky

2019

Copyright © Qingchao Qiu 2019

ABSTRACT OF DISSERTATION

TGF-β, WNT, AND FGF SIGNALING PATHWAYS DURING AXOLOTL TAIL REGENERATION AND FORELIMB BUD DEVELOPMENT

Tgf-β, Wnt, and Fgf signaling pathways are required for many developmental processes. Here, I investigated the requirement of these signaling pathways during tail regeneration and limb development in the Mexican axolotl (*Ambystoma mexicanum*).

Using small chemical inhibitors during tail regeneration, I found that the Tgf-β signaling pathway was required from 0-24 and 48-72 hours post tail amputation (hpa), the Wnt signaling pathway was required from 0-120 hpa, and the Fgf signaling pathway was required from 0-12hpa. Tgf-β1 was upregulated after amputation and thus may mediate Tgf-β signaling pathway during tail regeneration. Both Smad-mediated and non-Smad mediated Tgf-β signaling were activated as early as 1hpa. Smad-mediated Tgf-β signaling via activated pSmad2 and pSmad3, and via phosphorylated Erk and Akt. Two different Tgf-β signaling pathway inhibitors, SB505124 and Naringenin, differentially regulated pSmad2, pSmad3, p-Erk, and p-Akt, while SB505124 and Naringenin both inhibited tail regeneration; only SB505124 reduced cell proliferation. Wnt/β-Catenin signaling was increased and was enhanced by Wnt-C59. Disruption of the Wnt signaling pathway directly or indirectly activated Erk and Akt signaling. Disruption of the Fgf signaling pathway decreased p-Erk and increased p-Akt. All three signaling pathways affected cell proliferation and mitosis during tail regeneration.

The Wnt pathway inhibitor Wnt-C59 prevented forelimb bud outgrowth. The critical window for Wnt signaling regulating forelimb bud outgrowth was approximately developmental stage 40-42. Wnt signaling ligand Wnt3a and tight junction protein Zo-1 were expressed in the epidermis of the forelimb bud and both were down-regulated by Wnt-C59. Moreover, both Wnt and Fgf signaling pathways affected cell proliferation and mitosis of mesodermal cells during forelimb bud outgrowth.

Overall, my results show that Tgf-β, Wnt, and Fgf signaling pathways are required for axolotl tail regeneration. All three pathways affect Erk and Akt signaling and guide cell proliferation and mitosis. The Wnt signaling pathway is required for forelimb bud outgrowth, and it appears to regulate expression of Wnt3a and Zo1, and control cell

proliferation and mitosis of mesodermal cells underlying the forelimb epidermis. These data enrich understanding of signaling network dynamics that underlie tissue regeneration and vertebrate limb development.

KEYWORDS: Tgf-β, Wnt, Fgf, tail regeneration, limb development, axolotl

Qingchao Qiu

July 18, 2019

TGF-β, WNT, AND FGF SIGNALING PATHWAYS DURING AXOLOTL TAIL REGENERATION AND FORELIMB BUD DEVELOPMENT

By

Qingchao Qiu

Dr. S. Randal Voss

Director of Dissertation

Dr. Wayne Cass

Director of Graduate Studies

July 18, 2019

Date

Dedicated to my family for their support and sacrifice

ACKNOWLEDGEMENTS

The following dissertation, while an individual work, benefited from the insights and direction of several people. I want to thank all the people for their support over the past five years.

Firstly, and foremost, I would like to thank my advisor, Dr. S. Randal Voss, for his providing me with a decent scientific environment, sufficient financial support, freedom to research, and outstanding mentoring. No words are enough to describe the sense of respect and appreciation I have developed for him as a scientist and as a person. I have learned a lot from his scientific enthusiasm, patience, and perseverance. He has been there to support me at every step of my graduate career. He has taught me critical thinking, problem resolving, self-motivation, smart working, and a habit of writing every day. It was impossible for me to carry out all the graduate research without his guidance.

I am grateful to all my committee members, Dr. Edward Hall, Dr. Joe Springer, Dr. Richard Grondin, and Dr. Jon Thorson for their valuable advice, proper direction, positive feedbacks, and immense support. I thank Dr. Gregory Frolenkov, my outside defense committee member, for sharing his wisdom and knowledge. I thank Dr. Ann Morris and Dr. Doug Harrison for sharing their valuable insights and expertise on my research projects and qualifying exams. I want to thank prior and present Voss Lab members including Mr. Kevin Kump, Mrs. Laura Muzinic, Mr. Chris Muzinic, Mrs. Nour Al Haj Badder, Dr. Ryan Woodcock, Mrs. Jennifer Vaughn-Wolfe, Mr. Varun Dwaraka, Mr. James Giordano, Mrs. Xiu Xu, Dr. Maria Torres Sanchez, and Dr.

Anna Rodgers, for their technical support, enlightening scientific discussions and great friendship.

I want to thank all the faculties and staff from the Department of Biology, the Department of Neuroscience, and the Spinal Cord and Brain Injury Research Center. I thank Dr. Bret N. Smith for his sharing his wisdom and broad knowledge with us, holding Christmas parties and providing opportunities for us to communicate with seminar speakers. I thank Mrs. Linda Simmerman for her technical support on cryo-sectioning and imaging taking. I thank Dr. Ashley W. Seifert and his lab members, Dr. Jeremiah Smith and his lab members, Dr. Warren J Alilain and his lab members, Dr. Adam Bachstetter and his lab members, Dr. Kathryn Saatman and her lab members for their letting me use their equipment, technical support, and great friendship.

I want to thank the staff of Graduate School of the University of Kentucky, the Department of Biology at the College of Art and Science, the Department of Neuroscience at the College of Medicine, and the Spinal Cord and Brain Injury Research Center for supporting my doctoral studies. I thank Dr. David Westneat and Dr. Wayne Cass for all their direction, help, and support during my Ph.D. candidacy. I thank department administrators Mrs. Jacqueline J. Burke, Mrs. Avalon Sandoval, and Mrs. Zel Frye for their administrative support and friendship.

I will always be appreciated for all my family members for their support and sacrifice. I thank my mom, Mrs. Jinwu Li, for her teaching me love, perseverance, and patience. I thank my dad, Mr. Shaoheng Qiu for his supporting me unconditionally in all my

endeavors. I thank my big brother, Qingsong Qiu and big sister, Qinghua Qiu for their being there supporting me over all these years. I thank my father-in-law, Mr. Liusheng Hu for all his sacrifice and support. I especially thank my beloved husband, Mr. Bo Hu, for his love, support, and sacrifice. I thank the loves of my life, Lucy, Charlie, and Sophia, for their giving me beautiful smile, high fives, and warm hugs to keep me happy and cheerful.

I would like to thank all my friends Nancy, Steven, Wendy, Sally, Tao, Imogene, Amy, Xiaohong, Teresa, Xiaohua, Wenfu, Wei, Sally, Wen, Ye, Yuecheng, Lingfeng, Yuting, CC, Lakshmi, Chanung, Bei, Lei, Chenguang, Lydia, Rachel, Jacob, Yuanyuan, Qianqian, and Aixia for their great friendship, encouragement, and support. Especially, I thank Nancy for her encouraging me and helping me to start this journey. I thank Steven and Wendy for their enthusiasm for their cheering me up and their open-minded conversation, helping me shake my stress off. I thank Amy, Xiaohong, and Teresa for their support and their wise suggestions in both my daily life and my work. I thank Tao for her tremendous amount of support, her delicious cooking and taking care of me whenever I need her help. I thank Wen for her help and optimistic suggestions during my graduate study. I thank Imogene and Sally for their kindness, peaceful mindsets, and sweet heart.

My special gratitude also goes to the thousands of salamander embryos who sacrificed their lives for my dissertation. My research was funded by the National Institute of Health, Office of the Director (R24OD010435).

TABLE OF CONTENTS

ACKNOWLEDGEMENTS..... iii

TABLE OF CONTENTS vi

LIST OF TABLES xi

LIST OF FIGURES xii

CHAPTER 1: INTRODUCTION..... 3

1.1 Preface 3

1.2 Tissue regeneration 3

1.2.1 Cellular basis of tissue regeneration in animals 3

1.2.2 Signaling pathways and tissue regeneration in vertebrates..... 4

1.2.3 The axolotl embryo tail regeneration model is an excellent animal model to use small molecule inhibitors to perturb and study signaling pathways associated with tissue regeneration. 5

1.3 Tgf-β signaling pathway and tissue regeneration 6

1.3.1 Tgf-β signaling pathway..... 6

1.3.2 Tgf-β signaling pathway inhibitor SB505124 7

1.3.3 Tgf-β signaling pathway inhibitor Naringenin 7

1.3.4 Tgf-β signaling during tissue regeneration 8

1.4 Wnt signaling pathway and tissue regeneration..... 10

1.4.1 Wnt signaling pathway 10

1.4.2 Porcupine inhibitor Wnt-C59..... 11

1.4.3 Wnt signaling pathway during tissue regeneration..... 12

1.5 Fgf signaling pathway and tissue regeneration 14
1.5.1 Fgf signaling pathway and Fgfr inhibitor BGJ398 14
1.5.2 Fgf signaling pathway during tissue regeneration 15
1.6 Interactions of signaling pathways during tissue regeneration 17
1.7 Wnt and Fgf signaling pathways during limb development 18
1.8 Conclusions and perspective 19
1.9 Rationale 20
CHAPTER 2 TGF-β SIGNALING IS REQUIRED DURING AXOLOTL TAIL REGENERATION 21
2.1 Abstract 21
2.2 Introduction 22
2.3 Materials and Methods 24
2.3.1 Regeneration experiments 24
2.3.2 Antibodies 25
2.3.3 Immunochemistry staining 25
2.3.4 Western blotting 26
2.3.5 EdU cell proliferation assay 27
2.4 Results 28
2.4.1 Tgf-β signaling is required during axolotl tail regeneration. 28
2.4.2 Tgf-β1 increases during tail regeneration. 30
2.4.3 Smad-mediated Tgf-β signaling increases during axolotl tail regeneration. 32
2.4.4 Non-Smad mediated Tgf-β signaling pathways are up-regulated by SB505124 and down-regulated by Naringenin at 1hpa. 34
2.4.5 SB505124, but not Naringenin, significantly reduces cell proliferation. 36
2.4.6 Tgf-β signaling regulates cell mitosis during tail regeneration. 39

2.5 Discussion 40

CHAPTER 3 WNT SIGNALING IS REQUIRED DURING AXOLOTL TAIL REGENERATION . 46

3.1 Abstract 46

3.2 Introduction 47

3.3 Methods 50

3.3.1 Regeneration experiments 50

3.3.2 Antibodies 51

3.3.3 Tissue processing and immunochemistry staining 51

3.3.4 Western blotting 52

3.3.5 EdU cell proliferation assay 53

3.4 Results 53

3.4.1 Blocking Wnt signaling prevents axolotl embryo tail regeneration 53

3.4.2 Wnt3a is suppressed during tail regeneration. 55

3.4.3 Wnt-C59 increases β-Catenin expression during tail regeneration. 56

3.4.4. Inhibiting Wnt signaling increases p-Erk and p-Akt expression. 57

3.4.5 Wnt signaling regulates cell mitosis during axolotl tail regeneration. 58

2.4.6 Wnt signaling regulates cell proliferation during axolotl tail regeneration. 59

3.5 Discussion 62

CHAPTER 4 FGF SIGNALING IS REQUIRED DURING 66

AXOLOTL TAIL REGENERATION 66

4.1 Abstract 66

4.2 Introduction 66

4.3 Methods 68

4.3.1 Regeneration experiments 68
4.3.2 Antibodies 69
4.3.3 Tissue processing and immunochemistry staining 70
4.3.4 Western blotting 70
4.3.5 EdU cell proliferation assay 71
4.4 Results 72
4.4.1 Blocking Fgf signaling inhibits axolotl embryo tail regeneration. 72
4.4.2 BGJ398 downregulates phosphorylation of Erk. 73
4.4.3 BGJ398 upregulates phosphorylation of Akt. 74
4.4.4 BGJ398 upregulates Wnt/β-Catenin signaling. 75
4.4.5 Fgf signaling regulates cell mitosis during axolotl tail regeneration. 76
4.4.6 BGJ398 reduces the number of cells in S-phase. 77
4.5 Discussion 79
CHAPTER 5 WNT SIGNALING IS REQUIRED FOR 83
FORELIMB BUD DEVELOPMENT 83
5.1 Abstract 83
5.2 Introduction 83
5.3 Methods 86
5.3.1 Animal husbandry and timing experiments for limb bud outgrowth. 86
5.3.2 Antibodies 87
5.3.3 H& E staining and immunochemistry staining 87
5.3.4 EdU cell proliferation assay 88
5.3.5 Cell orientation and cell density measurements. 89
5.4 Results 90

5.4.1 Wnt signaling is required around developmental stage 40 for axolotl forelimb bud development. 90
5.4.2 Long-term phenotype of the Wnt-C59 treated animals 91
5.4.3 Down-regulation of Wnt3a expression by Wnt-C59 treatment is associated with inhibition of forelimb bud development. 92
5.4.4 Polarity of mesodermal cells is disrupted by Wnt-C59 treatment. 95
5.4.5 Wnt and Fgf signaling pathways promote cell progression at M-phase during forelimb bud outgrowth. 97
5.4.6 Wnt signaling is critical for mesodermal cell proliferation in the forelimb bud. 101
5.5 Discussion 102
CHAPTER 6: SUMMARY AND DISCUSSION: SIGNALING PATHWAYS DURING AXOLOTL TAIL REGENERATION AND FORELIMB BUD OUTGROWTH 106
BIBLIOGRAPHY 119
VITA 128

LIST OF TABLES

Table 6.1 Inhibitors of cell proliferation and mitosis. 107

Table 6.2 SB505124 and Naringenin differentially affect Smad-mediated TGF-β signaling. 110

Table 6.3 SB505124 and Naringenin differentially affect non-Smad mediated TGF-β signaling. 112

Table 6.4 Effects of Wnt-C59 and BGJ398 on Erk and Akt signaling. 113

Table 6.5 Effects of Wnt-C59 and BGJ398 on Wnt3a and β-Catenin expression. 114

LIST OF FIGURES

Figure 2.1 Inhibiting Alk4/5/7 by SB505124 blocks axolotl tail regeneration. 29

Figure 2.2 Naringenin inhibits axolotl tail regeneration. 30

Figure 2.3 Tgf-β1 is broadly expressed in the axolotl tail and increases in the epidermis during tail regeneration. 31

Figure 2.4 SB505124 significantly affects p-Smad2 and p-Smad3 expression. 33

Figure 2.5 Naringenin significantly affects activation of Smad2 and Smad3. 34

Figure 2.6 SB505124 increases phosphorylation of non-Smad mediated signaling Erk and Akt at 1hpa. 35

Figure 2.7 Naringenin down-regulates p-Erk and p-Akt signaling at 1hpa. 36

Figure 2.8 SB505124, but not Naringenin, significantly reduces cell proliferation at 72hpa. 38

Figure 2.9 SB505124 inhibits the mitotic index within tail tips at 48hpa. 39

Figure 3.1 Inhibiting Wnt signaling by Wnt-C59 blocks axolotl tail regeneration. 55

Figure 3.2 Wnt3a expression decreases during tail regeneration. 56

Figure 3.3 Wnt-C59 increases β-Catenin expression at 48hpa. 57

Figure 3.4 Wnt-C59 increases phosphorylation of Erk at 24, 48, and 72hpa. 58

Figure 3.5 Wnt-C59 increases phosphorylation of Akt at 48 and 72hpa. 58

Figure 3.6 Wnt-C59 inhibits the mitotic index at 48hpa. 59

Figure 3.7 Wnt-C59 reduces cell proliferation. 61

Figure 3.8 Wnt-C59 blocks dorsal and ventral fin regeneration and forelimb outgrowth permanently. 62

Figure 4.1 Blocking Fgf receptors prevents axolotl embryo tail regeneration. 73

Figure 4.2 BGJ398 decreases phosphorylation of Erk at 24hpa. 74

Figure 4.3 BGJ398 downregulates phosphorylation of Akt. 75

Figure 4.4 BGJ398 upregulates Wnt ligand expression. 76

Figure 4.5 BGJ398 inhibits mitosis in axolotl tails at 48hpa. 77

Figure 4.6 BGJ398 reduces S-phase entry of cells in the tail but not the spinal cord. 79
Figure 5.1. Wnt signaling is required at developmental stage 40 for axolotl forelimb development. 91
Figure 5.2. Wnt-C59 prevents forelimb bud development and decreases hindlimb size..... 92
Figure 5.3 Down-regulation of Wnt3a expression by Wnt-C59 treatment is associated with inhibition of forelimb bud development. 94
Figure 5.4 Planar cell polarity of forelimb mesodermal cells is disrupted by Wnt-C59. 96
Figure 5.5. Wnt signaling supports the mitosis of forelimb mesodermal cells..... 99
Figure 5.6 Fgf signaling supports the mitosis of forelimb mesodermal cells. 100
Figure 5.7 Aurora Kinase inhibitors inhibit forelimb bud outgrowth. 100
Figure 5.8 Wnt and Fgf signaling pathways regulate cell proliferation of mesodermal cells of the forelimb bud. 102
Figure 6.1 Crucial ligands regulate Tgf-β, Wnt, and Fgf signaling pathways. 109
Figure 6.2 Preliminary network for Tgf-β, Wnt, and Fgf signaling pathways during axolotl tail regeneration. 115

CHAPTER 1: INTRODUCTION

Qingchao Qiu[1]

[1]Department of Neuroscience, University of Kentucky, Lexington, Kentucky

KEYWORDS: Tgf-β, Wnt, Fgf, regeneration, limb development

1.1 Preface

How organisms regenerate body parts is not entirely understood. Using genetic and pharmaceutical methods, several signaling pathways have been shown to play essential roles during tissue regeneration. In this chapter, I review the Transforming growth factor beta (Tgf-β), Wingless/Integrated (Wnt), and Fibroblast growth factor (Fgf) signaling pathways in regulating wound epithelium formation, blastema formation, and cell proliferation during tissue regeneration. I also review Wnt and Fgf signaling pathways during limb development. Understanding signaling pathway dynamics during tissue regeneration and embryonic development may shed light on mechanisms of tissue regeneration and suggest therapeutic strategies to enhance regenerative ability in mammals.

1.2 Tissue regeneration

1.2.1 Cellular basis of tissue regeneration in animals

In recent years, cell lineage tracing and transplantation studies have identified progenitor cell populations that orchestrate tissue regeneration responses in many classical model organisms (Tanaka and Reddien 2011; Cary et al. 2019; Fink, Andersson-Rolf, and Koo 2015). Planaria regenerate an entire body from a tiny body fragment with pluripotent stem cells called clonogenic neoblasts (Wagner, Wang, and Reddien 2011; Scimone et al. 2014). A small body fragment of Hydra regenerates an individual similar to the original through ectodermal and endodermal epithelial stem

cells and interstitial stem cells (Bosch 2007; Govindasamy, Murthy, and Ghanekar 2014). Axolotl appendages and Xenopus tails harbor tissue and germ layer restricted progenitors that are recruited to form a regeneration blastema (Tanaka and Reddien 2011; Bryant, Endo, and Gardiner 2002; Gargioli and Slack 2004; Mochii, Taniguchi, and Shikata 2007). For example, axolotl Schwann cells regenerate from Schwann cells only, progenitor cells in muscle regenerate muscle, and progenitor cells in cartilage regenerates cartilage. In contrast, dermal cells regenerate dermis, connective tissue, and cartilage in a germ layer-specific manner (Kragl et al. 2009). These lineage tracing studies provide valuable information for understanding the cellular basis of tissue regeneration. How signaling pathways control these cellular behaviors during tissue regeneration is poorly understood.

1.2.2 Signaling pathways and tissue regeneration in vertebrates

Salamanders regenerate many body parts such as limb, tail, lens, heart, spinal cord, and brain (Sugiura et al. 2016; Nacu et al. 2016; Franklin, Voss, and Osborn 2017; Suetsugu-Maki et al. 2012; Nakamura et al. 2016; Tazaki, Tanaka, and Fei 2017; Amamoto et al. 2016). Upon limb amputation, epithelial cells migrate to the exposed wound surface and form a wound epithelium (Carlson, Bryant, and Gardiner 1998; Nye et al. 2003; Satoh et al. 2008). This wound epithelium thickens and matures into a signaling center that is called the Apical Epithelial Cap (AEC) (Christensen and Tassava 2000). Interactions between the AEC and underlying cells in the stump are considered to activate and support the proliferating undifferentiated blastemal cells, of which the majority are thought to be connective tissue cells (Satoh, Bryant, and Gardiner 2012). Multiple signaling pathways, including Tgf-β, Wnt, and Fgf signaling pathways are known to be deployed during tissue regeneration to regulate cellular and

developmental processes associated with tissue repair and the formation of new tissues (Ho and Whitman 2008; Singh et al. 2018; Peiris et al. 2016; Herman et al. 2018). Detailing where and when signaling pathways are deployed during regeneration is essential to understanding how regeneration programs are regulated.

1.2.3 The axolotl embryo tail regeneration model is an excellent animal model to use small molecule inhibitors to perturb and study signaling pathways associated with tissue regeneration.

It is through the perturbation of signaling pathways that we learn about their necessity and requirement for regeneration. The axolotl assay uses hatching stage 42 embryos (Ponomareva et al. 2015) that are capable of regenerating amputated distal tail tips in 7 days. Although axolotl limb regeneration has been studied most, it is not well suited for signaling pathway analysis. First, it takes several months for a fully developed limb to form. Second, the size of an axolotl with fully developed limbs is too large for the whole body, chemical treatment. Third, it takes about 40-50 days for a juvenile axolotl to regenerate a limb and even longer time for post-metamorphic adult axolotls to regenerate their limbs (Young, Bailey, and Dalley 1983). In contrast, the axolotl embryo tail regeneration model has several advantages for studying cell signaling pathways. First, hatching stage embryos have well-developed tails in less than 30 days. Second, the size of the hatching stage embryo is about 1cm long, allowing them to be reared individually in 12-well, microtiter plates with small volumes of chemical solution. Third, a hatching stage embryo is capable of regenerating 2mm of the distal amputated tail in 7 days. Fourth, the endpoint of the experiment is an easy to score, morphological difference in body length, fin width, and fin shape. Fifth, chemicals can be directly dissolved in embryo rearing water to study molecular events during

tail regeneration. Lastly, axolotl embryo development is slow, allowing higher temporal resolution of molecular and cellular events that overlap in rapidly growing model organisms like Danio rerio (zebrafish) and Xenopus laevis (Xenopus). Axolotl embryos are also good to use for limb development studies, which will be discussed later.

1.3 Tgf-β signaling pathway and tissue regeneration

1.3.1 Tgf-β signaling pathway

The Tgf-β signaling pathway has been well characterized in many species and cell culture studies. The Tgf-β signaling pathway is mediated by multiple ligands and receptors (Wrana et al. 1992; Attisano et al. 1993; Zhang et al. 1996). In general, Tgf-β, Activin or Nodal bind with Tgf-β type II receptors on the cell membrane, causing the recruitment and transphosphorylation of Tgf-β type I receptors, Alk5, Alk4, and Alk7 (DaCosta Byfield et al. 2004). Activated Tgf-β type I receptors phosphorylate Smad2 and Smad3, which then interact with Smad4, a co-Smad that mediates translocation into the nucleus. The Smad2/Smad3/Smad4 complex binds specific DNA motifs to regulate transcription through various co-activator or co-repressor proteins (Derynck and Zhang 2003). Therefore, phosphorylated Smad2 and Smad3 are essential transcription factors in Smad-mediated Tgf-β signaling pathways. On the other hand, non-Smad-mediated Tgf-β signaling pathway can be activated by phosphorylating extracellular-signal-regulated kinase (Erk) and Akt signaling pathways (Zhang 2009). Erk and Akt signaling are central cassettes of the mitogen-activated protein kinase (Mapk) signaling pathway that regulates wound contraction and cell proliferation during Xenopus embryonic wound healing (Shaul and Seger 2007; Li et al. 2013; Li et al. 2016). Tgf-β signaling also rapidly activates Akt signaling. Akt signaling is essential in regulating neoblast behavior and mediates

injury-mediated cell death during planarian tissue regeneration (Peiris et al. 2016). Down-regulation of Akt function by RNAi increased cell death throughout the body of a planarian (Peiris et al. 2016).

1.3.2 Tgf-β signaling pathway inhibitor SB505124

SB505124 is a selective and specific inhibitor for Tgf-β Type I receptors Alk4, Alk5, and Alk7, but not Alk1, Alk2, Alk3, and Alk6 (DaCosta Byfield et al. 2004). Treating cells with Tgf-β1 or Activin leads to phosphorylation of Alk5 and Alk4, respectively, which activate their downstream substrates Smad2 and Smad3 (DaCosta Byfield et al. 2004), while BMP treated cells result in phosphorylation of Alk1, Alk2, Alk3, and Alk6, which then enable phosphorylation of Smad1, 5, and 8 (Heldin, Miyazono, and ten Dijke 1997). Alk7 mediates signaling by Nodal, another member of the Tgf-β superfamily. SB505124 has been developed initially as a competitive inhibitor of Alk5 by binding its ATP binding site, but it also inhibits Alk4 and Alk7. It is more potent and less toxic than a related Alk5 inhibitor SB431542 (DaCosta Byfield et al. 2004). Therefore, SB505124 provides a valuable small molecule for perturbing the Tgf-β signaling pathway. In chapter 2, I used SB505124 to disrupt the Tgf-β signaling pathway during axolotl tail regeneration.

1.3.3 Tgf-β signaling pathway inhibitor Naringenin

Naringenin has been described as a pSmad3 inhibitor. It is the most abundant natural component from grapefruit and related citrus (Guengerich and Kim 1990). Interestingly, it was not shown to inhibit axolotl limb regeneration (Denis et al. 2016). In chapter 2, I used Naringenin to evaluate its effects on inhibiting phosphorylation of Smad3 during axolotl tail regeneration.

1.3.4 Tgf-β signaling during tissue regeneration

The full nucleotide sequence of Tgf-β1 has been cloned, and three Tgf-β receptors, Tgf-β receptor I, II, and III have been identified in axolotl tissues. Tgf-β1 expression is strongly upregulated at 6hpa and maintained throughout axolotl limb regeneration (Denis et al. 2016; Levesque et al. 2007). Tgf-β2 is upregulated at 4hpa and Tgf-β5 is up-regulated at 2hpa during Xenopus tail regeneration (Ho and Whitman 2008). During lizard tail regeneration, activin-βA is strongly upregulated during the early stages of regeneration (Gilbert, Vickaryous, and Viloria-Petit 2013). Morpholino knockdown of activin-βA or its receptor Alk4 impairs zebrafish fin regeneration by affecting the migration of wound epithelial cells and formation of the blastema (Jazwinska, Badakov, and Keating 2007). The Tgf-β signaling pathway is also implicated in early wound healing processes during Xenopus tail regeneration (Ho and Whitman 2008). Both Tgf-β/Smad and Tgf-β/p38/Jnk pathways play roles in wound epithelial formation by affecting wound closure, which is associated with changes in the expression of epithelium mesenchymal transition markers Slug, Zeb2, Twist3, Vimentin, and N-cadherin (Sader et al. 2019). Tgf-β signaling also plays an important role in regulating the cell proliferation response during tissue regeneration. SB431542 inhibition of Tgf-β signaling pathway for seven days and 14 days irreversibly prevented limb regeneration by downregulating blastemal cell proliferation during axolotl limb regeneration (Levesque et al. 2007). Similarly, chemical inhibition of Tgf-β in the Xenopus tadpole tail model blocked blastema cell proliferation (Ho and Whitman, 2008).

The Tgf-β signaling pathway regulates the transcription, translation, and post-translation modification of target genes through phosphorylation of Smad2 and Smad3 (Christensen and Tassava 2000; Chablais and Jazwinska 2012; Denis et al. 2016). P-Smad2, but not p-Smad3 is required in axolotl limb regeneration (Denis et al. 2016). Activation of Smad3 via Tgf-β/activin signaling pathway is essential for the formation of a transient scar that is permissive for zebrafish heart regeneration (Chablais and Jazwinska 2012). P-Smad2 is also expressed at 6 hpa in the *Xenopus laevis* tadpole tail and SB431542 inhibition of Tgf-β signaling reduced p-Smad2 expression during Xenopus tail regeneration (Sato, Umesono, and Mochii 2018). A Tgf-β signaling pathway target gene, fibronectin, is strongly expressed in the basal layer of the AEC (Christensen and Tassava 2000). Inhibition of the Tgf-β signaling pathway by SB431542 reduced fibronectin expression and blocked blastema formation during axolotl limb regeneration (Levesque et al. 2007). A proteomic study using regenerating axolotl limbs presented a model wherein Tgf-β and fibronectin activate transcription factors Sp1 and c-Myc, respectively, which potentially play essential roles during axolotl limb regeneration (Jhamb et al. 2011). The Tgf-β signaling pathway also activates non-Smad mediated signaling via Erk during Xenopus tadpoles tail regeneration (Ho and Whitman 2008). Thus, in the axolotl limb and Xenopus tail regeneration models, Tgf-β signals through both Smad-mediated and non-Smad mediated signaling pathways. However, it is unknown if Smad-mediated and non-Smad-mediated Tgf-β signaling regulates essential processes during axolotl tail regeneration. In chapter 2, I present data showing that Smad-mediated and non-Smad mediated signaling regulate cell mitosis and cell proliferation during axolotl tail regeneration.

1.4 Wnt signaling pathway and tissue regeneration

1.4.1 Wnt signaling pathway

The central logic of the Wnt signaling pathway has emerged from three decades of study. Wnt proteins are conserved, secreted signaling molecules that play a myriad of biological roles in controlling developmental processes (Willert and Nusse 2012). Multiple cytoplasmic, nuclear, and extracellular components modulate Wnt signaling (Nusse 2005). There are 19 *Wnt* genes found in human and the mouse. The *Xenopus tropicalis* genome contains orthologues of all 19 mammalian *Wnt* genes (Yang 2003). Wnt protein binds the N-terminal extracellular cysteine-rich domain of a seven transmembrane molecule Frizzled (Fz) family receptor, alongside interactions with co-receptors including lipoprotein receptor-related (Lrp)5/6, Ror2 and receptor tyrosine kinase (Rtk) (Komiya and Habas 2008). Upon activation of the receptor, the Fz directly binds to Dsh which has three conserved protein domains: a central PDZ domain, an amino-terminal DIX domain, and a carboxy-terminal DEP domain (Wong et al. 2003). It is through the three domains of Dsh that canonical Wnt/β-Catenin, and non-canonical planar cell and calcium Wnt signaling, are accomplished (Habas and Dawid 2005).

In the absence of Wnt ligand, cytoplasmic β-Catenin is degraded continuously by the action of a destruction complex composed of scaffolding protein Axin, the adenomatous polyposis coli gene product Apc, glycogen synthase kinase 3 (Gsk3), protein phosphatase 2A (Pp2A), and casein kinase 1. Upon activation of Dsh through phosphorylation, DIX and PDZ domains of Dsh inhibit activity of Gsk3 in the destruction complex and lower the activity of the destruction complex (MacDonald, Tamai et al. 2009, Minde, Anvarian et al. 2011). The consequence of the low the

activity of destruction complex leads to accumulation and stabilization of the β-Catenin protein. The β-Catenin translocates into the nucleus and acts as a coactivator of Tcf/Lef family transcription factors (Minde et al. 2013; Minde et al. 2011; MacDonald, Tamai, and He 2009).

The non-canonical Wnt pathways are independent of β-Catenin. The noncanonical Wnt/PCP pathways use the PDZ and DIX domains of Dsh binding to Dishevelled-associated activator of morphogeneis1(DAAM1) and activate the G-protein Rho (MacDonald, Tamai, and He 2009). Rho activates Rho-associated kinase (Rock) and regulates the cytoskeleton (Amano, Nakayama, and Kaibuchi 2010). Dsh also binds to Rac1 to mediate profilin binding to actin, which activates Jnk and affects actin polymerization (Spiering and Hodgson 2011).

In the noncanonical Wnt/calcium pathways, Fz recruits Dsh through PDZ and DEP domains and directly interacts with a trimeric G-protein (MacDonald and He 2012). This co-stimulation of Dsh and G-protein leads to activation of either PLC, which promotes calcium release, or cGMP-specific PDE, which inhibits calcium release from the ER (Thakur et al. 2016). The Wnt/Calcium signaling pathway regulates many processes during development, including convergent extension movement, dorsoventral polarity, and organ formation (Lin et al. 2010; Freisinger, Fisher, and Slusarski 2010).

1.4.2 Porcupine inhibitor Wnt-C59

Wnt proteins are modified by palmitoylation. Palmitoylation is a hydrophobic modification of a conserved cysteine reside that affects Wnt protein transport and

distribution (Kurayoshi et al. 2007; Zhai, Chaturvedi, and Cumberledge 2004). Wnt proteins treated with enzyme acyl protein thioesterase are not hydrophobic or active, thus establishing that palmitate is essential for Wnt signaling (Nusse 2005). Studies in *Drosophila* and vertebrates have shown that Wnt palmitoylation is controlled by a membrane-bound O-acyl transferase called Porcupine, which is critical for generating Wnt secretion and gradients. Lack of Porcupine activity produces a phenotype similar to those of the Wg mutant in Drosophila (Medina, Taylor, and Donovan 1997). During chick neural tube development, Porcupine-mediated lipid modification reduces the activity of Wnt1 and Wnt3a (Galli et al. 2007). These studies show that by blocking Porcupine activity, Wnt secretion and activity is decreased. A Porcupine inhibitor, Wnt-C59, was used to block Wnt signaling during tail regeneration in chapter 3 and axolotl forelimb bud outgrowth in chapter 5. My results show that Wnt signaling is required for tail regeneration and limb development.

1.4.3 Wnt signaling pathway during tissue regeneration

The Wnt signaling pathway controls many tissue regeneration processes (Kawakami et al. 2006; Ghosh et al. 2008; Shimokawa et al. 2013; Hamilton, Sun, and Henry 2016; Yokoyama et al. 2011; Sugiura et al. 2009; Lin and Slack 2008). In non-vertebrates, Wnt/β-Catenin signaling pathway defines anteroposterior identity during regeneration. Upon depletion of β-Catenin, an amputated planarian tail regenerates into a head instead of a tail, and this leads to the generation of multiple heads suggesting that β-Catenin maintains anteroposterior identity during homeostasis and regeneration in planarians (Petersen and Reddien 2008; Gurley, Rink, and Sanchez Alvarado 2008). In Hydra, Wnt3a is expressed at the tip of the head of an intact animal and is rapidly re-expressed in head regenerate tips after amputation through

triggering an autocatalytic feedback loop (Hobmayer et al. 2000; Nakamura et al. 2011). Knock down of Sp5, a transcriptional repressor of Wnt3, yields a robust multi-headed phenotype after head amputation in Hydra (Nakamura et al. 2011). Beane et, al (2012) used RNAi to target components of the PCP pathway in planarian to dysregulate visual neuronal cell growth. Their findings suggest that PCP signaling is required to halt neuronal growth after the completion of tissue patterning during planarian regeneration. Both canonical and non-canonical Wnt signaling pathways are also involved in vertebrate tissue regeneration. Wnt-7a is expressed throughout axolotl limb regeneration (Shimokawa et al. 2013). Inhibiting the Wnt/β-Catenin signaling pathway prevents limb regeneration in axolotl larvae and fin regeneration in zebrafish by inducing alterations in the formation of the AEC that associated with the spatiotemporal regulation of p63 (Kawakami et al. 2006). β-Catenin overexpression induces limb regeneration in non-regeneration competent pre-apical ectodermal ridge (AER) chick embryos; in contrast, overexpression of p63 does not induce regeneration (Kawakami et al. 2006). The non-canonical Wnt signaling pathway is also crucial to regulate tissue regeneration. Overexpression of Wn5a during Xenopus tail regeneration induces ectopic larval tails at the injury site, presumably by altering JNK signaling (Sugiura et al. 2009). Interestingly, not only does blocking Wnt protein secretion and activity by Wnt-C59 prevent axolotl tail regeneration, but also activation of Wnt signaling by Wnt agonists differentially impairs axolotl limb regeneration, and prevents Xenopus cornea-lens regeneration and newt Wolffian-lens regeneration (Wischin et al. 2017; Hamilton, Sun, and Henry 2016). Suppression of Wnt/β-Catenin signaling is required for Xenopus limb regeneration and cornea-lens regeneration (Yokoyama et al. 2011; Hamilton, Sun, and Henry 2016). These findings suggest that Wnt/β-Catenin signaling is temporally regulated during regeneration.

Wnt ligands have opposing effects on β-Catenin and tissue regeneration (Stoick-Cooper et al. 2007). Generally, Wnt3a stabilizes β-Catenin and mediates canonical Wnt/β-Catenin signaling (Hino et al. 2003). Noncanonical Wnt signaling pathway is independent of β-Catenin and is mediated by Wnt5a. However, it is reported that Wnt5a promotes Gsk-3-independent β-Catenin degradation and inhibits the canonical Wnt pathway (Topol et al. 2003). Therefore, Wnt5a is regarded as a link between canonical and non-canonical Wnt signaling. Ponomareva et al (2015) used both inhibitors and agonists to disrupt Wnt signaling pathway during axolotl tail regeneration. They found that Wnt antagonist IWR-1-end, Porcupine inhibitor Wnt-C59, and Wnt agonist II SKL blocked axolotl tail regeneration (Ponomareva et al. 2015). Transcriptional data showed that Wnt-C59 treatment affected transcription of genes associated with Wnt, Fgf, Tgf-β, Hox, Egf, Myc, Notch, Ngf, Ras/Mapk, p53, and retinoic acid (RA) pathways. Thus, Wnt signaling, via the transcriptional regulation of key target genes, may integrate multiple pathways during tissue regeneration (Ponomareva et al. 2015). Most differentially expressed genes were discovered between Wnt-C59 treated and control embryos after 24 hours post tail amputation (hpa) (Ponomareva et al. 2015). I used the same tail regeneration model and Porcupine inhibitor Wnt-C59 to more finely investigate the requirement of Wnt signaling during axolotl tail regeneration in Chapter 3.

1.5 Fgf signaling pathway and tissue regeneration

1.5.1 Fgf signaling pathway and Fgfr inhibitor BGJ398

Fgf signaling is essential for cell proliferation, differentiation, migration, mitogenesis, angiogenesis, and embryogenesis (Ornitz and Marie 2015). In vertebrates, there are 22

Fgf genes grouped into seven subfamilies and four Fgf receptors (Fgfrs) in vertebrates (Dorey and Amaya 2010). Fgf signaling is initiated by the binding of Fgf ligands to Fgfrs. A ligand-dependent dimerization event yields a complex consisting of two Fgfs, two heparin sulfate chains, and two Fgfrs (Plotnikov et al. 1999). Each Fgf ligand binds to two Fgf receptors contacted with each other via the D2 domain and trans-phosphorylates each Fgf receptor monomer (Schlessinger 2000). Upon the binding of Fgf ligands and its receptors, the tyrosine residues on the docking protein Frs2-α is phosphorylated (Hadari et al. 2001). The Ras/Map kinase and PI3/Akt pathways act downstream of Fgf signaling (Armstrong et al. 2006). The Ras/Map kinase pathway is associated with cellular proliferation and differentiation (Shapiro 2002). Map kinase effectors include extracellular signal-related kinase (Erk), c-Jun N-terminal kinase (Jnk), and p38 mitogen-activated kinase (Cargnello and Roux 2011). The PI3/Akt pathway is implicated in cell survival and cell fate determination during mammal embryonic development (Yu and Cui 2016). BGJ398 is a selective and potent Fgfr inhibitor of Fgfr1/2/3 (Guagnano et al. 2011). I used BGJ398 in chapter 4 to block Fgf signaling during axolotl tail regeneration. I also used BGJ398 in chapter 5 to assess the requirement of Fgf signaling during axolotl forelimb development.

1.5.2 Fgf signaling pathway during tissue regeneration

Fgfs have been studied as neurotrophic and mitogenic factors during tissue regeneration for more than 40 years (Gospodarowicz 1976). Fgf1 signaling is associated with AEC formation and activation of underlying progenitor cells in the axolotl limb that have the potential to differentiate into different tissues (Dungan et al. 2002). Fgf8 is expressed in the basal layer of the AEC, and Fgf8 and Fgf10 are upregulated in cells underlying the AEC during axolotl limb regeneration.

Denervation prevents Fgf8 and Fgf10 upregulation during axolotl limb regeneration, suggesting that Fgf signaling is nerve-dependent (Kolodziej et al. 2001; Han, An, and Kim 2001). Indeed, Fgf2 and Fgf8 are expressed in nerve tissue and the AEC during axolotl limb regeneration (Mullen et al. 1996). Fgf2 and Fgf8 act as trophic factors to maintain Prrx-1 expression in progenitor cells and promote blastema formation during axolotl limb regeneration (Mullen et al. 1996; Satoh et al. 2011). Fgf2 and Fgf8, together with growth and differentiation factor-5 (Gdf5), are sufficient to substitute for nerve induction of limb regeneration (Makanae et al. 2013). Fgf2 and Fgf8 induce bump formation during limb regeneration, and Fgf2+Fgf8+Bmp7 or Bmp2 induce limb formation during skin wound healing using the accessory axolotl limb model (Makanae, Mitogawa, and Satoh 2014). Fgf2+Fgf8+Bmp7 also induce tail regeneration in the axolotl (Makanae, Mitogawa, and Satoh 2016). Ectopic Fgf8 and endogenous Hh signaling pathway are sufficient to induce posterior axolotl limb regeneration (Nacu et al. 2016). The requirement for Fgf has also been shown to be relatively late for outgrowth of tail tissue in Xenopus by using Fgfr antagonist SU5402 and heat shock inducible XFD. The Fgf signaling pathway is also required for Xenopus lens regeneration (Lin and Slack 2008; Fukui and Henry 2011). In the zebrafish "devoid of blastema" mutant, a blastema fails to form during fin regeneration. It was discovered that this mutant is caused by a *Fgf20a* null allele, thus establishing Fgf signaling is essential for blastema formation during zebrafish fin regeneration (Whitehead et al. 2005). Fgf3 and Fgf10a are responsible for the later stage of blastemal formation in zebrafish fin regeneration (Shibata et al. 2016). Taken together, Fgf signaling is associated with neurotrophic factors that sustain progenitor cell proliferation and blastema formation during tissue regeneration.

1.6 Interactions of signaling pathways during tissue regeneration

In response to artificial amputation or natural injury, animals activate a complex series of responses which lead to local and systemic changes in molecules that function in signaling pathways. Studies have shown that TGF-β, Wnt, and Fgf signaling pathways are activated during tissue regeneration in many different species. Signaling pathways comprise complex networks that are regulated through positive and negative regulatory interactions. Here I provide a brief overview of regulatory interactions among the TGF-β, Wnt, and Fgf pathways.

Tgf-β, Wnt, and Fgf signaling pathways interact at multiple levels. First, these signaling pathways reciprocally regulate ligand production during development and regeneration. For example, Wnt signal pathway inhibitor Wnt-C59 decreases transcription of Tgf-β1 and Fgf9 during axolotl tail regeneration (Ponomareva et al. 2015). Second, nucleus components of different signaling pathways can form complexes to regulate shared target genes in a synergistic manner, at least in cell culture studies (Edlund et al. 2005). Third, cytoplasmic components of different pathways interact to repress or activate specific mechanisms of signal transduction. For example, the interaction of Bmp/TGF-b signaling component Smad7, and Wnt signaling component Axin stabilizes β-catenin, forming a complex with E-cadherin to modulate cell-cell adhesion (Tang et al. 2008).

Because components of signaling pathways interact, it is essential to determine their organization in time and space; in other words, it is essential to determine if pathways function hierarchically or in parallel, which has proven difficult in tissue regeneration studies. For example, inhibiting Wnt/β-Catenin signaling pathway abolishes Fgf8

expression in the blastema during Xenopus limb regeneration (Lin and Slack 2008). Moreover, Fgf signaling acts downstream of Wnt/β-Catenin in both Xenopus limb regeneration and zebrafish fin regeneration (Poss et al. 2000; Yokoyama et al. 2007; Stoick-Cooper et al. 2007). However, Fgfr antagonist SU-5402 decreases Wnt3a and Wnt5a expression during Xenopus tail regeneration, suggesting that feedback regulation of Wnt expression by Fgf signaling is not a simple upstream-downstream relationship (Lin and Slack 2008). Although studies have independently established the requirement of TGF-β, Wnt, and Fgf signaling pathways in different tissue regeneration models, there is a need to examine all three pathways within the context of a single model. Such data are fundamental to tackling the more difficult question of how signaling pathways interact to regulate tissue regeneration processes.

1.7 Wnt and Fgf signaling pathways during limb development

Signaling pathway interactions have received greater study in models of limb development. During chicken limb development, limb bud outgrowth depends on signals from the apical ectodermal ridge (AER) (Hamburger and Hamilton 1992). Fibroblast growth factors expressed in the AER are sufficient and necessary for AER function in proximal-distal limb outgrowth and patterning (Niswander and Martin 1993; Saunders 1998; Mariani, Ahn, and Martin 2008). Absence of Fgf4 and Fgf8 leads to failure of limb development. Wnt signals, including Wnt7a expression in non-AER limb ectoderm, determines dorsal limb cell identity and thus dorsal-ventral axis regulation (Riddle et al. 1995). Therefore, Fgf and Wnt signaling pathways crucially determine limb axial polarity (Tickle 2015). A regulatory loop of multiple Wnt (Wnt3a, Wnt2b, and Wnt8c) and Fgf (Fgf8 and Fgf10) genes controls limb initiation and AER induction (Kawakami et al. 2001). Wnt3a is the earliest known AER marker

during limb development, it signals through the canonical β-Catenin pathway and mediates the induction of Fgf8 in the limb ectoderm by Fgf10 during AER formation (Kengaku et al. 1998; Kawakami et al. 2001). Moreover, gradients of Wnt5a establish planar cell polarity in chondrocytes along the P-D axis by regulating Vangl2 phosphorylation during mice limb development (Gao and Yang 2013; Qian et al. 2007).

During axolotl limb development, a visible AER does not form. Fgf8 is initially expressed in the epidermis in the prospective forelimb region of the limb bud at developmental stage 42. Fgf8 is expressed in both epidermis and mesenchyme at one day after stage 42, then Fgf8 is expressed mainly in the mesenchyme of the bud until digits form approximately 14 days later (Han, An, and Kim 2001). As in other vertebrates, sonic hedgehog (Shh) is expressed in posterior regions of the developing limb bud (Torok et al. 1999; Nacu et al. 2016). Wnt5a is expressed mainly in the distal apical ectoderm at stage 36 of the forelimb and hindlimb bud. Wnt5b is observed in the mesenchyme of the forelimb and hindlimb bud at developmental stage 36 (Ghosh et al. 2008). Wnt7a is expressed diffusely in the distal part of the limb throughout limb development (Shimokawa et al. 2013). Most studies of axolotl limb development to date have been descriptive and have not used functional approaches to test the requirement of key signaling pathways.

1.8 Conclusions and perspective

Many signaling pathways are activated during tissue regeneration and limb development in vertebrates. Studies have shown that TGF-β, Wnt, and Fgf signaling pathways are among the most important pathways controlling processes that are

necessary for limb development, including limb bud initiation, cell proliferation, and patterning. These pathways also play essential roles in regulating processes during tissue regeneration, including the formation of the wound epithelium, stimulation and migration of progenitor cells, and progenitor cell proliferation. Functional studies are needed to test the requirement of TGF-β, Wnt, and Fgf signaling pathways during limb development and tail regeneration.

1.9 Rationale

Recently, a chemical screen was performed to identify molecules that alter molecular functions, signaling pathways, and biological processes associated with axolotl tail regeneration (Ponomareva et al. 2015). Three specific inhibitors SB505124, Wnt-C59 and BGJ398 targeting TGF-β, Wnt, and Fgf signaling pathways, respectively, were found to block axolotl tail regeneration. In this dissertation, I performed experiments to determine how these chemical inhibitors affected processes that are necessary for tail regeneration, including mitosis, cell proliferation, and cell orientation during axolotl tail regeneration and limb bud outgrowth.

CHAPTER 2 TGF-β SIGNALING IS REQUIRED DURING AXOLOTL TAIL REGENERATION

Qingchao Qiu[1]

[1]Department of Neuroscience, University of Kentucky, Lexington, Kentucky

KEYWORDS: Axolotl, regeneration, tail, Tgf-β, Erk, Akt

2.1 Abstract

The Tgf-β signaling pathway is required for many regenerative processes in vertebrates, including salamander limb, frog tadpole tail, and fish fin regeneration. Here, I investigated the requirement of Tgf-β signaling pathway on tail regeneration using Mexican axolotl (*Ambystoma mexicanum*) embryos and chemical inhibitors of Smad and non-Smad signaling pathways (SB505124 and Naringenin). Both SB505124 and Naringenin completely blocked tail regeneration and reduced levels of p-Smad2 and p-Smad3 as early as 1-hour post-amputation. However, more complex changes in p-Erk and p-Akt were observed between the chemical treatments. At 1hpa, levels of p-Erk and p-Akt were significantly higher in SB505124-treated embryos, but significantly lower in Naringenin-treated embryos. At 6hpa and 12hpa, SB505124 significantly affected levels of p-Erk while Naringenin significantly affected levels of p-Akt. Further analyses showed that SB505124 but not Naringenin decreased cell proliferation. My results show that Tgf-β signaling pathway via Smad and non-Smad signaling pathways are activated very early after axolotl tail amputation and chemical perturbation of these pathways blocks tail regeneration. Overall, my study enriches the understanding of signaling network dynamics that underlie tissue regeneration.

2.2 Introduction

Multiple signaling pathways are deployed during regeneration to regulate cellular and developmental processes associated with repair and formation of new tissue (Ho and Whitman 2008; Singh et al. 2018; Peiris et al. 2016; Herman et al. 2018). Detailing where and when signaling pathways are deployed during regeneration is essential to understand how regeneration programs are regulated. Cellular and developmental processes are often regulated in parallel, and it can be difficult to resolve the onset or offset timing of signaling pathway deployment in rapidly developing model organisms (Fields and Johnston 2005). To address this issue, we recently developed an embryo tail amputation model using the Mexican axolotl (Ponomareva et al. 2015). The assay uses hatching stage embryos that are capable of regenerating amputated distal tail tips in 7 days. Relative to rapidly growing organisms like *Danio rerio* (zebrafish) and *Xenopus laevis* (Xenopus), axolotl embryos grow slowly, allowing greater temporal resolution of early events during regeneration (Fields and Johnston 2005; Voss, Epperlein, and Tanaka 2009).

The axolotl embryo model was first used to investigate the Wnt signaling pathway during tail regeneration (Ponomareva et al. 2015). Wnt proteins are secreted ligands that bind to extra-cellular receptors of the Frizzled family (Willert and Nusse 2012; MacDonald and He 2012). In the presence of Wnt ligand, intracellular levels of β-Catenin increase, and transcriptional target genes are activated (MacDonald, Tamai, and He 2009). Using chemical compound Wnt-C59, a potent inhibitor of Wnt ligand secretion, Ponomareva et al (2015) inhibited tail regeneration, thus establishing a requirement for Wnt signaling. Surprisingly, few differentially expressed genes were discovered between Wnt-C59 treated and control embryos before 48 hours post-

amputation. Still, the few genes that were discovered at 24hpa and the greater number of genes discovered at later time points included many ligands and components of cell signaling pathways (e.g. Wnt, Fgf, Bmp, Tgf-β, Egf, Ras/Mapk, Ngf, Notch, Ra, Myc, and P53) (Ponomareva et al. 2015). Thus, Wnt signaling yields transcripts that code for proteins of multiple signaling pathways, but the timing is delayed relative to early wound healing events (< 24hpa) that are likely regulated by other signaling pathways (Shah et al. 2012).

A pathway that is likely activated upstream of Wnt during tail regeneration is the Tgf-β signaling pathway, as it is known to be activated very early in response to injury, and it is required for successful zebrafish fin, Xenopus tadpole tail, and axolotl limb regeneration (Levesque et al. 2007; Ho and Whitman 2008; Denis et al. 2016; Pfefferli and Jazwinska 2017). Tgf-β signaling is generally mediated by Tgf-β, Nodal and Activin ligands that bind Tgf-β type II receptors on the cell membrane, causing the recruitment and transphosphorylation of Tgf-β type I receptors (Aykul and Martinez-Hackert 2016; Zhu et al. 2012; Wrana et al. 1992; Attisano et al. 1993). Activated Tgf-β type I receptors phosphorylate Smad2 and Smad3, which then complex with Smad4, a co-Smad that mediates translocation into the nucleus to regulate transcription (Derynck and Zhang 2003). In addition to canonical Smad2/Smad3 signaling, the Tgf-β signaling pathway utilizes non-Smad pathways, including Map kinase and phosphatidylinositol-3-kinase/Akt (Zhang 2009; Li et al. 2013; Li et al. 2016). Recently, inhibitors of Smad3 were used to show that p-Smad2 but not p-Smad3 mediates Tgf-β signaling during axolotl limb regeneration (Denis et al. 2016). Whether this mechanism generally applies to animal models with regenerative capacity, as well as other tissues in the axolotl, is unknown.

In this study, I used chemical compounds to inhibit components of the Tgf-β signaling pathway during axolotl embryo tail regeneration. I show that SB505124 and Naringenin both inhibit tail regeneration, and this is associated with alterations in canonical Smad2/3 signaling and non-Smad signaling pathways. Interestingly, only SB505124 inhibited cell proliferation and thus the mechanism by which Naringenin inhibited regeneration remains unknown.

2.3 Materials and Methods

2.3.1 Regeneration experiments

Axolotl embryos were reared at 16°C in 40% Holtfreter's solution. Embryos at developmental stage 42 (Bordzilovskaya & Dettlaff, 1989) were used for all the tail regeneration experiments (Ponomareva et al. 2015). SB505124 (Selleckchem, Cat. #S2186) was dissolved in DMSO to make a 50mM stock solution and used at 10μM for regeneration experiments (DaCosta Byfield et al. 2004). DMSO at 0.02% was used for controls. Naringenin (Selleckchem, Cat. #S2394) was dissolved in DMSO to make a 50mM stock solution and used at 20μM for the regeneration experiments (Denis et al. 2016). DMSO at 0.04% was used as controls for Naringenin treatment to match the DMSO concentration in the treatment group. Axolotl embryos were dechorionated and anesthetized in 0.02% benzocaine, and 2mm of the distal tail tip was amputated using a sterile blade. Embryos were reared singly, one per well, in 12-well microtiter plates for the timing experiments and immunofluorescence (IF) staining. Five embryos were reared per well for Western Blot tissue collection. There were 9 groups in the titration experiment: 0.02% DMSO control, and 10^{-4}, 10^{-3}, 10^{-2}, 10^{-1}, 1, 2.5, 5, and 10μM SB505124. There were 7 groups in the timing experiment:

0.02% DMSO control and SB505124 administered from 0-12, 12-24, 24-48, 48-72, 72-120, and 120-144hpa. The embryos were photographed at different post-amputation time points, and tail length and snout-vent length were measured from the images. Statistical analysis was performed using GraphPad Prism software version 6.0 using Student's t-test.

2.3.2 Antibodies

Anti-TGF-β antibody (Cat. #bs-0086R) was obtained from Bioss. Anti-p-Smad2 (Cat. #3108), Anti-Smad2 (Cat. #5339S), Anti-Smad3 (Cat. #9523S), Anti-Erk (Cat. #4348), Anti-phospho-Erk (Thr202/Tyr204) (Cat. #4370), Anti-Akt (Cat. #9272), Anti-phospho-Akt (Ser473) (Cat. #9271), Anti-β-Actin (Cat. #5125S), and Anti-GAPDH (Cat# 2118) were purchased from Cell Signaling Technology. Anti-p-Smad3 was a gift from Dr. Stephane Roy (Succursal Centresville Montreal, Quebec Canada). Anti-phospho-Histone H3 (Ser10) (Cat. # 05-1336) was purchased from Millipore. Goat anti-Rabbit IgG, (H+L) HRP conjugate (Cat. # AP307P) and Goat anti-Mouse IgG, (H+L) HRP-conjugated secondary antibodies (Cat. #AP308P) were purchased from Millipore. Cy3™ AffiniPure Donkey Anti-Mouse IgG (H+L) (Cat. #715-165-151) was purchased from Jackson Immune Research. DAPI (4', 6-diamidino-2-phenylindole, dihydrochloride, Cat. #62247) was purchased from Thermo Scientific.

2.3.3 Immunochemistry staining

A previous protocol was modified for immunochemistry staining (Qiu et al. 2015). In brief, samples were fixed in 4% Paraformaldehyde (PFA) overnight. Samples were dehydrated through a methanol series, starting in 100% PBS and then 25, 50, 75, and 100% methanol. These samples were saved at -20ºC for later use. Samples were

rehydrated for whole-mount staining or OCT embedding. After OCT embedding, 8μM sections were prepared for staining or saved at -80°C for later use. Primary Anti-TGF-β 1antibodies were used at 1: 200. Primary Anti-phospho-Histone H3 (Ser10) antibodies were used at 1:1000. The secondary Cy3™ AffiniPure Donkey Anti-Mouse IgG (H+L) antibodies were used at 1:200. Blocking solution was 5% sheep serum. Total DNA was labeled by DAPI. Stained slides were imaged using a confocal microscope (Nikon Tie and C2+ Confocal). A mitotic index was determined by dividing the number of histone H3 positive cells by the number of DAPI positive cells within 200μm of the tail tip. Statistical analysis was performed using GraphPad Prism software version 6.0 using Student's t-test.

2.3.4 Western blotting

Embryos that had been administered tail amputations were anesthetized with 0.02% benzocaine and 1mm of the distal tail tip was cut using a sterile blade. Tail tips of 30 embryos were pooled for each sample. The pooled tail tips were washed two times using 1x PBS solution with proteinase/phosphatase inhibitor mixture (#5872S, Cell Signaling Technology), and then lysed in RIPA buffer (#R0278, Sigma) with proteinase/phosphatase inhibitor mixture by using a 22.5-gauge needle and 1 ml syringe. The protein concentrations were determined by a BCA protein assay (#23225, Thermo Scientific). Equal amounts of tissue lysate were loaded into lanes of 10% SDS polyacrylamide gels and transferred to PVDF membranes. The membranes were blotted with 5% non-fat milk and then incubated overnight at 4°C with primary antibodies and were followed by HRP-conjugated secondary antibodies. The immune complexes were detected by enhanced chemiluminescence (Cat# NEL103001, PerkinElmer). Quantification of band intensities was performed using the ImageJ

software (http://rsbweb.nih.gov/ij/). The data were shown as mean ± SD. Statistical analyses were performed by GraphPad Prism software version 6.0. using Student's t-test.

2.3.5 EdU cell proliferation assay

An EdU cell proliferation assay was performed using FAM picolyl azide from Click Chemistry Tools (Cat. # 1180-1), along with CuSO4 and sodium ascorbate in the Click-iT™ EdU Alexa Fluor™ 488 Imaging Kit from Invitrogen (Cat. # C-10337). The protocol was modified for whole-mount staining and cryo-section staining. Briefly, axolotl embryos were tail amputated and placed in 12-well-plates with 0.02% DMSO, 0.04% DMSO, 10μM SB505124, or 20μM Naringenin solution. At 48hpa, embryos were injected intraperitoneally with 1ul of 8μM 5-ethynyl-2'-deoxyuridine (EdU). At 72hpa, embryos were anesthetized with 0.02% benzocaine and fixed in 4% paraformaldehyde overnight. The samples were dehydrated and rehydrated using a methanol series (0, 25, 50, 75, and 100% in PBS). The samples were washed with PBS with 1% Triton for 3x5 minutes, then bathed in 2.5% trypsin for 30 minutes and washed with icy cold acetone for 10 minutes following PBS with 1% Triton 3x5 minutes. Click-iT EdU reaction solution containing 1x Tris-buffered saline, 4mM CuSO4, FAM 488 picolyl azide, and 100mM sodium ascorbate was used to visualize EdU incorporation into the DNA of proliferating cells. DAPI was used to counter stain DNA within cells. Cells staining positive for EdU within 400μm of the tail tip were counted as well as cells staining positive for DAPI within the same area. A proliferative index was calculated as a ratio of EdU positive cells over DAPI positive cells. For cryo-section staining, trypsinization and ice-cold acetone washing steps

were skipped. Results were analyzed in GraphPad Prism software version 6.0 (San Diego California USA) using Student's t-test.

2.4 Results

2.4.1 Tgf-β signaling is required during axolotl tail regeneration.

A Tgf-β receptor Alk5/4/7 inhibitor, SB505124, was previously shown to inhibit axolotl tail regeneration using a 10μM dose (Ponomareva et al. 2015; DaCosta Byfield et al. 2004). To verify this result and more comprehensively examine dosage, I treated embryos with different concentrations of SB505124 (0, 10^{-4}, 10^{-3}, 10^{-2}, 10^{-1}, 1, 2.5, 5, and 10μM) (Figure2.1 A). The treated embryos appeared healthy and active for all treatments tested. Doses of SB505124 above 0.01μM inhibited tail regeneration at 7dpa (Figure2.1 B). By varying the time that SB505124 was administered, I detected significant differences in tail length at 7dpa when treating embryos from 0-12hpa, 12-24hpa, and 48-72hpa (Figure2.1 C). In contrast, I did not detect significant differences in snout-vent length at 7dpa (Figure2.1 D). These results show that SB505124 efficiently blocks tail regeneration without affecting overall embryo growth and development. These results suggest that Tgf-β signaling is required for axolotl tail regeneration.

To further investigate the requirement of Tgf-β signaling, I treated embryos with Naringenin, a small molecule that inhibits phosphorylation of Smad3, an intracellular protein that mediates Tgf-β signal transduction (Ortiz-Andrade et al. 2008; Denis et al. 2016). I tested 8 embryos for 4 different concentrations of Naringenin (0, 10, 20, and 35μM) (Figure2.2 A-C). The 35μM treatment was toxic, all embryos died. Relative to controls, embryos treated with 10μM showed a marginal decrease in tail

length at 7dpa, indicating partial inhibition of regeneration. In contrast, 20μM Naringenin significantly inhibited tail regeneration at 7dpa (Figure2.2 D). Although the 20μM treated embryos appeared healthy and normal, I noted that the outer margins of their tailfins presented an abnormal white coloration. This white tissue may reflect necrosis of epithelial cells during prolonged treatment of Naringenin at 20μM. However, Naringenin completely inhibited regeneration at this concentration, consistent with an early disruption of the Tgf-β signaling pathway.

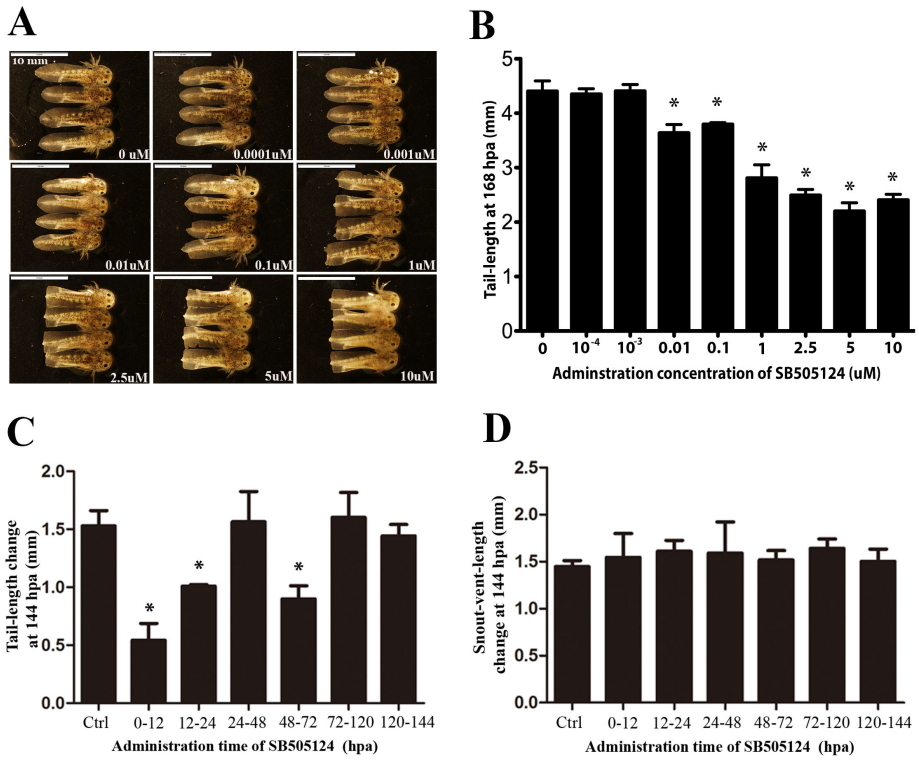

Figure 2.1 Inhibiting Alk4/5/7 by SB505124 blocks axolotl tail regeneration.

A and B) SB505124 treatments above 0.01μM significantly inhibited axolotl embryo tail regeneration. C) 10μM of SB505124 was administered at different time periods and tail length was measured. Tail length at 7dpa differed significantly between DMSO treated controls (1.53 ± 0.26mm) and SB505124 treatments of 0-12 (0.54 ± 0.29mm), 12-24 (1.01 ± 0.03mm), and 48-72hpa (0.90 ± 0.22mm). D) No significant

difference in snout-vent length was detected between SB505124 treated and DMSO treated controls. *: p value < 0.05 for contrasts of DMSO control vs SB505124.

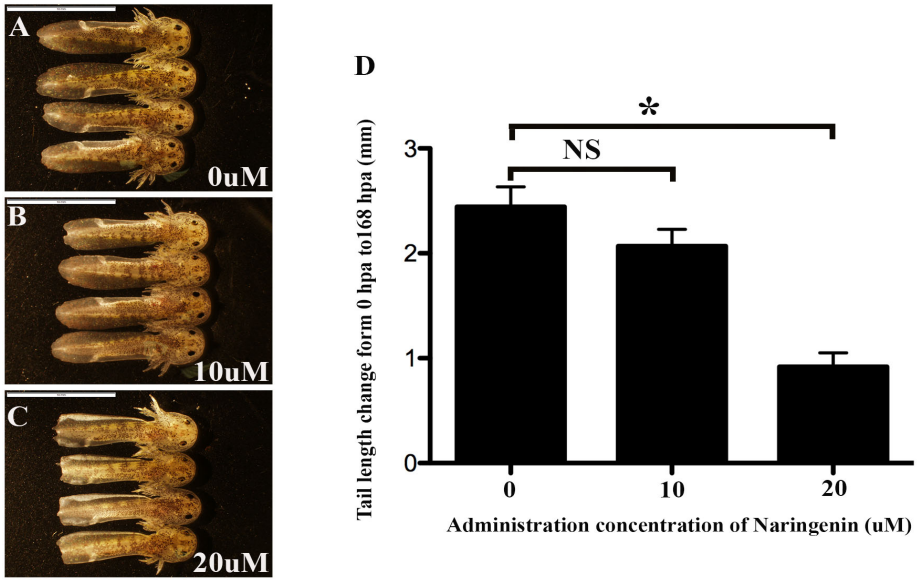

Figure 2.2 Naringenin inhibits axolotl tail regeneration.

A-D) Naringenin inhibited axolotl tail regeneration at 7dpa. D) Tail growth was significantly less for 20μM Naringenin treated embryos (0.92 ± 0.22mm) relative to DMSO controls (2.45 ± 0.38mm). *: p value < 0.001 for contrasts of DMSO control vs Naringenin.

2.4.2 Tgf-β1 increases during tail regeneration.

Previous studies have established that the Tgf-β signaling pathway is required for axolotl limb regeneration (Levesque et al. 2007; Jhamb et al. 2011; Denis et al. 2016). In particular, Levesque et al. (2007) showed that *Tgf-β1* mRNA is upregulated very early (6hpa) following limb amputation and strongly expressed in the blastema at the early bud stage. To determine if Tgf-β1 is also expressed during axolotl embryo tail regeneration, I stained for Tgf-β1 at 0, 3, and 6hpa. Tgf-β1 was broadly expressed in the tail at the time of amputation, particularly in the epidermis and myotomes

(Figure2.3 A). Tgf-β1 expression significantly decreased at 3hpa (Figure2.3 A-D, n = 6, $p < 0.05$) but was significantly higher than basal levels at 6hpa, prominently in cells of the wound epidermis (Figure2.3 A-D, n = 6, $p < 0.05$). These data show that Tgf-β1 is dynamically regulated in response to tail amputation.

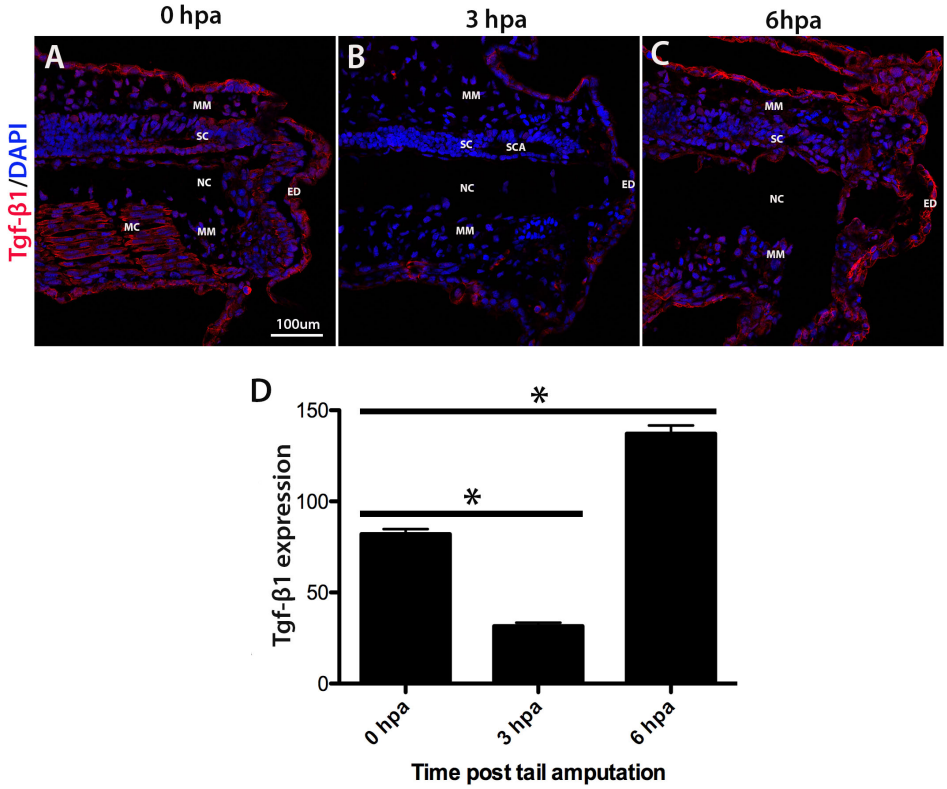

Figure 2.3 Tgf-β1 is broadly expressed in the axolotl tail and increases in the epidermis during tail regeneration.

A) Tgf-β1 expression at 0hpa in the tail tip. Relative to Tgf-β1 expression in the epidermis at 0hpa, expression was significantly lower at 3hpa (B) but significantly higher at 6hpa (C). * $p < 0.001$ for contrasts of DMSO control vs SB505124. MM: Mesenchymal tissue; SC: Spinal cord; NC: Notochord; MC: Muscle cells; ED: Epidermis tissue. SCA: Spinal cord ampulla.

2.4.3 Smad-mediated Tgf-β signaling increases during axolotl tail regeneration.

Tgf-β signaling during axolotl limb regeneration is associated with phosphorylation of Smad2 and Smad3 (Denis et al 2016). To determine if Smad2/3-mediated Tgf-β signaling during axolotl tail regeneration, I quantified phosphorylated Smad2 (p-Smad2) and Smad3 (p-Smad3) expression using pooled 2 mm tail tips by Western Blotting. Levels of Smad2 and Smad3 were constant for all samples analyzed, while p-Smad2 and p-Smad3 levels were more variable (Figure2.4A). P-Smad2 increased from 1hpa to 12hpa (Figure2.6 A and B) while the expression of p-Smad3 was relatively constant (Figure2.4A and C). Embryos were next treated with SB505124 to determine if p-Smad2 and p-Smad3 were specifically mediated by Tgf-β signaling, in comparison to control embryos; SB505124 significantly decreased p-Smad2 at 1, 6, and 12hpa (45.1%, 71.1%, and 74.5%, respectively) (Figure2.4 A and B). P-Smad3 was not significantly inhibited by SB505124 at 1 h, but p-Smad3 levels were significantly lower at 6 and 12hpa (57.9% and 36.9%, respectively) (Figure2.4A-C). The results show that SB505124 treatment affected p-Smad2 earlier and to a greater degree than p-Smad3, but inhibition of Tgf-β signaling decreased phosphorylation of both proteins.

I next performed Western blotting to determine if Naringenin inhibited tail regeneration via its predicted blockade of Smad3 phosphorylation (Denis et al. 2016). In control embryos, p-Smad2 levels increased slightly at 1hpa, but greatly at 6 and 12hpa. At each of these time points, Naringenin treated embryos showed significantly reduced levels of p-Smad2 (Figure2.5 A and B). The p-Smad3 expression profiles for control and treated embryos also showed differences in both timing and magnitude of expression. In control embryos, p-Smad3 increased precipitously at 1hpa, but after

this time levels decreased. Levels of p-Smad3 also increased in Naringenin treated embryos. However, peak expression was observed at 6hpa. As a result, p-Smad3 levels were significantly lower in Naringenin treated embryos at 1hpa, but significantly higher than those of controls at 6hpa (Figure2.5 A and C). Thus, Naringenin decreases and delays p-Smad3 expression after tail amputation. Overall, these expression patterns show that Naringenin alters phosphorylation dynamics of Smad2 and Smad3 proteins that mediate Tgf-β signaling.

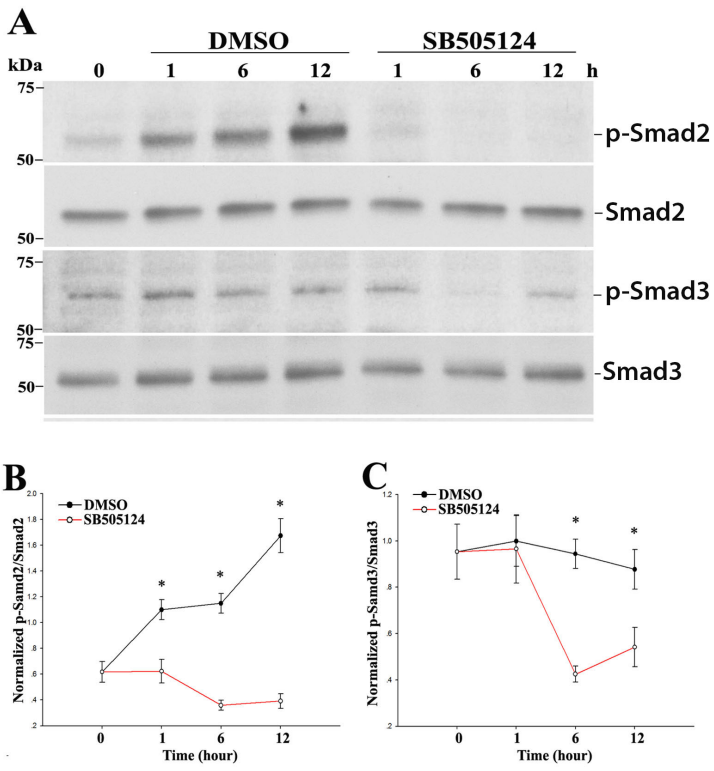

Figure 2.4 SB505124 significantly affects p-Smad2 and p-Smad3 expression.
A) Smad2, p-Smad2, Smad3, and p-Smad3 were detected by Western blotting using pooled 1mm tail tips from SB505124 treated or DMSO control embryos at 0, 1, 6, and 12hpa. B) P-Smad2 expression was normalized against total Smad2. C) P-Smad3 expression was normalized against total Smad3. *: p-value < 0.05 for contrasts of DMSO control vs SB505124.

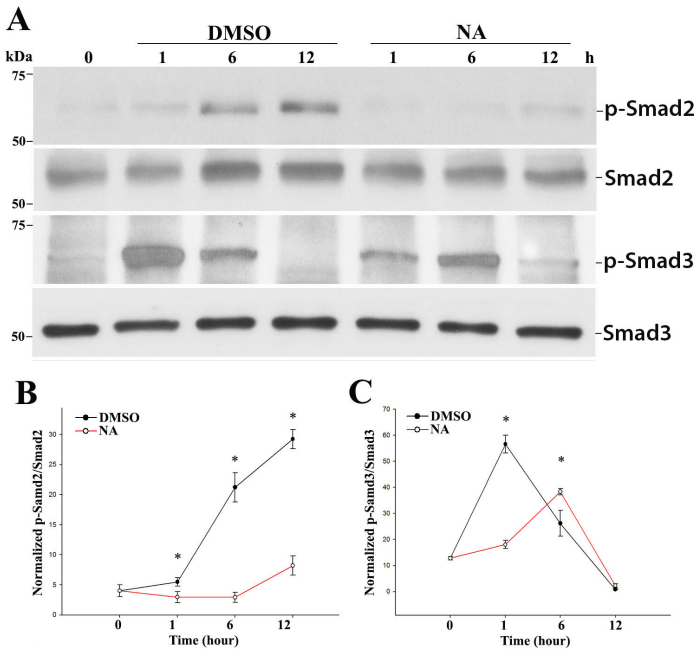

Figure 2.5 Naringenin significantly affects activation of Smad2 and Smad3. A) Western blotting of Smad3, p-Smad3, Smad2, and p-Smad2 using pooled 1mm tail tips from 20μM Naringenin (NA) treated or DMSO treated embryos tail tips collected at 0, 1, 6, and 12hpa. B) P-Smad2 expression was normalized against total Smad2. C) P-Smad3 expression was normalized against total Smad3. *: p-value < 0.05 for contrasts of DMSO control vs Naringenin.

2.4.4 Non-Smad mediated Tgf-β signaling pathways are up-regulated by SB505124 and down-regulated by Naringenin at 1hpa.

Previous studies have shown that Tgf-β ligands mediate intracellular signaling via non-Smad mediated pathways (Ho and Whitman 2008; Bassat et al. 2017; Bakin et al. 2000). To investigate non-Smad mediated Tgf-β signaling pathways, phosphorylated Erk (p-Erk) and Akt (p-Akt) signaling were quantified by Western blotting. Both p-Erk and p-Akt were detected at the time of tail amputation. However, these proteins presented different post-amputation expression profiles between control and SB505124-treated tails. While p-Erk was increased in both control and SB505124-

treated embryos at 1hpa, expression was significantly higher in the later (Figure2.6 A and B). Phosphorylated Akt did not significantly change at 1hpa but decreased at 6 and 12hpa in control embryos. SB505124 treatment increased Akt phosphorylation at 1hpa and had no significant effect at 6 and 12hpa (Figure2.6 A and C). P-Erk was significantly down-regulated in Naringenin-treated embryos at 1hpa compared with controls (Figure2.7 A and B). Naringenin also significantly down-regulated p-Akt following tail amputation at all time points (Figure2.7 A and C). These results show that Erk and Akt activation are up-regulated by SB505124 and down-regulated by Naringenin during early tail regeneration.

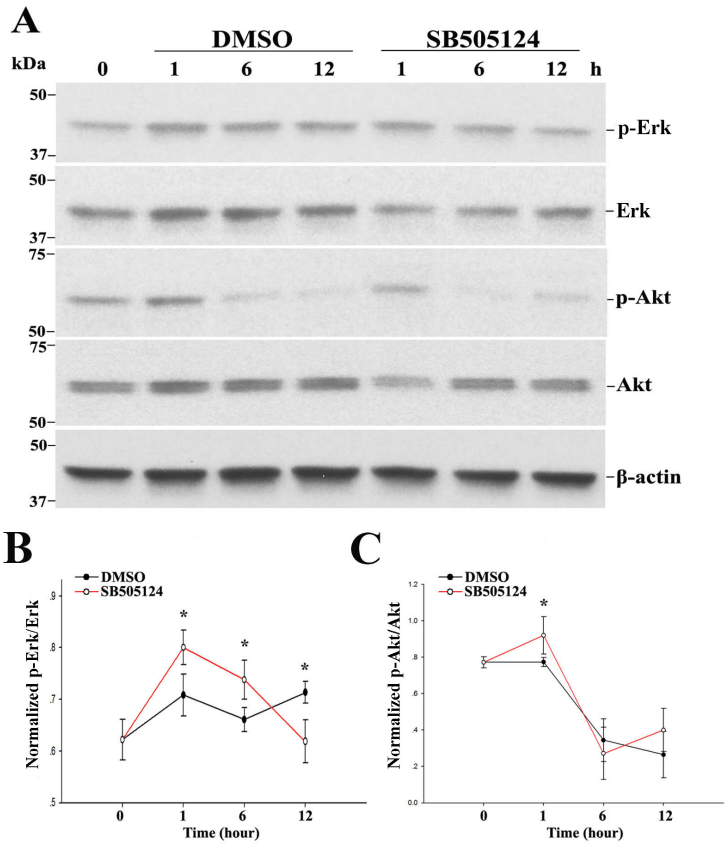

Figure 2.6 SB505124 increases phosphorylation of non-Smad mediated signaling Erk and Akt at 1hpa. A) Erk, p-Erk, Akt, p-Akt, and β-actin were detected by Western blotting using pooled 1mm tail tips from SB505124 treated or DMSO control

embryos at 0, 1, 6, and 12hpa. B) P-Erk expression was normalized against Erk. C) P-Akt expression was normalized against Akt. *: *p*-value <0.05 for contrasts of DMSO control vs SB505124.

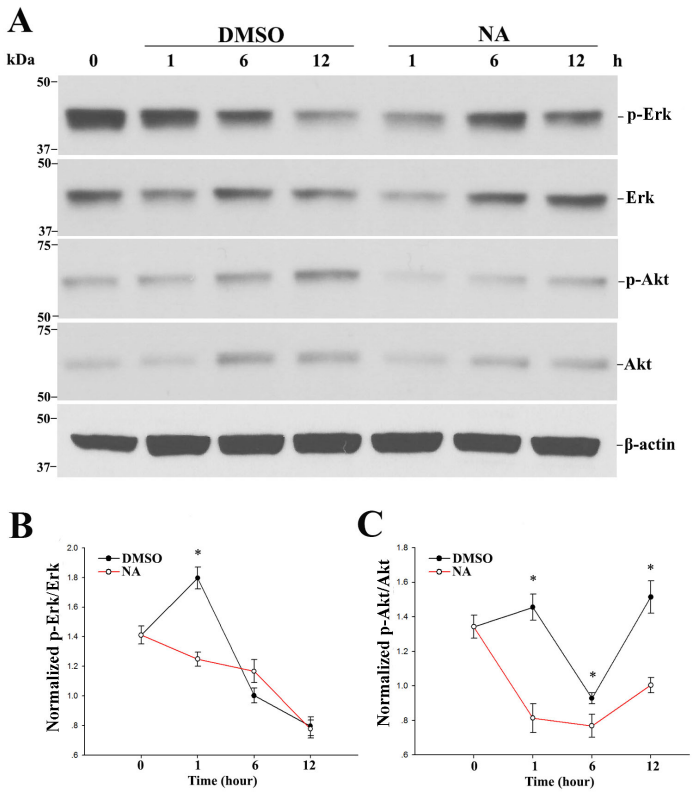

Figure 2.7 Naringenin down-regulates p-Erk and p-Akt signaling at 1hpa. A) Western blotting of total Erk, p-Erk, Akt, p-Akt, and β-actin using pooled 1mm tail tips from Naringenin treated or DMSO control tails. B) P-Erk expression was normalized against Erk. C) P-Akt expression was normalized against Akt. *: *p* value < 0.05 for contrasts of DMSO control vs Naringenin.

2.4.5 SB505124, but not Naringenin, significantly reduces cell proliferation.

Tgf-β signaling pathway is required for cell proliferation during tail regeneration in *Xenopus laevis* tadpoles (Ho and Whitman 2008). To determine whether Tgf-β signaling regulates cell proliferation during axolotl tail regeneration, EdU

incorporation was used to detect proliferating cells from 48 to 72hpa. In DMSO control tails, proliferating cells were observed in the regenerating bud, especially within 400μm of the tail tip (Figure2.8 A-A''), while SB505124 treatment reduced cell proliferation within multiple regions of the tail including dorsal fins, ventral fins, and spinal cord (Figure2.8 B-B'' and D, n = 6, $p < 0.001$). In contrast, Naringenin treatment did not reduce cell proliferation significantly in these tissues (Figure2.8 C-C'' and E, n = 4, $p > 0.05$). These data show that SB505124 downregulates cell proliferation during tail regeneration, while Naringenin does not.

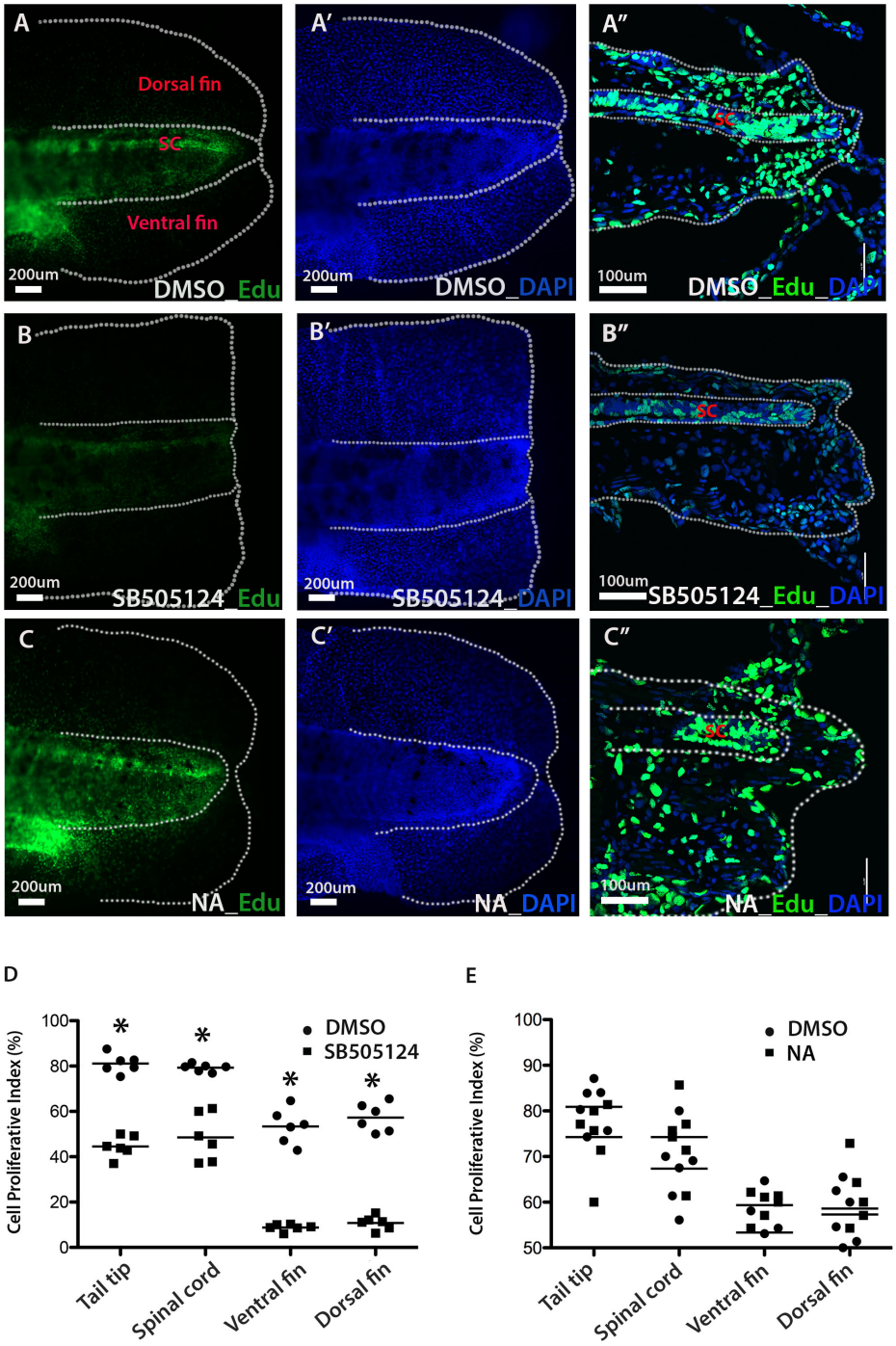

Figure 2.8 SB505124, but not Naringenin, significantly reduces cell proliferation at 72hpa. Images A", B", and C" are cryo-sections of regenerating tails. All the other images are the whole-mount and regenerating tails. A) DMSO control stained for EdU. A') DMSO control stained with DAPI. A'') DMSO control stained for EdU and DAPI. B) Tail treated with SB505124 and stained for EdU. B') Tail treated with SB505124 and stained with DAPI. B'') Tail treated with SB505124 and stained for

EdU and DAPI. C) Tail treated with Naringenin and stained for EdU. C') Tail treated with Naringenin and stained with DAPI. C'') Tail treated with Naringenin and stained with EdU and DAPI. D) Proliferative index for the tail tip and spinal cord. For dorsal or ventral fins, cells were counted in whole-mount staining samples. E) Proliferative index for Naringenin treated and control samples. *: p-value < 0.001 for contrasts of DMSO control vs SB505124.

2.4.6 Tgf-β signaling regulates cell mitosis during tail regeneration.

To determine whether the cell proliferation response during tail regeneration associates with cell mitosis, a mitotic marker, anti-phospho-histone H3 (Ser10), was used to detect mitotic cells. In DMSO treated controls, the mitotic index was 7.6 ± 2.8%. SB505124 treatment significantly reduced the mitotic index to 2.4 ± 1.0% (Figure2.9 A-C, n = 3, p < 0.05). These results strongly suggest that Tgf-β signaling regulates cell mitosis during tail regeneration.

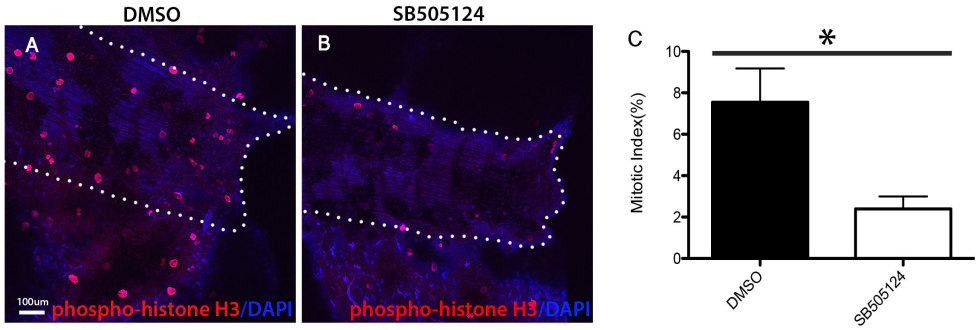

Figure 2.9 SB505124 inhibits the mitotic index within tail tips at 48hpa. A) DMSO control tail stained with phospho-histone H3 in red. The total nuclear DNA was labeled with DAPI. The white stippled lines outline the tail. B) SB505124 treated tail stained with phospho-histone H3. C) Graph comparing the mitotic index in DMSO control and SB505124 treated tails. *: p-value < 0.05 for contrasts of DMSO control vs SB505124.

2.5 Discussion

Ligands of the Tgf-β super family associate with axolotl tail regeneration.

Tgf-β ligands are pleiotropic cytokines whose activities depend on their receptor-binding partner and intracellular signaling components. In mammals, there are approximately 33 ligands in the Tgf-β family (Aykul and Martinez-Hackert 2016). In this chapter, Tgf-β1 was shown to be up-regulated during axolotl tail regeneration. This result is consistent with studies of other tissue regeneration models. For example, Tgf-β1 is upregulated during axolotl limb and tadpole tail regeneration (Denis et al. 2016; Levesque et al. 2007). However, SB505124 inhibits multiple type I receptors (Alk5/4/7). Ligands, in addition to Tgf-β1, which are thought to signal through Alk5, may orchestrate Tgf-β signaling during axolotl tail regeneration. For example, Tgf-β2 and Tgf-β5 are up-regulated during Xenopus tail regeneration, and they are thought to function in wound epithelium formation and establishment of the regeneration bud, a structure that forms very early in tadpole regeneration (Ho and Whitman 2008). Also, these Tgf-β ligands are thought to regulate cell proliferation through their effects on Erk signaling (Ho and Whitman 2008). In lizard tail regeneration, Tgf-β1 expression is limited while activin-βA is strongly upregulated. Morpholino knockdown of activin-βA or its receptor Alk4 impairs zebrafish fin regeneration (Jazwinska, Badakov, and Keating 2007). Inhibin could be another important ligand during tail regeneration based on results of a previous axolotl tail microarray study which showed significant upregulation of *inhbb* at 48hpa (Ponomareva et al. 2015). *Inhbb* shares a β subunit with *activin* and its function is thought to oppose *activin* (Zhu et al. 2012; Namwanje and Brown 2016). In future studies, it will be important to investigate activin and inhibin during axolotl tail regeneration. Overall, my results and other studies clearly implicate Tgf-β ligands in early tissue regeneration responses.

Dynamic regulation of p-Smad2 and p-Smad3 by Tgf-β signaling during tail regeneration

In this study, I showed that chemical disruption of Tgf-β signaling altered Smad2 and Smad3 phosphorylation. In control embryos, p-Smad2 and p-Smad3 dynamically increased following tail amputation. Both Smad2 and Smad3 were activated upon tail amputation as early as 1hpa and p-Smad2 steadily increased after this time while p-Smad3 decreased. Application of SB505124 down-regulated both p-Smad2 and p-Smad3 at all post-amputation time points and blocked tail regeneration. Naringenin also down-regulated p-Smad2 at all post-amputation time points and delayed peak p-Smad3 expression and completely blocked tail regeneration. However, SB505124 treatment affected p-Smad2 at an earlier time and to a greater degree than p-Smad3, while Naringenin affected p-Smad3 at an earlier time and to a greater degree than p-Smad2. Activation of p-Smad2 has been reported at 1hpa during Xenopus tail regeneration and 6hpa during axolotl limb regeneration; these results are consistent with my findings (Ho and Whitman 2008; Denis et al. 2016). Denis et, al (2016) reported that only phosphorylation of Smad2, but not phosphorylation of Smad3, is required for axolotl limb regeneration (Denis et al. 2016). This contrasts with my findings, as I found that pSmad3 inhibitor Naringenin blocked tail regeneration. Additional studies are needed to understand the differential requirements for Smad2 and Smad3 signaling during axolotl limb and tail regeneration.

Dynamic regulation of p-Erk and p-Akt by the Tgf-β signaling pathway during tail regeneration

Erk and Akt are two non-Smad mediated Tgf-β signaling pathways (Zhang 2009). Erk signaling is a central cassette of the mitogen-activated protein kinase (Mapk) signaling pathway that regulates mammalian wound contraction and cell proliferation (Shaul and Seger 2007; Li et al. 2013; Li et al. 2016). Tgf-β signaling also activates Akt signaling; inhibition of Tgf-β type I receptor prevented the activation of Akt that functions in mammalian cell survival (Bakin et al. 2000). In this study, I found that p-Erk and p-Akt responded to tail amputation at an early phase of tail regeneration. In DMSO control embryos, the expression pattern of p-Erk and p-Akt in SB505124 and Naringenin were different. One possible reason is that embryos used for these different experiments came from different genetic backgrounds that may exhibit variability in cell signaling. Another possible reason is that the DMSO concentration in the Naringenin experiments was 0.04%, which is 1x higher than the DMSO concentration in the SB505124 experiment. Studies have shown that DMSO concentration may differentially alter cell membrane structure, ubiquitination sites, and affect oxidative phosphorylation (ATP synthesis) leading to variation in signal transduction, protein degradation, and protein phosphorylation (Majdi et al. 2017; Doellinger et al. 2018; Syed, Skonberg, and Hansen 2013; Julien et al. 2012). However, the effects of DMSO on axolotl cells is unknown. In regard to protein phosphorylation, I used a high concentration of proteinase/phosphatase inhibitor during sample collection. Despite differences in the expression levels of p-Erk and p-Akt in the DMSO controls, their patterns were somewhat similar for the first 6hpa. In both of the DMSO control samples, p-Erk was expressed at the time of tail amputation, increased at 1hpa and then decreased at 6hpa, although the decrease was

much greater in the Naringenin experiment. P-Akt was expressed at the time of tail amputation. It changed very little at 1hpa and decreased at 6hpa. These data suggest that both Erk and Akt were dynamically changed following tail regeneration. Overall, increased expression of p-Erk and decreased expression of p-Akt appear to be important early signaling responses. Furthermore, p-Erk and p-Akt were significantly up-regulated in SB505124-treated tails, but significantly down-regulated in Naringenin-treated tails at 1hpa, showing that p-Erk and p-Akt are affected by disruptions of Tgf-β signaling. Temporal changes in p-Erk and p-Akt have been observed in other studies. For example, Erk phosphorylation is upregulated in the wound epithelium at 8hpa and in mesenchymal cells under the wound epithelium at 48hpa during Xenopus tail regeneration (Ho and Whitman 2008). These two periods of Erk phosphorylation are consistent with my results which showed inhibition of tail regeneration at these times. The first 0-24 hours is an important injury response phase wherein genes are expressed to facilitate wound healing. Transcription between 48-72hpa time course may regulate cell proliferation. Also, in the Xenopus limb regeneration model, Erk phosphorylation is upregulated in the wound epithelium at 48hpa and mesenchymal cells under the wound epithelium at 96hpa while Akt phosphorylation is up-regulated in the mesenchymal cells from 24hpa to 96hpa (Suzuki et al. 2007). Overall, these studies suggest an important role for pathways that mediate non-Smad Tgf-β signaling during early amphibian appendage regeneration.

Tgf-β signaling regulates mitogenic activity and cell proliferation response during axolotl tail regeneration.

In cell culture models, it is widely accepted that Tgf-β signaling inhibits the growth of certain non-transformed epithelial, endothelial, and primary fibroblasts of embryonic

origin (Moses 1992; Ten Dijke et al. 2002). However, Tgf-β signaling facilitates mitogenic activity in some transformed cells and immortalized fibroblasts (Alexandrow and Moses 1995). In cancer biology, it is known that the action of Tgf-β signaling depends on cell type and growth conditions; it acts as a tumor suppressor at early stages and stimulates tumor proliferation at later stages (Fabregat et al. 2014). In tissue regeneration models, Tgf-β pathway regulation of cell proliferation is also tissue-dependent. In zebrafish, Tgf-β signaling promotes cell proliferation during fin and heart regeneration, but negatively regulates cell proliferation in retinal regeneration (Tappeiner et al. 2016). In axolotl tail regeneration, I detected significantly higher cell proliferation and mitosis in control embryos than in SB505124 treated embryos at 72hpa and 48hpa, respectively. Therefore, my data indicate that Tgf-β signaling plays an important role in regulating cell proliferation responses during tail regeneration.

Naringenin targets multiple signaling pathways in addition to p-Smad3 phosphorylation.

Naringenin inhibited p-Smad2, p-Smad3, p-Erk, and p-Akt as early as 1hpa, and blocked tail regeneration. The inhibitory effect of Naringenin on axolotl tail regeneration contrasts with the result of Denis et al (2016), who did not find that Naringenin inhibited axolotl limb regeneration. They concluded that p-Smad3 is not required during axolotl limb regeneration while my result suggests that p-Smad3 is required for axolotl tail regeneration. It is possible that Naringenin may have a broader inhibitory effect in the axolotl embryo model than the adult limb model, as multiple signaling pathways are operative during early development. In other words, Naringenin targets multiple signaling pathways in addition to p-Smad3. Consistent

with this interpretation, my study is the first to show that Naringenin downregulates p-Smad2, p-Erk, and p-Akt during tissue regeneration.

A cell proliferation response at 72hpa is necessary, but not sufficient for tail regeneration.

SB505124 treatment decreased cell proliferation at 72hpa and prevented tail regeneration. These results suggest that Tgf-β signaling regulates a cell proliferation response that is necessary for successful tail regeneration. However, other processes than cell proliferation are necessary for tail regeneration because Naringenin did not inhibit cell proliferation at 72hpa but did block tail regeneration. It will be important in future studies to perform dose and timing experiments for Naringenin to identify the key periods for Naringenin inhibition of tail regeneration and more thoroughly investigate how this drug affects cell mitosis.

In this chapter, I found: 1) Tgf-β1 is upregulated during tail regeneration. 2) Both Smad mediated Tgf-β signaling and non-Smad mediated Tgf-β signaling are activated as early as 1hpa during axolotl tail regeneration. 3) Blocking Tgf-β signaling by SB505124 or Naringenin prevents axolotl tail regeneration. 4) Tgf-β signaling regulates cell proliferation and cell mitosis during axolotl tail regeneration. Overall, my study enriches understanding of Tgf-β signaling pathway dynamics underlies tissue regeneration.

CHAPTER 3 WNT SIGNALING IS REQUIRED DURING AXOLOTL TAIL REGENERATION

Qingchao Qiu[1]

[1]Department of Neuroscience, University of Kentucky, Lexington, Kentucky

KEYWORDS: axolotl, regeneration, tail, Wnt, Erk, Akt

3.1 Abstract

Wnt signaling pathway is activated during tissue regeneration. Palmitoylation of Wnts by Porcupine is critical for Wnt protein secretion and activity. Here I investigated the requirement of Wnt signaling on tail regeneration using Mexican axolotl (*Ambystoma mexicanum*) embryos and Porcupine inhibitor Wnt-C59. Continuous Wnt-C59 treatment completely blocked tail regeneration at 7 days post tail amputation (dpa). Temporal dosing experiments showed that Wnt signaling is required from 0-120 hours post-amputation (hpa). Individuals that were removed from Wnt-C59 treatment at 7dpa regenerated somatic tissues of the body axis, but not dorsal and ventral fins. Strikingly, Wnt-C59 released individuals did not develop their forelimbs, and hindlimb development was abnormal. Levels of Wnt3a were significantly lower than pre-amputation levels at 24 and 72hpa. β-Catenin levels decreased in DMSO-treated embryos after tail amputation and were significantly lower than pre-amputation levels at 48hp, but significantly higher at 72hpa. Inhibiting Wnt signaling by Wnt-C59 increased the β-Catenin level and upregulated Erk and Akt phosphorylation. Additionally, inhibition of Wnt signaling reduced cell mitosis at 24 hpa and cell proliferation at 72hpa. These data suggest that Wnt signaling regulates β-Catenin, Erk, and Akt signaling and controls cell mitosis and cell proliferation during axolotl tail regeneration. My results show that Wnt signaling is required for axolotl tail regeneration.

3.2 Introduction

Salamanders regenerate many body parts including limbs, tail, lens, heart, spinal cord, and brain (Sugiura et al. 2016; Nacu et al. 2016; Franklin, Voss, and Osborn 2017; Suetsugu-Maki et al. 2012; Nakamura et al. 2016; Tazaki, Tanaka, and Fei 2017; Amamoto et al. 2016). Salamander appendages harbor lineage-restricted progenitor cells and multipotent cells that are recruited after injury to reform missing or damaged tissues (Tanaka and Reddien 2011). For example, cell lineage tracing during Xenopus tail regeneration showed that the spinal cord regenerates from progenitors within the spinal cord, while new muscle is reformed by satellite cells within muscle tissue (Gargioli and Slack 2004). Despite those advances in understanding tissue regeneration at the cellular level, how injury activates signaling pathways to guide progenitor cell behaviors is still poorly understood. For example, while it has been established that Wnt signaling is required for axolotl embryo tail regeneration (Ponomareva et al. 2015), the temporal requirements and effects of Wnt signaling on cellular and developmental processes have not been characterized in this model.

Wnt proteins have been found to play a myriad of biological roles in controlling tissue regeneration among many species (Zhao et al. 2019; Fan et al. 2018; Wischin et al. 2017; Ghosh et al. 2008; Kawakami et al. 2006). Wnt protein binds N-terminal extracellular cysteine-rich domain of a 7 transmembrane molecule Frizzled (Fz) family receptor, which interacts with co-receptors including lipoprotein receptor-related (LRP) 5/6, ROR2, and receptor tyrosine kinase (RTK) (Komiya and Habas 2008). Upon activation, Fz directly binds to Dsh, which has three conserved protein domains: a central PDZ domain, an amino-terminal DIX domain, and a carboxy-terminal DEP domain (Wong et al. 2003). There are three Wnt signaling pathways:

the canonical Wnt/β-Catenin pathway and two pathways that function independent of β-Catenin, the Wnt/planar cell polarity (PCP) pathway and Wnt/calcium pathway (Habas and Dawid 2005).

Canonical and non-canonical Wnt signaling pathways are required during tissue regeneration to control different aspects of tissue regeneration (Kawakami et al. 2006; Ghosh et al. 2008; Shimokawa et al. 2013; Hamilton, Sun, and Henry 2016; Yokoyama et al. 2011; Sugiura et al. 2009; Lin and Slack 2008). Upon depletion of β-Catenin, an amputated planarian tail regenerates into a head. This suggests that β-Catenin maintains anteroposterior identity during homeostasis and regeneration in planarians (Petersen and Reddien 2008; Gurley, Rink, and Sanchez Alvarado 2008). Using a genetic construct to inhibit Wnt/β-Catenin signaling, Kawakami et al (2006) prevented limb regeneration in axolotl larvae and fin regeneration in zebrafish. Moreover, they showed that the surprising ability of early-stage chick embryos to regenerate limbs is associated with β-Catenin signaling (Kawakami et al. 2006). Non-canonical Wnt signaling pathways are also crucial to regulate tissue regeneration. Two non-canonical Wnt genes, *Wnt5a* and *Wnt5b,* are expressed during axolotl limb regeneration (Ghosh et al. 2008). Overexpression of Wn5a induces the development of ectopic tails in Xenopus tadpoles at the site of a dorsal incision; presumably, this is mediated by Wnt/Jnk signaling (Sugiura et al. 2009). Thus, both canonical and non-canonical Wnt signaling pathways are required in multiple types of tissue regeneration across species.

However, in some cases, the use of tools to inhibit Wnt signaling has not yielded inhibitory regeneration outcomes. For example, a heat-shock inducible genetic

construct encoding the Wnt antagonist Dkk1 did not prevent Xenopus limb or lens regeneration (Yokoyama et al. 2011; Hamilton, Sun, and Henry 2016). Yokoyama et al (2011) hypothesized that nerve-derived signals could compensate for Wnt signaling during the initiation of Xenopus limb regeneration. Other studies have shown that Wnt-pathway agonists can inhibit regeneration, including axolotl limb and Xenopus lens regeneration (Wischin et al. 2017; Hamilton, Sun, and Henry 2016). In the axolotl study, Wnt agonist treatment before blastema formation inhibits limb regeneration, possibly by affecting innervation, while treatment after blastema formation causes disorganized skeletal elements to form (Wischin et al. 2017). A similar phenomenon has been shown during limb development; stabilization of β-Catenin during early stages of limb development leads to early regression of the apical epidermal ridge and results in truncated limbs (Hill et al. 2006), while it causes skeletal abnormalities during later stages (Akiyama et al. 2004). During axolotl tail regeneration, both Wnt agonist SKL, which increases Wnt/β-Catenin signaling, and Wnt antagonist IWR-1-endo which decreases Wnt/β-Catenin signaling, inhibits tail regeneration (Ponomareva et al. 2015). This suggests that successful tissue regeneration requires proper spatial-temporal regulation of Wnt/β-Catenin signaling, especially the timing of β-Catenin activation (Kawakami et al. 2006).

Ponomareva et al. (2015) found that inhibiting Wnt signaling pathway by Wnt-C59 blocks axolotl tail regeneration. Moreover, Wnt-C59 treatment affects transcription of genes associated with Wnt, Fgf, Tgf-β, Hox, Egf, Myc, Notch, Ngf, Ras/Mapk, p53, and retinoic acid (RA) pathways. Most differentially expressed genes were discovered between Wnt-C59 treated and control embryos after 24 hours post tail amputation (hpa). These data demonstrated that Wnt signaling interacts with other signaling

pathways to regulate tail regeneration. However, the temporal requirement of Wnt/β-Catenin signaling pathway during axolotl tail regeneration is unknown. In this study, I used the chemical compound Wnt-C59 to inhibit Wnt protein secretion and activity during axolotl embryo tail regeneration. I demonstrate that Wnt signaling is required from 0 to 120 hours post tail amputation. The Wnt-C59 treatment completely prevented tail regeneration, and this was associated with increasing β-Catenin, p-Erk, p-Akt, and a reduction in cell mitosis and cell proliferation in the tail. These findings suggest that Wnt/ β-Catenin signaling regulates p-Erk and p-Akt signaling pathways to maintain cell mitosis and cell proliferative responses during axolotl tail regeneration.

3.3 Methods

3.3.1 Regeneration experiments

Axolotl embryos were reared at 16°C in 40% Holtfreter's solution. Embryos at developmental stage 42 (Bordzilovskaya & Dettlaff, 1989) were used for all tail regeneration experiments (Ponomareva et al. 2015). Wnt-C59 (Selleckchem, Cat. #S7037) was dissolved in DMSO at 10mM to make a stock solution and then diluted further to make a 10μM working solution. 0.1% DMSO was used for controls. Axolotl embryos were dechorionated and anesthetized in 0.02% benzocaine, and 2mm of tail tips were amputated using a sterile blade. Embryos were reared singly, one per well, in 12-well microtiter plates for dose-timing experiments and immunofluorescence (IF) staining. Five embryos were reared per well for tissue collection to perform Western Blotting experiments. There were 7 groups in the timing experiment: 0.1% DMSO control and Wnt-C59 administered from 0-12, 12-24, 24-48, 48-72, 72-120, and 120-144hpa. The embryos were photographed at

different post-amputation time points. Tail length and snout-vent length were measured from the images. Statistical analyses were performed using GraphPad Prism software version 6.0 using Student's t-test.

3.3.2 Antibodies

Anti-β-Catenin (Cat. # 610154) was purchased from BD Biosciences. Anti-Wnt3a (Cat. # bs-1700R), Anti-Erk (Cat. #4348), Anti-phospho-Erk (Thr202/Tyr204) (Cat. #4370), Anti-Akt (Cat. #9272), Anti-phospho-Akt (Ser473) (Cat. #9271), and Anti-β-actin (Cat. #5125S) were purchased from Cell Signaling Technology. Anti-phospho-Histone H3 (Ser10) (Cat. # 05-1336) was purchased from Millipore. Goat anti-Rabbit IgG, (H+L) HRP conjugate (Cat. # AP307P) and Goat anti-Mouse IgG, (H+L) HRP-conjugated secondary antibodies (Cat. #AP308P) were purchased from Millipore. Cy3™ AffiniPure Donkey Anti-Mouse IgG (H+L) (Cat. #715-165-151) was purchased from Jackson immune Research. DAPI (4', 6-diamidino-2-phenylindole, dihydrochloride, Cat. #62247) was purchased from Thermo Scientific.

3.3.3 Tissue processing and immunochemistry staining

An existing protocol was modified for immunostaining (Qiu et al. 2015). In brief, samples were fixed in 4% paraformaldehyde overnight. Samples were dehydrated through a methanol series, starting in 100% PBS and then 25, 50, 75, and 100% methanol. These samples were saved at -20ºC for later use. Samples were rehydrated for whole-mount staining or OCT embedding. After OCT embedding, 8µM sections were prepared for staining or saved at minus 80°C for later use. Primary Anti-phospho-Histone H3 (Ser10) antibodies were used at 1:1000, and the secondary Cy3™ AffiniPure Donkey Anti-Mouse IgG (H+L) antibodies were used at 1:200.

Blocking solution was modified as 5% sheep serum. Total DNA was labeled by DAPI. Stained slides were imaged using a confocal microscope (Nikon Tie and C2+ Confocal). A mitotic index was determined by dividing the number of histone H3 positive cells by the number of DAPI positive cells within 200μm of the tail tip. Statistical analyses were performed using GraphPad Prism software version 6.0 using Student's t-test.

3.3.4 Western blotting

Embryos were anesthetized with 0.02% benzocaine and 1mm of the distal tail tip was cut using a sterile blade. Tail tips of 30 embryos were pooled for each sample. Each pooled sample was washed two times using a 1x PBS solution with proteinase/phosphatase inhibitor mixture (#5872S, Cell Signaling Technology), and then lysed in RIPA buffer (#R0278, Sigma) with proteinase/phosphatase inhibitor mixture using a 22.5-gauge-needle and 1 ml syringe. Protein concentrations were determined by a BCA protein assay (#23225, Thermo Scientific). Equal amounts of tissue lysate were loaded into lanes of 10% SDS polyacrylamide gels and transferred to a PVDF membrane. The membranes were blotted with 5% non-fat milk, incubated overnight at 4°C with primary antibodies, and then incubated with HRP-conjugated secondary antibodies. The immune complexes were detected by enhanced chemiluminescence (Cat# NEL103001, PERKin Elmer). Quantification of band intensities was performed using the ImageJ software (http://rsbweb.nih.gov/ij/). The data were presented as the mean ± SD. Statistical analyses were performed using GraphPad Prism software version 6.0 using Student's t-test.

3.3.5 EdU cell proliferation assay

An EdU cell proliferation assay was performed using FAM picolyl azide from Click Chemistry Tools (Cat. # 1180-1), along with CuSO4 and sodium ascorbate in the Click-iT^{TM} EdU Alexa Fluor^{TM} 488 Imaging Kit from Invitrogen (Cat. # C-10337). The protocol was modified for whole-mount staining and cryo-sections at 8μm. Briefly, axolotl embryos were tail amputated and placed in 12-well-plates with 0.1% DMSO or 10μM Wnt-C59 solution. At 48hpa, embryos were injected peritoneally with 1ul of 8μM 5-ethynyl-2'-deoxyuridine (EdU). At 72hpa, embryos were anesthetized and fixed in 4% paraformaldehyde overnight. The samples were dehydrated and rehydrated using a methanol series (0, 25, 50, 75, 100% in PBS). The samples were washed 3x with 1% Triton for 5 minutes, then bathed in 2.5% trypsin for 30 minutes, washed with ice-cold acetone for 10 minutes, followed by PBS and 1% Triton 3x for 5 minutes. Click-iT EdU reaction solution containing 1x Tris-buffered saline, 4mM CuSO4, FAM 488 picolyl azide, and 100mM sodium ascorbate was used to visualize EdU incorporation into the DNA of proliferating cells. DAPI was used to stain total nuclear DNA. Cells staining positive for EdU within 400μm of the tail tip were counted as well as cells staining positive for DAPI within the same area. A proliferative index was calculated as a ratio of EdU positive cells to DAPI positive cells. Results were analyzed in GraphPad Prism software version 6.0 (San Diego California USA) using one-way ANOVA test.

3.4 Results

3.4.1 Blocking Wnt signaling prevents axolotl embryo tail regeneration.

A Porcupine inhibitor, Wnt-C59, was previously demonstrated to inhibit axolotl tail regeneration using a 10μM dose (Ponomareva et al. 2015). To confirm this result and

titrate the best dosage, concentrations of Wnt-C59 at 0, 10^{-4}, 10^{-3}, 10^{-2}, 10^{-1}, 1, 2.5, 5, and 10μM were used to treat developmental stage 42 embryos. The treated embryos were healthy and active for all treatments tested. Doses of Wnt-C59 above 1μM inhibited tail regeneration at 168hpa (Figure 3.1, A and B). By varying the time of Wnt-C59 administration, I detected significant differences in tail length at 7dpa for 0-12, 12-24, 24-48, 48-72, and 72-120hpa treatments. In contrast, I did not detect a significant difference in snout-vent length at 168hpa between the DMSO control and any treatment (Figure 3.1 D). The 120-144hpa group had shorter tails in comparison to the DMSO controls, but the difference was not statistically significant, presumably due to the short administration time. The above results indicate a requirement for Wnt signaling throughout most of the tail regeneration process.

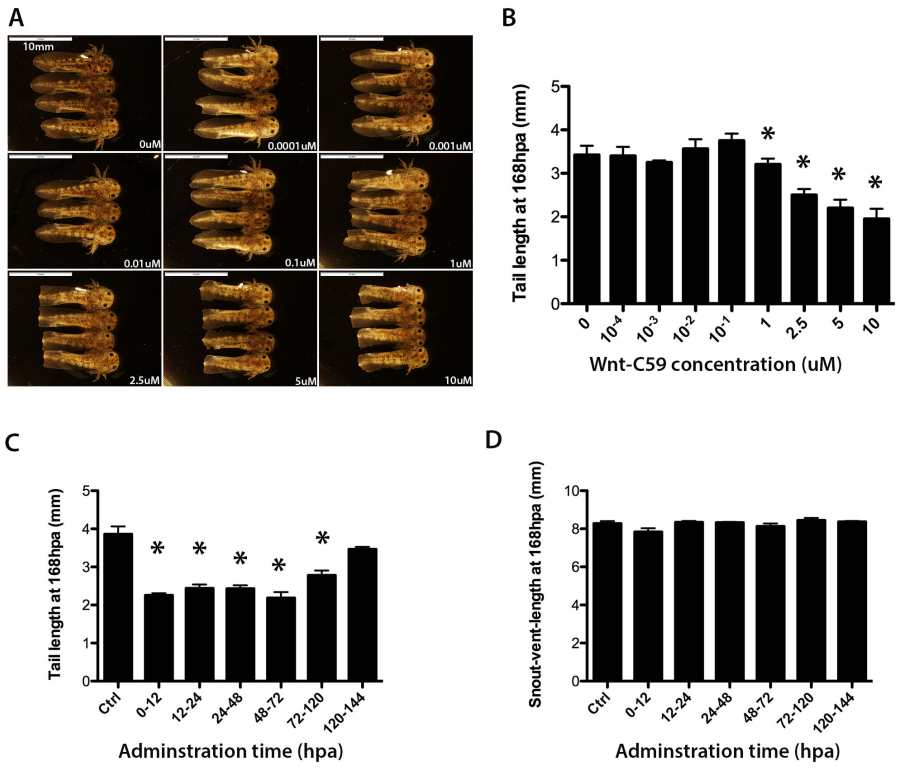

Figure 3.1 Inhibiting Wnt signaling by Wnt-C59 blocks axolotl tail regeneration. A and B) Wnt-C59 above 1μM significantly inhibited axolotl embryo tail regeneration. C) 10μM of Wnt-C59 was administered for different lengths of time, and tail length was measured. Tail length at 168hpa differed significantly between DMSO control and Wnt-C59 treatments of 0-12, 12-24, 24-48, 48-72, and 72-120hpa. D) No significant differences in snout-vent length were detected between Wnt-C59 treated and DMSO control embryos. *: p-value < 0.05 for contrasts of DMSO control vs Wnt-C59, n = 4.

3.4.2 Wnt3a is suppressed during tail regeneration.

Previous studies have established that canonical Wnt/β-Catenin signaling promotes blastema formation and subsequent proliferation in zebrafish fin regeneration (Stoick-Cooper et al. 2007). Wnt3a is a major Wnt ligand mediating Wnt/β-Catenin signaling. To evaluate if Wnt3a is also expressed during axolotl embryo tail regeneration, Wnt3a

was detected in pooled tail tips at 24, 48, and 72hpa. In comparison to pre-amputation levels, Wnt3a expression significantly decreased at 24hpa and 72hpa (Figure 3.2 A and B, p value < 0.05, n = 3). These data show dynamic changes in Wnt3a expression during the first 72 hours of tail regeneration.

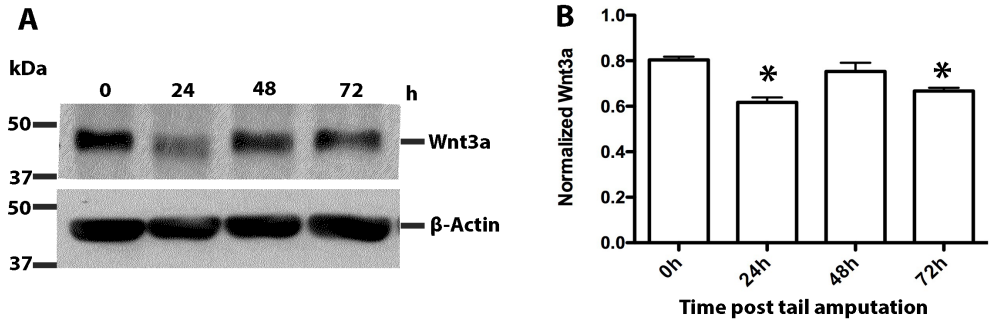

Figure 3.2 Wnt3a expression decreases during tail regeneration. A) Wnt3a was detected by western blotting using pooled distal tail tips. β-Actin was blotted as a loading control. B) Wnt3a was expressed at 0hpa and decreased at 24hpa and 72hpa. *: p-value < 0.05 for contrasts between 0hpa vs 48hpa or 72hpa, n = 3.

3.4.3 Wnt-C59 increases β-Catenin expression during tail regeneration.

β-Catenin is an important transcription factor that mediates canonical Wnt/β-Catenin signaling. To investigate β-Catenin expression and determine how Wnt-C59 regulates β-Catenin levels, I quantified β-Catenin levels in regenerating distal tail tip tissues that were treated with DMSO or Wnt-C59 at 0, 24, 48, and 72hpa. β-Catenin was expressed at the time of amputation. Relative to pre-amputation levels, I detected a significant decrease in β-Catenin expression at 48hpa (Figure 3.2, p < 0.05, n = 3) and a significant increase in β-Catenin at 72hpa (Figure 3.3, p < 0.01, n = 3). Wnt-C59 increased β-Catenin at 48hpa (Figure 3.3, p < 0.01, n = 3). These results suggest that canonical Wnt signaling is dynamically changed during tail regeneration and β-Catenin increases upon Wnt signaling pathway inhibition.

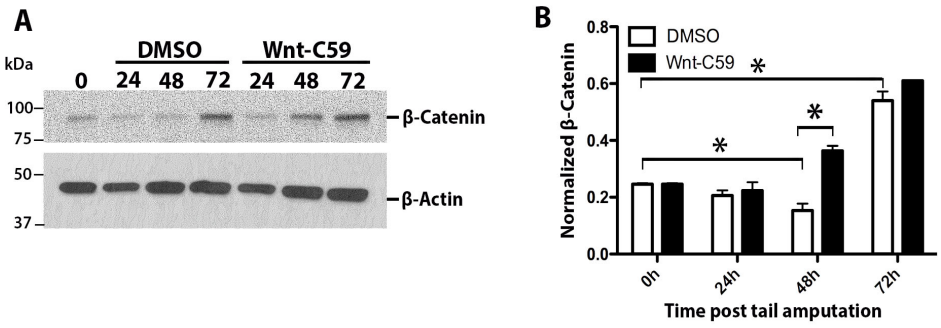

Figure 3.3 Wnt-C59 increases β-Catenin expression at 48hpa. A) β-Catenin was detected by western blotting using Wnt-C59 treated or DMSO control tails. β-Actin was blotted as a loading control. B) Relative to 0hpa, β-Catenin was significantly lower at 48hpa and significantly higher at 72hpa. Wnt-C59 increased β-Catenin expression at 48hpa. *: p-value < 0.05 for contrasts between DMSO control at 0hpa vs 48hpa or 72hpa, and between DMSO control and Wnt-C59 at 48hpa.

3.4.4. Inhibiting Wnt signaling increases p-Erk and p-Akt expression.

A few studies have shown that Wnt signaling regulates Erk or Akt signaling pathways (Zhang, Pizzute, and Pei 2014; Bikkavilli and Malbon 2009; Georgopoulos, Kirkwood, and Southgate 2014). To determine if Wnt signaling affects these pathways during axolotl tail regeneration, I detected p-Erk and p-Akt using distal pooled tail tips treated with Wnt-C59 and DMSO at 0, 24, 48, and 72hpa. Both p-Erk and p-Erk were expressed at the time of amputation but decreased at 24hpa and increased significantly at 72hpa (Figure 3.4, $p < 0.001$, n = 3). Wnt-C59 treatment increased p-Erk at all tested times and increased p-Akt expression at 48hpa and 72hpa (Figure 3.5, $p < 0.001$, n = 3). These results suggest that Wnt-C59 up-regulates Erk and Akt during tail regeneration.

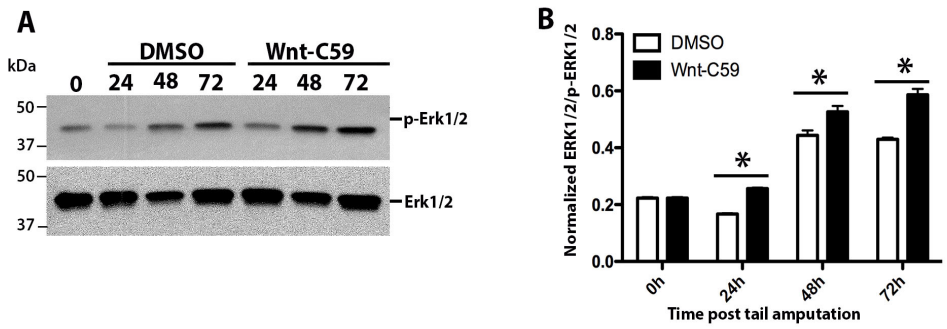

Figure 3.4 Wnt-C59 increases phosphorylation of Erk at 24, 48, and 72hpa. A) P-Erk and Erk expression in Wnt-C59 treated and DMSO controls. B) P-Erk was lowly expressed at 0hpa and 24hpa but increased significantly at 48hpa and 72hpa. Wnt-C59 treatment increased p-Erk expression at 24hpa, 48hpa, and 72hpa. *: *p*-value < 0.01 for contrasts of DMSO control vs Wnt-C59, n = 3.

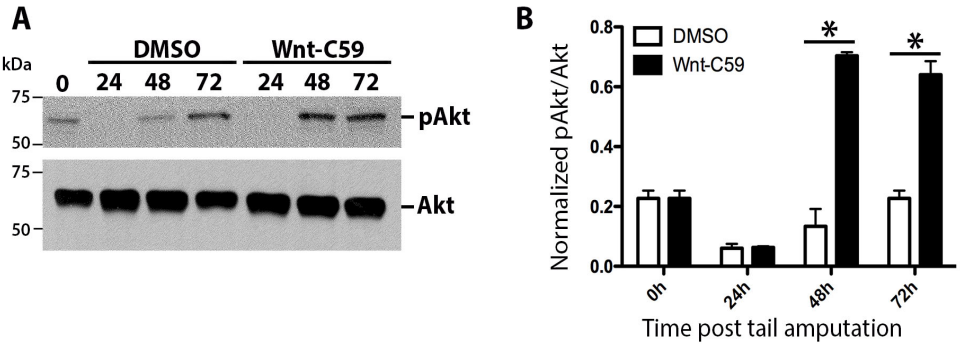

Figure 3.5 Wnt-C59 increases phosphorylation of Akt at 48 and 72hpa. A) P-Akt and Akt expression in Wnt-C59 treated and DMSO controls. B) P-Akt was low at 0hpa. It significantly decreased at 24hpa and increased at 48hpa and 72hpa in regenerating tail tips. Wnt-C59 treatment significantly increased p-Akt expression at 48hpa and 72hpa. *: *p* value < 0.01 for contrasts of DMSO control vs Wnt-C59, n = 3.

3.4.5 Wnt signaling regulates cell mitosis during axolotl tail regeneration.

To determine if Wnt signaling regulates cell mitosis, a mitotic marker, anti-phospho-histone H3 (Ser10), was used to stain mitotic cells in the tail using whole-mount

staining. Most of the phospho-histone H3 positive cells were located in the mesenchyme underlying the epidermis. The mitotic index of the DMSO control within 400µm of the distal tail tip was 7.5 ± 1.5%. Wnt-C59 treatment reduced the mitotic index by 2.5 ± 0.6% (Figure 3.6, $p < 0.01$, n = 3). These results show that Wnt signaling regulates cell mitosis in the distal tail tip during axolotl tail regeneration.

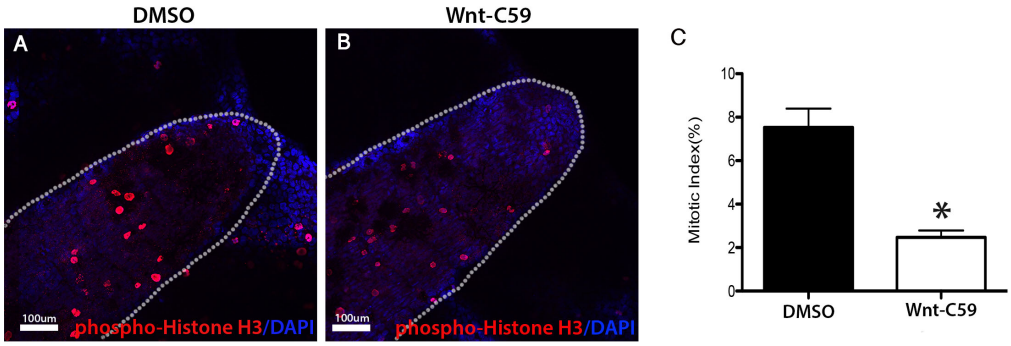

Figure 3.6 Wnt-C59 inhibits the mitotic index at 48hpa. A) DMSO control tail stained with phospho-histone H3 in red. The white stippled lines outline medial tail tissues to the exclusion of tail fins. B) Wnt-C59 treated tail stained with phospho-histone H3. C) Graph comparing the mitotic index in DMSO control and Wnt-C59 treated tails. *: p-value < 0.05 for contrasts of DMSO control vs Wnt-C59.

2.4.6 Wnt signaling regulates cell proliferation during axolotl tail regeneration.

Wnt signaling is required for proliferation of progenitor cells in the blastema during zebrafish fin regeneration (Stoick-Cooper et al. 2007). To determine whether Wnt signaling regulates cell proliferation during axolotl tail regeneration, an EdU incorporation assay was used to detect proliferating cells from 48 to 72hpa. In DMSO treated samples, proliferating cells were observed in the regenerating tail, especially within 400µm of the tail tip (Figure 3.7 A-A''), while Wnt-C59 treatment reduced

proliferating cells in the tail tip, dorsal fin, ventral fin, and spinal cord (Figure 3.7 B-B'', and D, n = 6, $p < 0.001$). These data show that Wnt signaling regulates cell proliferation during tail regeneration. Note that the proliferation index in the spinal cord of Wnt-C59 treated tails was still very high (44.8% ± 7.6%, n = 6).

Embryos were reared without Wnt-C59 for 33 days to test for a long-term effect of early Wnt-C59 treatment. Interestingly, a fin-less phenotype was observed, consistent with a long-term block of fin regeneration. Moreover, Wnt-C59 treated animals did not develop forelimbs (Figure 3.8). This finding led me to investigate the Wnt signaling pathway during forelimb bud outgrowth, the results of which are presented in Chapter 5.

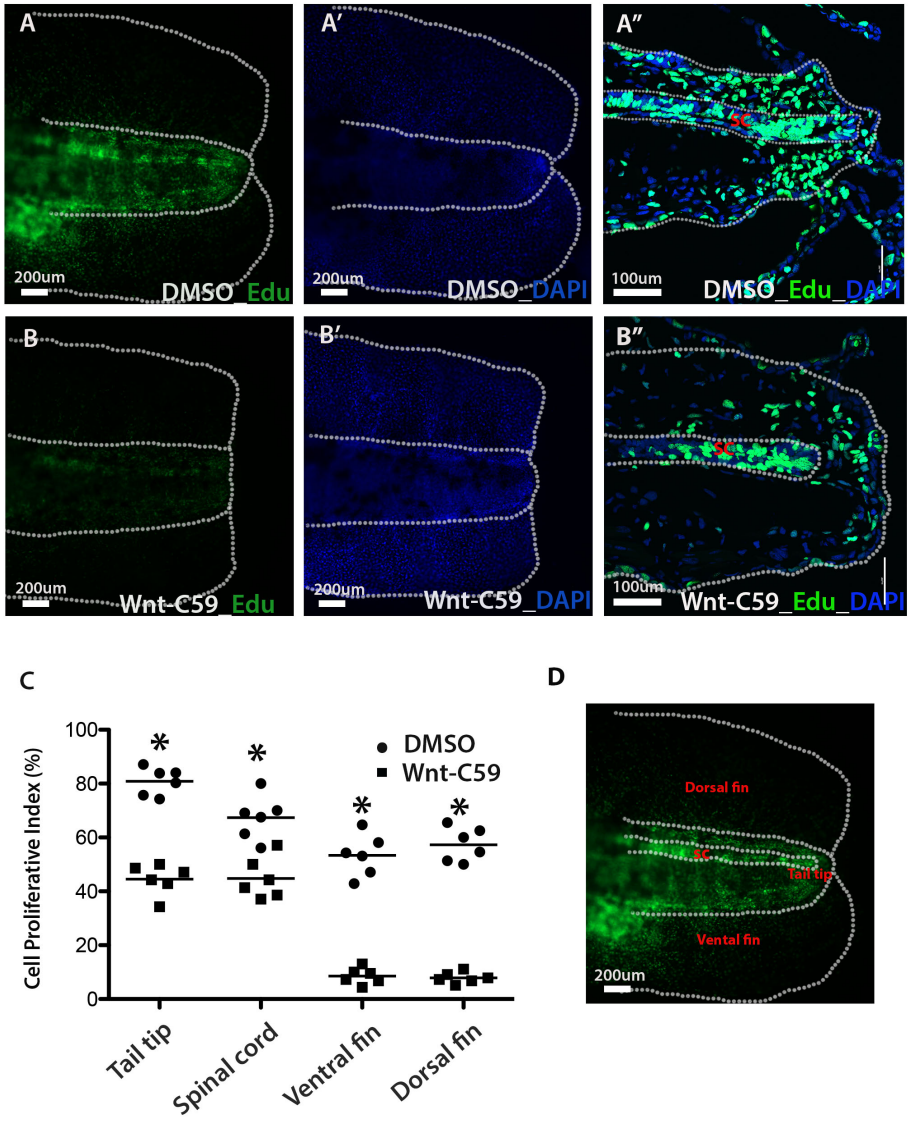

Figure 3.7 Wnt-C59 reduces cell proliferation. Images A" and B" are cryo-sections of regenerating tails. All other images are the whole-mount and regenerating tails. A) DMSO control stained for EdU. A') DMSO control stained with DAPI. A'') DMSO control stained for EdU. B) Tail treated with Wnt-C59 and stained for EdU. B') Tail treated with Wnt-C59 and stained with DAPI. B'') Tail treated with Wnt-C59 and stained for EdU. C) Wnt-C59 significantly reduced cell proliferation. The proliferation index for the tail tip and spinal cord was determined from cryo-sections. For dorsal and ventral fin, proliferating cells were counted in whole-mount samples. *: p-value < 0.001 for contrasts of DMSO control vs Wnt-C59.

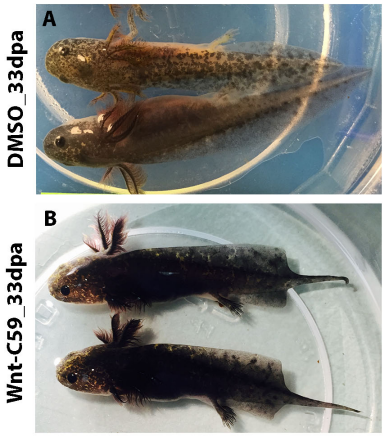

Figure 3.8 Wnt-C59 blocks dorsal and ventral fin regeneration and forelimb outgrowth permanently. A) DMSO control with a fully regenerated tail at 33dpa. B) Amputated tail treated with Wnt-C59 for 7 days and reared to 33 days post tail amputation. The tail fins were not regenerated and no forelimb was observed.

3.5 Discussion

Wnt signaling pathway is required throughout axolotl tail regeneration.

Wnt signaling is required for many different aspects of tissue regeneration (Kawakami et al. 2006; Ghosh et al. 2008; Shimokawa et al. 2013; Hamilton, Sun, and Henry 2016; Yokoyama et al. 2011; Sugiura et al. 2009; Lin and Slack 2008). The amputated tail is regenerated in 7 days. In this chapter, I blocked Wnt signaling by varying the time of Wnt-C59 application. I found that Wnt signaling was required from 0-120hpa, essentially the entirety of axolotl tail regeneration.

β-Catenin and Wnt3a expression during axolotl tail regeneration

β-Catenin is thought to be very important for tissue regeneration because β-Catenin induces limb regeneration in chick embryos that do not normally regenerate (Kawakami et al. 2006). β-Catenin is a dual function molecule that coordinates gene

transcription and also functions in cell-cell adhesion (Giarre, Semenov, and Brown 1998). Cytosolic pools of β-Catenin enter the nucleus and modulate the expression of specific genes that regulate cell cycle progression (Giarre, Semenov, and Brown 1998). The plasma membrane β-Catenin fraction acts as a component of cell-cell adhesion interactions that affect cell specification (Giarre, Semenov, and Brown 1998). It is thought that Wnt-induced β-Catenin conformational changes favor assembly of transcriptional complexes that are key regulators of cell cycle progression to S phase (Harris and Peifer 2005; Giarre, Semenov, and Brown 1998). Globally blocking Wnt signaling pathway by Wnt-C59 did not block β-Catenin expression; in contrast, it increased β-Catenin expression at 48 and 72hpa. It has been shown that Wolffian lens regeneration in newt requires Wnt/β-Catenin signaling (Hayashi et al. 2006), but Hamilton et al (2016) found that activation of Wnt signaling impairs cornea-lens regeneration which requires suppression of Wnt/β-Catenin signaling. These findings suggest that the requirement for Wnt/β-Catenin signaling depends on tissue type and mode of regeneration.

I found that tail amputation decreased β-Catenin expression at 24hpa and 48hpa and increased β-Catenin at 72hpa. This suggests that β-Catenin levels are dynamically regulated during axolotl tail regeneration. This finding is consistent with a recent study that showed inhibition of tail regeneration using Wnt agonist II SKL, a compound thought to increase β-Catenin expression (Ponomareva et al. 2015). Moreover, Wnt agonist treatment before blastema formation inhibited Xenopus limb regeneration through inhibiting innervation, while treatment after blastema formation caused disorganization of skeletal features (Wischin et al. 2017). Amputated limbs treated with Wnt agonist at the onset of Xenopus limb regeneration did not form a

blastema (Wischin et al. 2017). It is also supported by similar findings in studies of Xenopus forelimb regeneration, where down-regulation of Wnt/β-Catenin signaling did not prevent limb regeneration (Yokoyama et al. 2011; Hamilton, Sun, and Henry 2016). Furthermore, I found that Wnt3a was decreased at 24 and 72hpa, which further supports the idea that β-Catenin levels dynamically change upon tail amputation, and these changes are essential for successful tail regeneration.

Upregulation of β-Catenin is associated with upregulation of Erk and Akt signaling in Wnt-C59 treated tails.

In this study, I found that p-Erk and p-Akt were down-regulated at 24hpa but increased at 72hpa in regenerating tails. P-Erk levels were up-regulated by Wnt-C59 at 24, 48 and 72hpa. P-Akt levels were upregulated by Wnt-C59 at 48 and 72hpa. High β-Catenin levels associated with high p-Akt and p-Erk levels in Wnt-C59 treated tails. Wnt signaling is known to affect Erk and/or Akt signaling in other models (Zhang, Pizzute, and Pei 2014). There is a positive feedback loop between Wnt and Erk pathways in which Erk activation upregulates β-Catenin through inactivation of Gsk-3β, and β-Catenin activates Raf1 through unknown mechanisms to activate Erk (Ding et al. 2005; Kim et al. 2007; Georgopoulos, Kirkwood, and Southgate 2014). While I observed similar changes in β-Catenin, p-Akt, and p-Erk, it remains to be shown how Wnt-C59-induced changes in the levels of these signaling molecules block axolotl tail regeneration.

Disruption of Wnt signaling differentially affects cell mitosis in proximal and distal regions of the tail.

Broadly blocking Wnt signaling by Wnt-C59 reduced both cell mitosis and cell proliferation within 400μm of the distal tail tip. Thus, Wnt-C59 may inhibit tail regeneration by blocking cell proliferation that is necessary to reform tissues, which suggests that Wnts act as mitogens to control cell proliferation in the tail tip during axolotl tail regeneration. Interestingly, while I found that Wnt-C59 affected cell proliferation in medial and tail fin tissues, only the tail fin was permanently inhibited after discontinuation of Wnt-C59 treatment. Thus, Wnt-C59 provides a valuable new tool for regenerative biology because it can be used to decouple regeneration processes and investigate tissue-level differences in the requirement for Wnt signaling. In the absence of Wnt signaling during regeneration, progenitor cells in the tail fin mesenchyme are seemingly depleted, perhaps through mechanisms of cell death, quiescence, or differentiation. This hypothesis awaits further study.

In summary, this study demonstrates the requirement of Wnt signaling during tail regeneration. Wnt inhibitor Wnt-C59 upregulated β-Catenin, p-Akt and p-Erk, and these changes were associated with a reduction in cell proliferation and mitosis of the regenerating tail tip. My findings suggest that temporal regulation of Wnt/β-Catenin is required for successful axolotl tail regeneration.

CHAPTER 4 FGF SIGNALING IS REQUIRED DURING AXOLOTL TAIL REGENERATION

Qingchao Qiu[1]

[1]Department of Neuroscience, University of Kentucky, Lexington, Kentucky

KEYWORDS: axolotl, regeneration, tail, Fgf, Erk, Akt

4.1 Abstract

Fgf signaling plays an essential role during amphibian appendage regeneration, but its function during axolotl embryo tail regeneration is unknown. Here I used an Fgf receptor inhibitor (BGJ398) to disrupt Fgf signaling during axolotl tail regeneration. Concentrations of BGJ398 above 1μM inhibited tail regeneration. By varying the time of delivery of BGJ398, I found that Fgf signaling is critical during the first 12 hours of tail regeneration. Inhibition of Fgf signaling affected multiple molecular and cellular level processes during tail regeneration, including phosphorylation of Erk and Akt, Wnt3a/β-Catenin signaling, cell proliferation, and cell mitosis. The effect of BGJ398 was reversible as embryos that were initially treated with BGJ398 and then washed out fully regenerated their tails. These results show that Fgf signaling is required for axolotl tail regeneration.

4.2 Introduction

An axolotl embryo tail regeneration model was recently established to investigate signaling pathway mechanisms associated with tissue regeneration. Ponomareva et al. (2015) showed a requirement for Fgf signaling during tail regeneration by blocking Fgf-receptor function with a small molecule (BGJ398). Also, in that study, chemical inhibition of Wnt-ligand secretion using Wnt-C59 decreased transcription of fibroblast growth factor 9 (*Fgf9*). These results suggest that Fgf signaling is

downstream of Wnt signaling, as has been reported in other tissue regeneration models (Lin and Slack 2008; Love et al. 2013). In this chapter, I describe experiments that were performed to more rigorously establish that Fgf signaling is required for tail regeneration.

Fgf signaling pathway plays roles in cell proliferation, mitogenesis, differentiation, angiogenesis, and embryogenesis (Ornitz and Marie 2015). There are 22 Fgf ligands grouped into seven subfamilies and four Fgf receptors (Fgfrs) in vertebrates (Dorey and Amaya 2010). Fgf signaling is initiated by binding of Fgf ligands to Fgfrs. A ligand-dependent dimerization event leads to the formation of a complex consisting of two Fgfs, two heparin sulfate chains, and two Fgfrs (Plotnikov et al. 1999). Each ligand binds to two receptors contacted with each other via a D2 domain, which results in the trans-phosphorylation of each receptor monomer (Schlessinger 2000). Upon the binding of Fgf ligands to receptors, the tyrosine residues on the docking protein Frs2-alpha are phosphorylated (Hadari et al. 2001). Two downstream pathways associated with Fgf signaling pathway are the Ras/Map kinase pathway and the PI3/Akt pathway (Armstrong et al. 2006). The Ras/Map kinase pathway is associated with many biological processes, including cellular proliferation and differentiation (Shapiro 2002). Map kinase effectors include Erk, c-Jun N-terminal kinase (Jnk), and p38 mitogen-activated kinase (Cargnello and Roux 2011). The PI3k/Akt pathway is also associated with many biological processes, including cell survival and cell fate determination (Yu and Cui 2016).

Several Fgf ligands have been shown to play key roles in tissue regeneration. Fgf signaling factors are considered neurotrophic factors because they are expressed in

nerve tissue during axolotl limb regeneration and promote blastema formation and outgrowth (Mullen et al. 1996; Satoh et al. 2011). Fgf8 is expressed in the basal layer of the AEC during blastema formation, and Fgf8 and Fgf10 are upregulated in underlying mesenchymal cells. Fgf8 is expressed in the anterior mesenchyme and its expression depends on sonic Hedgehog (Shh) signaling from posterior tissue during axolotl limb regeneration. Ectopic Fgf8 and endogenous Hh signaling are sufficient to induce axolotl limb regeneration from cells of a posterior blastema (Nacu et al. 2016). Consistent with the idea that Fgfs are neurotrophic factors, denervation of the limb prevents Fgf8 and Fgf10 upregulation during axolotl limb regeneration (Kolodziej et al. 2001; Han et al. 2001). Fgf2 and Fgf8, together with growth and differentiation factor-5 (Gdf5), are sufficient to substitute nerve induction of limb and tail regeneration in urodele amphibians (Makanae et al. 2013).

In this study, I examined Fgf signaling pathway components during axolotl tail regeneration. Disruption of Fgf signaling by BGJ398 inhibited tail regeneration. Interestingly, BGJ398 treatment upregulated both Wnt3a and β-Catenin. Under the assumption that Fgf signaling is regulated by Wnt signaling, this suggests that Fgf signaling activity regulates Wnt ligand expression. BGJ398 treatment also downregulated Erk signaling, upregulated Akt signaling, and reduced cell proliferation and mitosis.

4.3 Methods

4.3.1 Regeneration experiments

Axolotl embryos were reared at 16°C in 40% Holtfreter's solution. Embryos at developmental stage 42 (Bordzilovskaya & Dettlaff, 1989) were used for all the tail

regeneration experiments (Ponomareva et al. 2015). BGJ398 (Selleckchem, Cat. #S2183) was dissolved in DMSO to make a 10mM stock solution and then diluted further to make 10μM working solutions. DMSO at 0.1% was used for controls. Axolotl embryos were dechorionated and anesthetized in 0.02% benzocaine, and 2mm of the distal tail tip was amputated using a sterile blade. Embryos were reared singly, one per well, in 12-well microtiter plates for the timing experiments and immunofluorescence (IF) staining. Five embryos were reared per well for tissue collection to perform Western blotting experiments. There were 7 groups in the timing experiment: 0.1% DMSO control, and 10μM Wnt-C59 administered from 0-12, 12-24, 24-48, 48-72, 72-120, and 120-144hpa. The embryos were photographed at different post-amputation times. Tail length and snout-vent length were measured from the images. Statistical analyses were performed using GraphPad Prism software version 6.0 using Student's t-test.

4.3.2 Antibodies

Anti-Erk (Cat. #4348), Anti-phospho-Erk (Thr202/Tyr204) (Cat. #4370), Anti-Akt (Cat. #9272), Anti-phospho-Akt (Ser473) (Cat. #9271), and Anti-β-Catenin (Cat. # 610154) were purchased from BD Biosciences. Anti-Wnt3a (Cat. # bs-1700R) was obtained from Bioss Antibodies. Anti-β-actin (Cat. #5125S) was purchased from Cell Signaling Technology. Anti-phospho-Histone H3 (Ser10) (Cat. # 05-1336) was purchased from Millipore. Goat anti-Rabbit IgG, (H+L) HRP conjugate (Cat. # AP307P) and Goat anti-Mouse IgG, (H+L) HRP-conjugated secondary antibodies (Cat. #AP308P) were purchased from Millipore. Cy3™ AffiniPure Donkey Anti-Mouse IgG (H+L) (Cat. #715-165-151) was purchased from Jackson Immune

Research. DAPI (4', 6-diamidino-2-phenylindole, dihydrochloride, Cat. #62247) was purchased from Thermo Scientific.

4.3.3 Tissue processing and immunochemistry staining

An existing protocol was modified for cryosection immunostaining (Qiu et al. 2015). In brief, samples were fixed in 4% paraformaldehyde (PFA) overnight. Samples were dehydrated through a methanol series, starting in 100% PBS and then 25, 50, 75, and 100% methanol. These samples were saved at -20ºC for later use. The samples were rehydrated for whole-mount staining or OCT embedding. After OCT embedding, 8μM sections were prepared for staining or saved at -80°C for later use. Primary Anti-phospho-Histone H3 (Ser10) was used at 1:1000, and the secondary Cy3™ AffiniPure Donkey Anti-Mouse IgG (H+L) was used at 1:200. Blocking solution was modified as 5% sheep serum. Total DNA was labeled by DAPI. Stained slides were imaged using a confocal microscope (Nikon Tie and C2+ Confocal). A mitotic index was determined by dividing the number of histone H3 positive cells by the number of DAPI positive cells within 200μm. Statistical analysis was performed using GraphPad Prism software version 6.0 using Student's t-test.

4.3.4 Western blotting

Embryos were anesthetized with 0.02% benzocaine and then 1mm of the distal tail tip was cut using a sterile blade. Tail tips of 30 embryos were pooled for each sample. The pooled tail tips were washed 2x using 1x PBS solution with proteinase/phosphatase inhibitor mixture (#5872S, Cell Signaling Technology), and then tissue was lysed in RIPA buffer (#R0278, Sigma) with proteinase/phosphatase inhibitor mixture by using a 22.5-gauge-needle and 1 ml syringe. Protein

concentrations were determined by a BCA protein assay (#23225, Thermo Scientific). Equal amounts of tissue lysate were loaded into lanes of 10% SDS polyacrylamide gels and transferred to a PVDF membrane. The membranes were blotted with 5% non-fat milk and then incubated overnight at 4°C with primary antibodies. After this, membranes were treated with HRP-conjugated secondary antibodies. The immune complexes were detected by enhanced chemiluminescence (Cat# NEL103001, PerkinElmer). Quantification of band intensities was performed using ImageJ software (http://rsbweb.nih.gov/ij/). Statistical analyses were performed using GraphPad Prism software version 6.0 using Student's t-test.

4.3.5 EdU cell proliferation assay

An EdU cell proliferation assay was performed using FAM picolyl azide from Click Chemistry Tools (Cat. # 1180-1), along with CuSO4 and sodium ascorbate in the Click-iT™ EdU Alexa Fluor™ 488 Imaging Kit from Invitrogen (Cat. # C-10337). The protocol was modified for whole-mount staining and cryo-sections at 8µm. Briefly, axolotl embryos were tail amputated and placed in 12-well-plates with 0.1% DMSO or 10µM BGJ398 solution. At 48hpa, embryos were injected peritoneally with 1ul of 8µM 5-ethynyl-2'-deoxyuridine (EdU). At 72hpa, embryos were anesthetized with 0.02% benzocaine and fixed in 4% paraformaldehyde overnight. The samples were dehydrated and rehydrated using a methanol series (0, 25, 50, 75, 100% in PBS). The samples were washed 3x with 1% Triton for 5 minutes, then bathed in 2.5% trypsin for 30 minutes, washed with ice-cold acetone for 10 minutes, followed by PBS and 1% Triton 3x for 5 minutes. Click-iT EdU reaction solution containing 1x Tris-buffered saline, 4mM CuSO4, FAM 488 picolyl azide, and 100mM sodium ascorbate was used to visualize EdU incorporation into the DNA of proliferating cells. DAPI

was used to counter stain the samples. Cells staining positive for EdU within 400μm of the tail tip were counted as well as cells staining positive for DAPI within the same area. A proliferative index was calculated as the ratio of EdU positive cells to DAPI positive cells. Results were analyzed in GraphPad Prism software version 6.0 (San Diego California USA) using one-way ANOVA.

4.4 Results

4.4.1 Blocking Fgf signaling inhibits axolotl embryo tail regeneration.

BGJ398, a potent inhibitor of Fgf signaling, was previously shown to inhibit axolotl tail regeneration in a chemical genetic screen (Ponomareva et al. 2015). Here I more rigorously investigated timing and dosage of BGJ398 during axolotl tail regeneration. Concentrations of BGJ398 at 0, 10^{-4}, 10^{-3}, 10^{-2}, 10^{-1}, 1, 2.5, 5, and 10μM were used to treat developmental stage 42 axolotl embryos. The treated embryos were healthy and active within all treatment groups. Concentrations of BGJ398 above 1μM significantly inhibited tail regeneration at 7 days post tail amputation (dpa). By varying the time of BGJ398 administration, I detected a significant difference in tail length at 7dpa for the 0-12hpa treatment group compared with DMSO controls. Interestingly, I observed cup-shaped tails that folded anteriorly in 1, 2.5, and 5μM BGJ398 treated tails, a phenotype described by Voss et al. (2019) (Figure 4.1 A). These results establish that Fgf signaling is required for tail regeneration and the critical time for Fgf signaling is 0-12hpa.

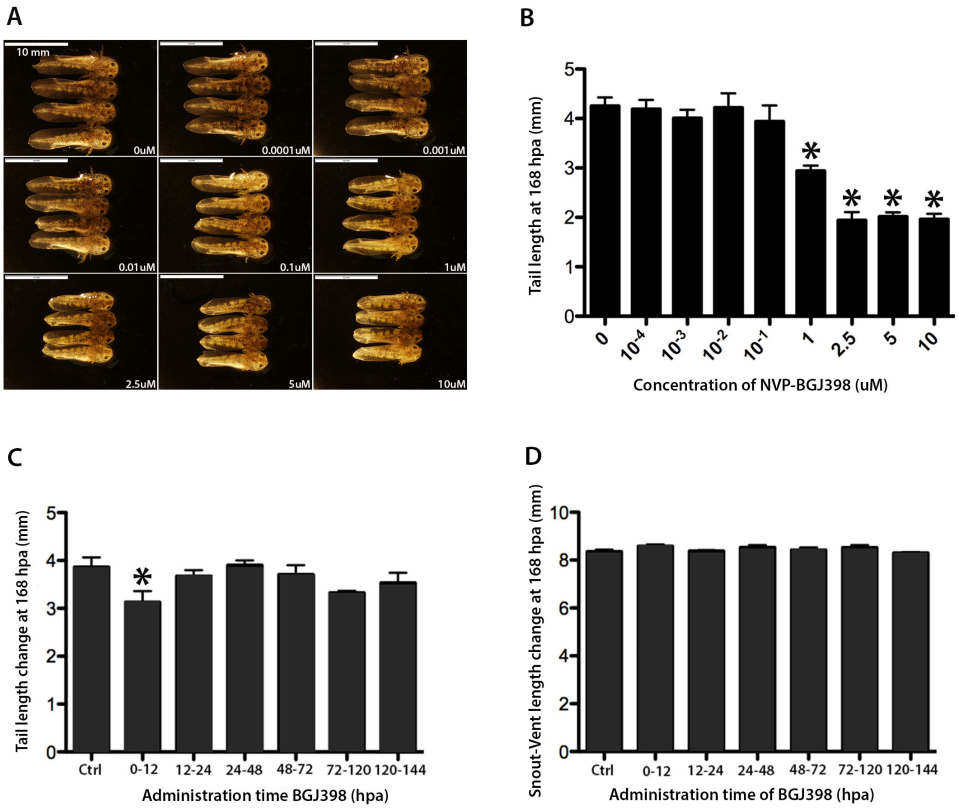

Figure 4.1 Blocking Fgf receptors prevents axolotl embryo tail regeneration. A) and B) BGJ398 above 1μM significantly inhibited axolotl embryo tail regeneration. C) 10μM of BGJ398 was administered for different periods, and the tail length was measured. Tail length at 7dpa differed significantly between DMSO control and the 0-12hpa BGJ398 treatment. D) No significant difference in snout-vent length was detected between BGJ398 treated and DMSO control embryos. *: p-value < 0.05 for contrasts of DMSO control vs Wnt-C59.

4.4.2 BGJ398 downregulates phosphorylation of Erk.

Upon Fgf ligand binding, Fgfr activates downstream signaling cascades, including the Mapk/Erk signaling pathway (Mukerjee 1947). To determine if Fgf/Erk signaling is activated during axolotl tail regeneration, I quantified phosphorylated Erk (p-Erk) expression by Western blotting. In DMSO control embryos, p-Erk was detected at the

time of amputation and increased at 24hpa (Figure 4.2, *p*-value < 0.001, n = 3). After this time, p-Erk levels at 48hpa (Figure 4.2, *p*-value < 0.05, n = 3), but not 72hpa (Figure 4.2, *p*-value > 0.05, n = 3), were significantly higher than basal (day0) levels. A similar pattern of expression was observed for embryos treated with continuous BGJ398 treatment. However, the spike in p-Erk at 24hpa was significantly lower than that observed in controls (Figure 4.2, *p*-value < 0.01, n = 3). These results show that inhibition of Fgf signaling reduces p-Erk at 24hpa.

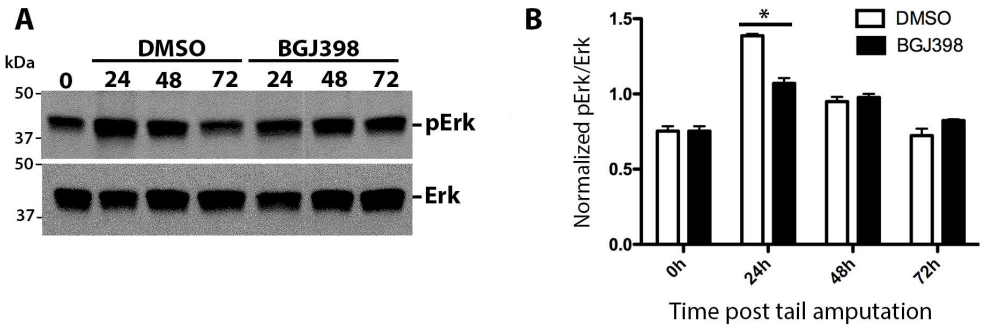

Figure 4.2 BGJ398 decreases phosphorylation of Erk at 24hpa. A) P-Erk and Erk were detected by Western blotting using pooled 1mm tail tips from BGJ398 treated or DMSO control embryos at 0, 24, 48, and 72hpa. B) P-Erk expression was normalized against Erk. *: *p*-value < 0.01 for contrast of DMSO control vs BGJ398.

4.4.3 BGJ398 upregulates phosphorylation of Akt.

Activated Fgf receptors also regulate the Akt pathway, which promotes cell survival and growth (Yu and Cui 2016). To determine if Fgf/Akt signaling is activated during axolotl tail regeneration, I quantified phosphorylated Akt (p-Akt) expression. In DMSO control embryos, p-Akt was detected at the time of amputation and decreased at 24hpa (Figure 4.3, *p* = 0.053, n = 3). Between 24-48hpa, p-Akt levels increased, roughly approximating basal levels. After this time, levels decreased at 72hpa. This

complex temporal pattern was also observed in embryos treated continuously with BGJ398. However, p-Akt levels were significantly higher in BGJ398 treated embryos than controls at 48hpa and 72hpa (Figure 4.3, *p*-value < 0.05, n = 3). These results show that Akt phosphorylation is dynamically regulated during tail regeneration and inhibition of Fgf signaling increases p-Akt at 48 and 72hpa.

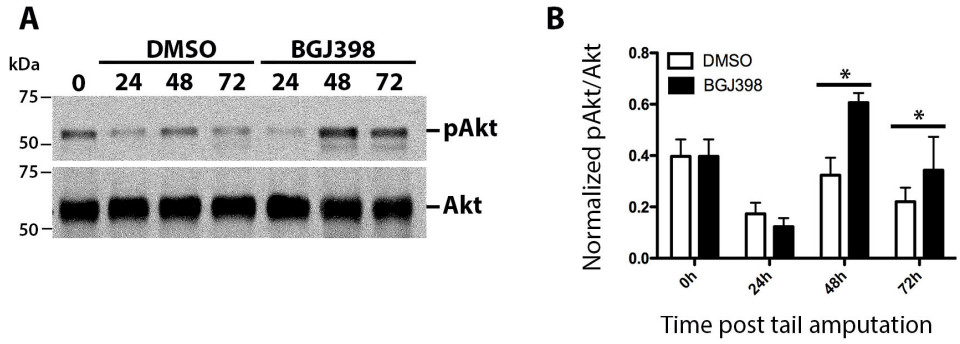

Figure 4.3 BGJ398 downregulates phosphorylation of Akt. A) P-Akt and Akt were detected by Western blotting using pooled 1mm tail tips from BGJ398 treated or DMSO control embryos at 0, 24, 48, and 72hpa. B) P-Akt expressions were normalized against Akt. *: *p*-value < 0.05 for contrast of DMSO control vs BGJ398.

4.4.4 BGJ398 upregulates Wnt/β-Catenin signaling.

The Wnt/β-Catenin and Fgf signaling pathways are required for zebrafish fin regeneration and Xenopus limb regeneration, and in both cases, Wnt/β-Catenin signaling acts upstream of Fgf signaling (Poss et al. 2000; Yokoyama et al. 2007; Stoick-Cooper et al. 2007). To test if Fgf signaling affects Wnt/β-Catenin signaling during tail regeneration, Wnt3a and β-Catenin were detected by western blotting. Wnt3a was detected at the time of tail amputation, decreased at 24hpa, and approximated basal (day0) levels at 48 and 72hpa (Figure 4.6, *p*-value < 0.05, n = 3). β-Catenin was also expressed at the time of tail amputation and increased at 72hpa

(Figure 4.6, *p*-value < 0.05, n = 3). Continuous BGJ398 treatment increased Wnt3a at 48 and 72hpa, and increased β-Catenin at 48hpa (Figure 4.6, *p*-value < 0.05, n = 3). These data show that BGJ398 inhibition of Fgf signaling increases the expression of Wnt ligands.

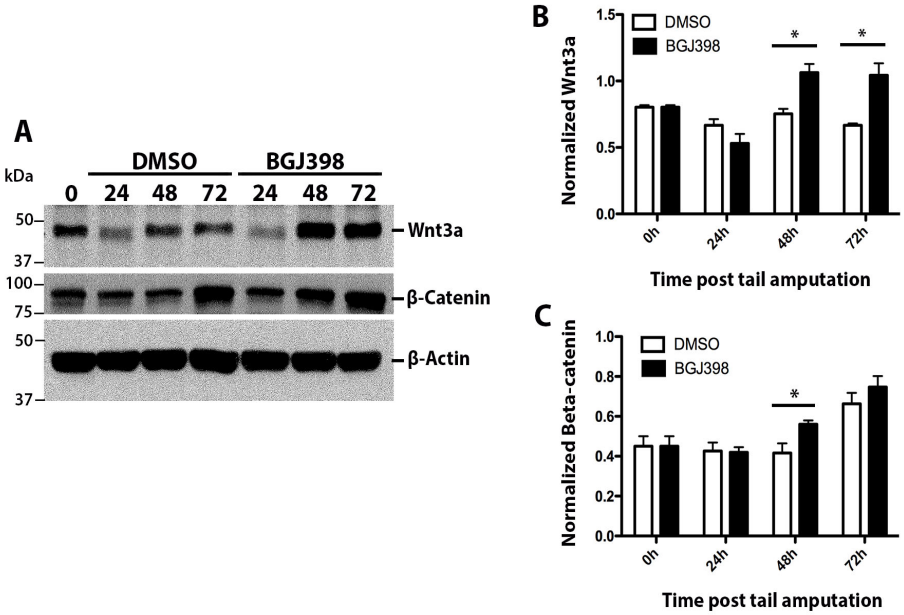

Figure 4.4 BGJ398 upregulates Wnt ligand expression. A) Wnt3a, β-Catenin, and β-Actin were detected by Western blotting using pooled 1mm tail tips from BGJ398 treated or DMSO control embryos at 0, 24, 48, and 72hpa. B) Wnt3a expression was normalized against total β-Actin. BGJ398 increased Wnt3a expression at 48hpa and 72hpa. B) β-Catenin expression was normalized against β-Actin. BGJ398 increased β-Catenin expression significantly at 48hpa. *: *p*-value < 0.05 for contrast of DMSO control vs BGJ398.

4.4.5 Fgf signaling regulates cell mitosis during axolotl tail regeneration.

Fgf signaling sustains progenitor cell mitogenic activity during zebrafish fin regeneration and muscle regeneration (Shibata et al. 2016; Saera-Vila, Kish, and Kahana 2016). To determine if Fgf signaling is similarly needed to sustain mitogenic

activity during axolotl tail regeneration, anti-phospho-histone H3 (Ser10) staining was performed to identify mitotic cells at 48hpa. Approximately twice (7.5± 1.5%) as many mitotic cells were observed in DMSO control versus BGJ398-treated embryos (Figure 4.5, $p < 0.05$, n = 3). These results suggest that Fgf signaling is required to sustain cell mitosis during axolotl tail regeneration.

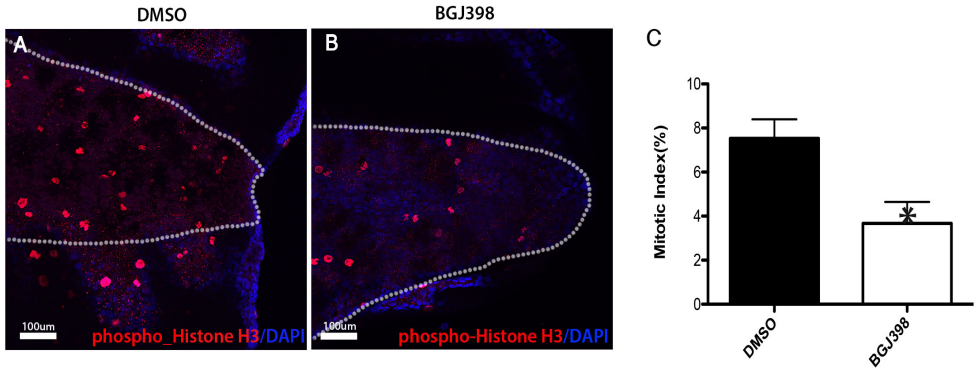

Figure 4.5 BGJ398 inhibits mitosis in axolotl tails at 48hpa. A) DMSO control tail stained with phospho-histone H3. The white stippled lines outlined the tail. The other tissues are fins. B) BGJ398 treated tail stained with phospho-histone H3. C) Graph comparing the mitotic index in DMSO control and BGJ398 treated tails (n = 3 embryos). *: p-value < 0.05 for contrast of DMSO control vs BGJ398.

4.4.6 BGJ398 reduces the number of cells in S-phase.

Fgf signaling is required for cell proliferation of blastema cells during zebrafish tail regeneration (Shibata et al. 2016). To determine if Fgf signaling regulates cell proliferation during axolotl tail regeneration, an EdU incorporation assay was used to detect S-phase cells at 72hpa. BGJ398 treatment reduced proliferating cells in the tail tips, dorsal fins, and ventral fins (Figure 4.6, $p < 0.001$, n = 6), but not the spinal cord (Figure 4.6, $p > 0.05$, n = 6). These results suggest that Fgf signaling regulates cell proliferation in the tail tip and fins during axolotl tail regeneration.

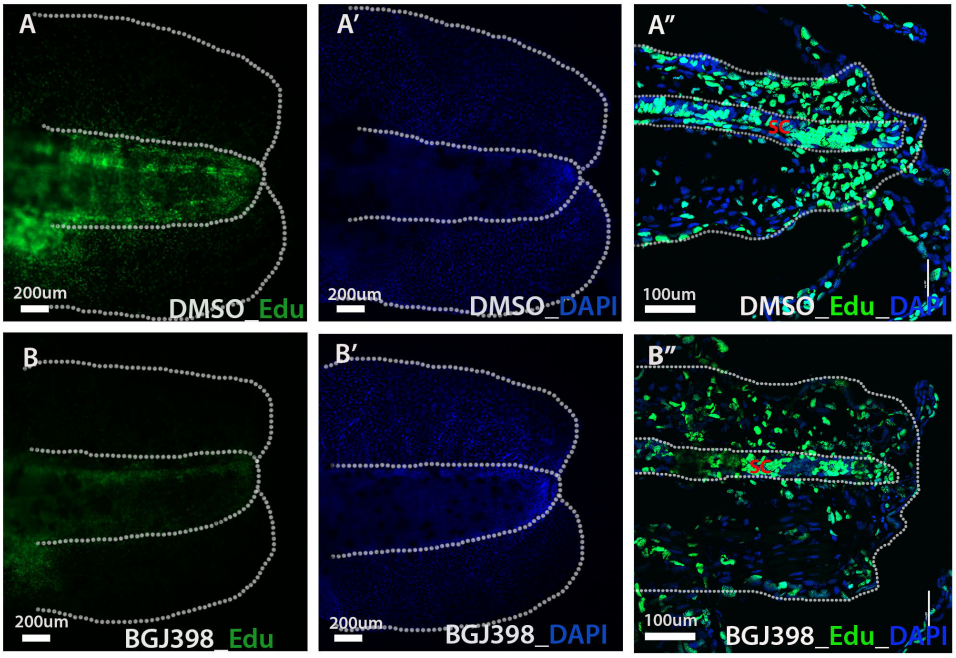
A
200um
DMSO_Edu
A′
200um
DMSO_DAPI
A″
SC
100um
DMSO_Edu_DAPI
B
200um
BGJ398_Edu
B′
200um
BGJ398_DAPI
B″
SC
100um
BGJ398_Edu_DAPI

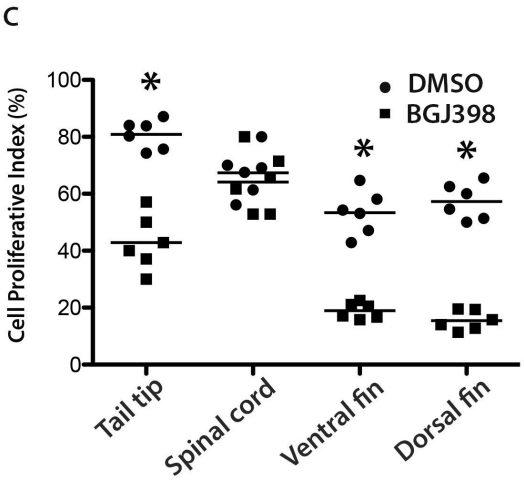
C
Cell Proliferative Index (%)
100
80
60
40
20
0
DMSO
BGJ398
Tail tip
Spinal cord
Ventral fin
Dorsal fin

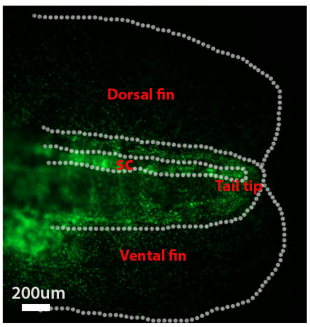
D
Dorsal fin
SC
Tail tip
Ventral fin
200um

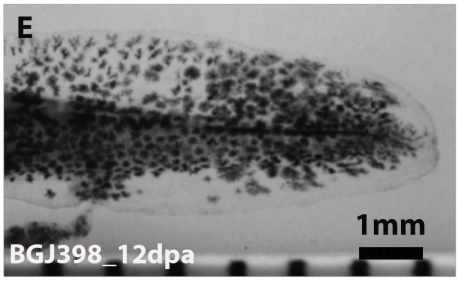
E
1mm
BGJ398_12dpa

Figure 4.6 BGJ398 reduces S-phase entry of cells in the tail but not the spinal cord. Image A'' and B'' are cryo-sections of regenerating tails. Images in panels C-D are whole-mounts. A) DMSO control stained with EdU A') DMSO control stained with DAPI A'') DMSO control stained with EdU and DAPI. B) Tail treated with BGJ398 and stained with EdU. B') Tail treated with BGJ398 and stained with DAPI. B'') Tail treated with BGJ398 and stained with EdU and DAPI. C) The proliferative index for tail tissues was estimated from counted cells in cryo-sections due to the thickness of the tail. For dorsal and ventral fins, cells were counted in whole-mount preparations. BGJ398 reduced cell proliferation of the tail except for the spinal cord. D) An image with labeled tissue types. E) Full tail regeneration at 12dpa of an embryo treated for 7 days with BGJ398. *: p-value < 0.05 for contrast of DMSO control vs BGJ398.

4.5 Discussion

The results in this chapter show that Fgf signaling pathway is required for axolotl tail regeneration. Embryos that were treated with BGJ398, a small molecule inhibitor of Fgf signaling did not regenerate their tail. In addition to blocking tail regeneration, BGJ398 reduced p-Erk levels at 24hpa and increased p-Akt at 48hpa and 72hpa. These pathways are known to regulate many biological processes, including cell division and growth, and embryos treated with BGJ398 presented fewer S-phase and mitotic phase cells, consistent with inhibition of cell proliferation.

Fgf signaling inhibitor BGJ398 acts during the first 12 hours of tail regeneration.

By varying the time that BGJ398 was administered to embryos, I identified a 12hr post-amputation window of time within which Fgf signaling is required for successful tail regeneration. This was an unexpected finding because Fgf signaling is thought to

be activated downstream of Wnt signaling, which is activated after this time. For example, I showed in Chapter 3 that Wnt ligands were not up-regulated until at least 48hpa, and in Ponamareva et al (2015), Wnt pathway target genes were not differentially expressed between Wnt-C59 treated and control axolotl embryos until 24 hpa. Thus, it seems likely that Fgf signaling is regulated independently of Wnt signaling, at least during the first 12 hours of regeneration. It is tempting to think that during this interval of time, Fgf signaling is required for proper formation of the wound epithelium, as is known for zebrafish fin regeneration (Whitehead et al. 2005). Studies of axolotl limb regeneration have shown that the basal layer of the wound epithelium, and underlying mesenchymal cells, secrete Fgf ligands that support progenitor cell proliferation (Mullen et al. 1996; Satoh et al. 2011). Perhaps, if the wound epithelium does not develop competence for Fgf ligand secretion during the first 12 hours of regeneration, activated progenitor cells are stalled in the cell cycle until the Fgf signaling block is released. After 12 hours, progenitor cell proliferation may no longer depend upon Fgf signaling. In other words, cells gain autonomy for cell proliferation after 12hpa, in much the same way that progenitor cells of regenerating limbs escape nerve-dependency at later stages of blastema maturation (Kumar et al. 2007; McCusker, Bryant, and Gardiner 2015). This hypothesis is consistent with the results of this study, including the reversibility of BGJ398 inhibition of Fgf signaling.

Erk and Akt signaling pathways during axolotl tail regeneration

In control embryos, Erk phosphorylation was significantly increased at 24hpa and high levels were sustained at 48hpa and 72hpa. BGJ398 treatment significantly decreased Erk phosphorylation at 24hpa. Erk phosphorylation is required for re-entry

of post-mitotic newt muscle cells by downregulation of P53 activity, while only transient Erk activation is observed in mammalian counterparts (Yun, Gates, and Brockes 2014). Although muscle de-differentiation and cell cycle entry do not occur in axolotls, differential changes in Erk signaling may be associated with cell cycle regulation. Indeed, fewer M-phase and S-phase cells were observed in BGJ398 treated embryos. Akt phosphorylation was decreased at 24hpa in DMSO control embryos and BGJ398 treatment increased Akt phosphorylation at 48 and 72hpa. Since the PI3k/Akt pathway plays a role in cell fate determination (Yu and Cui 2016), suppression of Akt phosphorylation during regeneration, as was observed in control embryos, may sustain progenitor cell proliferation. This hypothesis awaits further study.

BGJ398 upregulates Wnt/β-Catenin signaling pathway.

Inhibition of Fgf signaling by BGJ398 was associated with a significant increase in Wnt3a and β-Catenin expression at 48 and 72hpa. This suggests that regulation of Wnt/β-Catenin signaling may depend upon the activity state of the Fgf pathway. When Fgf signaling activity is dampened, β-Catenin mediated signaling increases to return Fgf signaling to basal levels under homeostatic conditions, or levels needed to support proliferating cells during tail regeneration. Such a model is consistent with the hierarchical regulation of Fgf signaling by canonical Wnt signaling during later phases of regeneration when cell proliferation and tail outgrowth are maximal. My results enrich this model by implicating a feedback mechanism between these two pathways. However, Fgfr1 antagonist SU-5402 decreased Wnt3a expression during Xenopus tail regeneration (Lin and Slack 2008). This may reflect a species-specific difference between axolotls and Xenopus, a difference in the action of Fgf inhibitors between studies, or a limitation of feed-back regulation to β-Catenin-mediated Wnt

signaling in Xenopus. Overall, my results suggest that Fgf and Wnt signaling pathways interact to regulate cell proliferation during axolotl tail regeneration.

CHAPTER 5 WNT SIGNALING IS REQUIRED FOR FORELIMB BUD DEVELOPMENT

Qingchao Qiu[1]

[1]Department of Neuroscience, University of Kentucky, Lexington, Kentucky

KEYWORDS: Wnt, Fgf, limb, axolotl, Wnt3a, Zo1

5.1 Abstract

Wnt signaling pathway and Fgf signaling pathway are key regulators of limb development in vertebrates such as chicken and mice. How Wnt and Fgf signaling pathways regulate forelimb bud outgrowth in the axolotl (*Ambystoma mexicanum*) is unknown. Here I demonstrate that Wnt signaling is required for forelimb bud development in the Mexican axolotl. Inhibiting Wnt signaling by Wnt-C59 prevented forelimb bud development. The critical window for inhibition was approximately developmental stage 40-42. Expression of canonical Wnt signaling ligand Wnt3a and cell polarity marker Zo1 were significantly decreased in epidermal cells of the forelimb bud in Wnt-C59 treated forelimbs. Moreover, Wnt-C59 treatment appeared to disrupt the orientation and density of mesodermal cells in the forelimb bud and significantly decreased mesodermal cell proliferation and mitosis. The results of this study indicate a requirement for Wnt signaling during forelimb bud development in the axolotl.

5.2 Introduction

Vertebrate limb development is a classic model for investigating patterning of three-dimensional structures during organ embryogenesis (Towers and Tickle 2009; Yang 2003). Three axes are used to characterize limb structure: a proximal-distal axis (P-D axis) runs along the arm from shoulder to digits; an anterior-posterior axis (A-P axis),

runs from the thumb to the little finger; and a dorsal-ventral axis (D-V axis), runs from the back of the hand to the palm. Three major signaling centers direct limb development along these axes. The first signaling center to appear during limb development is the apical ectodermal ridge (AER), which forms as a thickened epithelial cell layer at the distal part of the early limb bud. Fibroblast growth factors (Fgfs) in the AER are sufficient and necessary for AER function in proximal-distal limb outgrowth and patterning (Mariani, Ahn, and Martin 2008; Saunders 1998; Niswander and Martin 1993). The second signaling center is the zone of polarizing activity (ZPA). Sonic Hedgehog (Shh) signaling from the ZPA regulates anterior-posterior patterning (Ogura et al. 1996). The third signaling center is the non-AER limb ectoderm. The limb ectoderm produces molecules which are essential for dorsal (e.g., Wnt7a: (Riddle et al. 1995) and ventral (e.g., Engrailed-1: (Loomis et al. 1996) patterning. Signaling from the AER, ZPA, and limb ectoderm are crucial for the formation of a limb with correct axial polarity (Tickle 2015).

Several signaling pathways (such as the Wnt signaling pathway, Fgf signaling pathway, retinoid acid signaling pathway, and Bmp signaling pathway) and transcription factors (Tbx4, Tbx5, Pitx1, Nf-kappaB, Hoxb13, and Hoxc10) have been associated with limb patterning (Carlson et al. 2001; Bushdid et al. 1998; Kanegae et al. 1998; Grandel and Brand 2011; Kawakami et al. 2001; Christen et al. 2012; Duboc and Logan 2011). These signaling pathways must be tightly regulated spatially and temporally to ensure limb bud outgrowth. A hallmark of early vertebrate limb development is the limb bud. Limb bud outgrowth depends on signaling from the AER (Hamburger and Hamilton 1992). A regulatory loop consisting of Wnt factors Wnt3a, Wnt2b and Wnt8c, and fibroblast growth factors Fgf8 and Fgf10, play a key

role in both AER induction and limb bud outgrowth (Kawakami et al. 2001). Wnt3a is the earliest known AER marker during chick limb development. It signals through the canonical β-Catenin pathway and mediates Fgf10 to induce Fgf8 expression in the limb ectoderm during AER formation in the chick (Kengaku et al. 1998; Kawakami et al. 2001). It is thought that the limb bud is defined by a temporal succession of signaling events. For example, Christen et al. (2012) demonstrated that retinoic acid from somites specifies the limb field by activating Wnt ligands (*wnt2b* in forelimb and *wnt8c* in hindlimb) in the intermediate mesoderm, which is followed by the expression of *tbx5* and *tbx4* in the lateral plate mesoderm at positions where fore- and hind limb develop, respectively. Fgf10 signaling from the mesoderm to the overlaying ectoderm then induces the formation of the apical epidermal ridge, thereby establishing a signaling center for proximal-distal limb outgrowth (Christen et al. 2012). These data suggest that Wnt signaling plays an essential during early limb development.

The “proliferation gradient” model has been the most prominent hypothesis of physical morphogenesis of limb bud outgrowth, first proposed by Ede and Law (Ede and Law 1969). They proposed that a mitogen released by the AER signals underlying mesodermal cells to proliferate and form a P-D progress or proliferation zone (Reiter and Solursh 1982). There is another hypothesis explaining limb bud morphogenesis: oriented cell divisions, which has been found during limb bud extension (Wyngaarden et al. 2010). To achieve uniform polarity, mesodermal cells of the limb bud must employ a mechanism establishing and coordinating polarized cell behaviors along their developmental axes (Gao and Yang 2013). Wnt5a signaling gradients establish

planar cell polarity in chondrocytes along the P-D axis via Vangl2 phosphorylation (Gao and Yang 2013).

Although many studies have shown the importance of Wnt signaling during vertebrate limb development, little is known about Wnt signaling during forelimb bud development in the axolotl. In this study, a Porcupine inhibitor, Wnt-C59, was used to show a requirement for Wnt signaling during forelimb bud development in the axolotl.

5.3 Methods

5.3.1 Animal husbandry and timing experiments for limb bud outgrowth.

Axolotl embryos were reared at 16°C in 40% Holtfreter's solution. Embryos at developmental stage 40 (Bordzilovskaya & Dettlaff, 1989) were used for all experiments. Wnt-C59 (Selleckchem, Cat. #S7030) was dissolved in DMSO to make a 10mM as stock solution and then diluted further to make 10μM working solutions (DaCosta Byfield et al. 2004). NVP-BGJ398 (Selleckchem, Cat. #S2183) was dissolved in DMSO at 10mM and then diluted to 10μM for regeneration experiments (Denis et al. 2016). DMSO at 0.1% was used as a control. Axolotl embryos were dechorionated one day before the embryos reached developmental stage 40. In the timing experiment for limb bud outgrowth, a total of 155 axolotls were divided into 30 treatment groups plus one 0.1% DMSO control group. Each Wnt-C59 treated group was treated for three days, thus providing an overlapping series of treatments throughout the time course of forelimb development (Figure 5.1). The axolotls were anesthetized in 0.02% benzocaine and photographed 33 days after developmental stage 40. A few controls and Wnt-C59 treated animals (Day1-3 treatment group) were

reared to approximately one year of age. At this time, they were anesthetized and then photographed. Three aurora kinase inhibitors, CYC116, MK-5108, and Danusertib at 10mM in DMSO solution were obtained from Dr. Jon Thorson's Lab and were diluted further to make 10μM working solutions. The stage 40 embryos were treated separately with the three aurora kinase inhibitors for 7 days, and then washed out and reared for another 7 days, at which time they were photographed.

5.3.2 Antibodies

Rabbit anti-Wnt3a antibodies were obtained from bioss (Cat. # bs-1700R). Rabbit anti-Zo1 (Cat. #61-7300) was purchased from Invitrogen. Anti-phospho-Histone H3 (Ser10) (Cat. # 05-1336) was purchased from Millipore. Cy3™ AffiniPure Donkey Anti-Mouse IgG (H+L) (Cat. #715-165-151) was purchased from Jackson immune Research. DAPI (4', 6-diamidino-2-phenylindole, dihydrochloride, Cat. #62247) was purchased from Thermo Scientific.

5.3.3 H& E staining and immunochemistry staining

An existing protocol was modified for immunostaining (Qiu et al. 2015). In brief, samples were fixed in 4% paraformaldehyde (PFA) overnight. Samples were dehydrated through a methanol series, starting in 100% PBS and move up through 25, 50, 75, and 100% methanol. These samples were used freshly or saved at -20ºC for later use. Samples were rehydrated for whole-mount staining or OCT embedding. After OCT embedding, 8μM sections were prepared at D-V/P-D plane or A-P/P-D plane of forelimb bud for staining or saving at -80°C for later use. For H&E staining, sections were stained using filtered hematoxylin (VWR, # 95057-844) and 0.5% Eosin and mounted with Permount (Fisher Chemical, #. SP15-100). For

immunochemistry staining, epitope retrieval was done by heating in 10mM Tris-HCl solution (pH 9.5) on a hot plate. Primary Anti-phospho-Histone H3 (Ser10) antibodies were used at 1:1000. Anti-Zo1 and anti-Wnt3a antibodies were used at 1:100. The secondary Cy3™ AffiniPure Donkey Anti-Mouse IgG (H+L) antibodies were used at 1:200. Blocking solution was modified into 5% sheep serum. Total DNA was labeled by DAPI. Stained slides were imaged using a confocal microscope (Nikon Tie and C2+ Confocal). A mitotic index was determined by dividing the number of histone H3 positive mesodermal cells by the number of DAPI positive mesodermal cells within the limb bud. Results were analyzed in GraphPad Prism software version 6.0 using Student's t-test.

5.3.4 EdU cell proliferation assay

An EdU cell proliferation assay was performed using FAM Picolyl Azide from Click Chemistry tools (Cat. # 1180-1), and CuSO4 and Sodium Ascorbate in the Click-iT™ Edu Alexa Fluor™ 488 Imaging Kit (Invitrogen, Cat. # C-10337). The protocol was modified for whole-mount 5-ethynyl-2'-deoxyuridine (EdU) staining or cryo-section staining. Briefly, axolotl embryos were placed in 12-well-plates with 0.1% DMSO (control) or 10μM Wnt-C59. At 24 hours post-treatment, embryos were injected peritoneally with 1ul of 8μM EdU. At 72 hours post-treatment, embryos were anesthetized with 0.02% benzocaine and fixed in 4% paraformaldehyde overnight. The samples were dehydrated and rehydrated using a methanol series (0, 25, 50, 75, and 100% in PBS). The samples were washed 3x with PBS with 1% Triton for 5 minutes, then bathed in 2.5% trypsin for 30 minutes, washed 3x with PBS with 1% Triton for 5 minutes, and finally washed with ice-cold acetone for 10 minutes. Click-iT EdU reaction solution containing 1x Tris-buffered saline, 4mM CuSO4, FAM 488

picolyl azide, and 100mM sodium ascorbate was used to visualize EdU incorporation into the DNA of proliferating cells. DAPI was used to counter stain the samples. Cells staining positive for EdU within 400μm of the tail tip were counted as well as cells staining positive for DAPI within the same area. A proliferative index was calculated as the ratio of EdU positive cells over DAPI positive cells. For cryo-section staining, trypsinization and the ice-cold acetone wash were skipped. Results were analyzed in GraphPad Prism software version 6.0 using one-way ANOVA.

5.3.5 Cell orientation and cell density measurements.

Cell orientation was measured using two-dimensional confocal imaging of fixed tissue. The orientation of DAPI-stained nuclei of mesodermal cells was determined relative to the forelimb bud epidermis. This was quantified as an angle by drawing a line through the longitudinal axis of each nucleus and relating this line to a line drawn parallel to the forelimb bud epidermis. There are several caveats of this approach for determining cell orientation, and thus the results should be considered as preliminary pending *in vivo* imaging using intracellular landmarks to determine the polarity of cells and transgenes that reveal cell membranes (Wyngaarden et al. 2010). Cells with nuclear angles were arbitrarily binned into 0-30, 30-60, or 60 to 90 degrees categories, for DMSO treated and Wnt-C59 treated embryos. Three progress zones were also arbitrarily defined to delineate proximal, middle, and distal regions of the forelimb bud. Cell numbers per 2500 μm^2 were counted in each progress zone. Results were analyzed in GraphPad Prism software version 6.0 using one-way ANOVA.

5.4 Results

5.4.1 Wnt signaling is required around developmental stage 40 for axolotl forelimb bud development.

The axolotl tail amputation assay was previously performed during the time that embryos initiate forelimb development from developmental stage 40 to stage 44. I anecdotally observed that Wnt-C59 treatment inhibited forelimb bud outgrowth. I confirmed these observations by treating developmental stage 40 embryos with Wnt-C59 or DMSO as controls, with eight embryos in each group. At stage 51, all eight control embryos presented limbs that were in the process of digit formation. A deep interdigital notch was observed between digits II and III, and a small indentation separated digits I and II. In comparison, Wnt-C59 embryos did not form forelimbs; representative images are shown in Figure 5.2 A and B. To determine if there is a critical window within which Wnt-C59 blocks forelimb development, I varied the time of dosing (Figure 5.1). Developmental stage 40 embryos that were treated with Wnt-C59 for the first three days of the experiment did not form forelimbs; this treatment also decreased the size of hindlimbs (Figure 5.2). All other treatment groups had well-developed forelimbs and hindlimbs. These results show that Wnt signaling is required at developmental stage 40 for axolotl forelimb development.

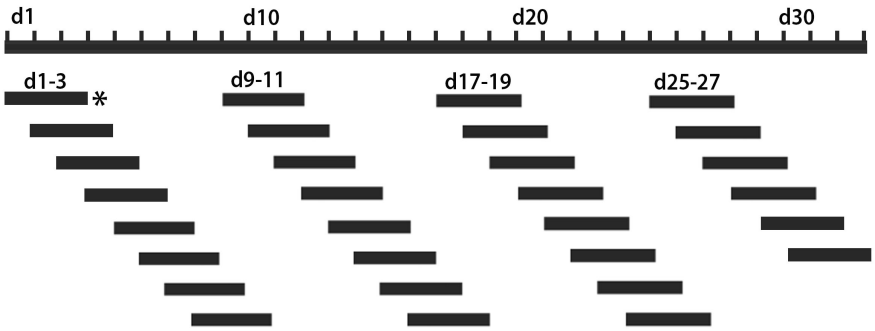

Figure 5.1. Wnt signaling is required at developmental stage 40 for axolotl forelimb development. A total of 155 embryos at stage 40 were used. Each group had five animals. There were 30 treatment groups, and each of these groups was treated with 10μM Wnt-C59 for three days with an overlapping series of treatments throughout the time course of forelimb development. There was one control group treated with 0.1% DMSO at day 1 to day 3. Only a narrow window from day 1 to day three was associated with Wnt-C59 inhibition of forelimb development.

5.4.2 Long-term phenotype of the Wnt-C59 treated animals

I treated developmental stage 40 embryos with 0.1% DMSO or Wnt-C59 for three days and then reared the embryos to 1 year of age (Figure 5.2 C). Hindlimbs of embryos with continuous Wnt-C59 treatment from Day1-3 were significantly smaller and shorter than those of the controls (Figure 5.2 C-E, $n=6$, $p < 0.01$). These results show that Wnt-C59 prevents forelimb development and decreases the size of hindlimbs.

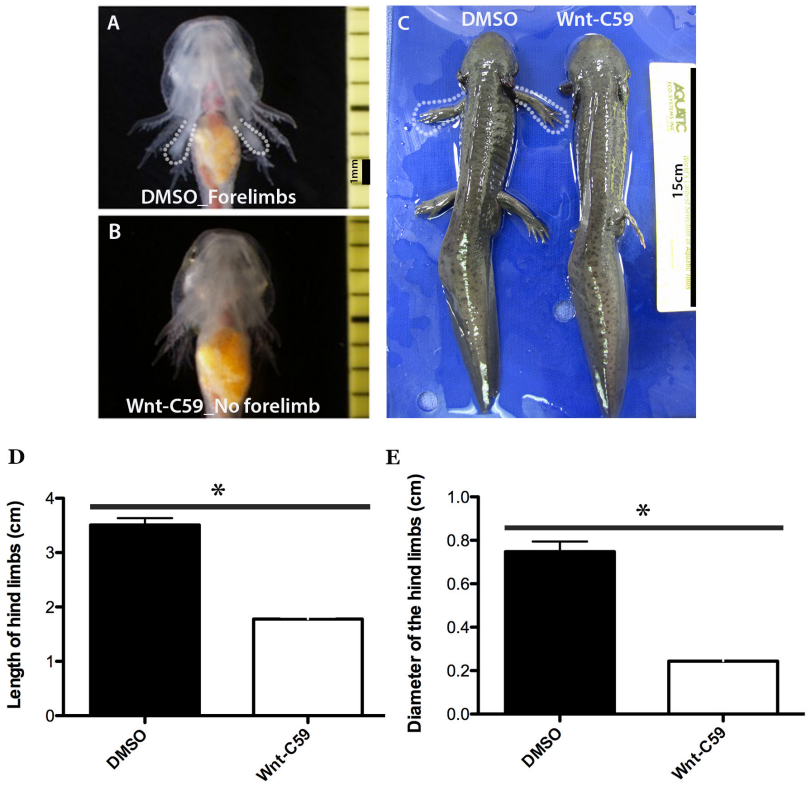

Figure 5.2. Wnt-C59 prevents forelimb bud development and decreases hindlimb size. White stippled lines outlined forelimbs. A) A DMSO treated embryo at developmental stage 51. B) Embryos treated with Wnt-C59 for the first three days did not form forelimbs. C) One-year-old adult axolotls treated with DMSO or Wnt-C59 as embryos. Left: The DMSO control animal had fully developed forelimbs and hindlimbs. Right: The Wnt-C59 treated animal had no forelimb, and smaller and shorter hindlimbs compared to DMSO controls. D) Wnt-C59 decreased hindlimb length. E) Wnt-C59 decreased the diameter of the hind limb at thigh level. *: $p < 0.01$ for contrasts of DMSO control vs Wnt-C59.

5.4.3 Down-regulation of Wnt3a expression by Wnt-C59 treatment is associated with inhibition of forelimb bud development.

Limb bud outgrowth depends on signals emanating from the AER. Wnt3a is the earliest known AER marker during chick limb development. It signals through the

canonical β-Catenin pathway and mediates Fgf10 to induce Fgf8 expression in the limb ectoderm during AER formation (Kengaku et al. 1998; Kawakami et al. 2001). To investigate canonical Wnt signaling during axolotl forelimb bud development, I performed Wnt3a immunostaining using embryos that were treated with either DMSO or Wnt-C59. Embryos were treated for 72 hours after reaching developmental stage 40 (the samples were collected at 72 hours after the treatment). There was no apparent AER observed during axolotl forelimb outgrowth. Wnt3a expression was higher in DMSO vs. Wnt-C59 treated embryos in the epidermis on D-V/P-D sections of the forelimb buds (Figure 5.3, $p < 0.01$, n = 6). Wnt3a did not appear to be differentially expressed among mesodermal cells of DMSO and Wnt-C59 treated forelimb bud, which suggests that the expression difference was specific to the epidermis. Assuming that the epidermis is 1-2 cells thick, Wnt3a expression was significantly higher on the apical side of epidermal cells in DMSO treated embryos (Figure 5.3, $p < 0.01$, n = 6), and Wnt-C59 treatment significantly decreased Wnt3a expression (Figure 5.3, $p > 0.01$, n = 6). These data suggest that down regulation of Wnt3a expression by Wnt-C59 treatment is associated with inhibition of forelimb bud development.

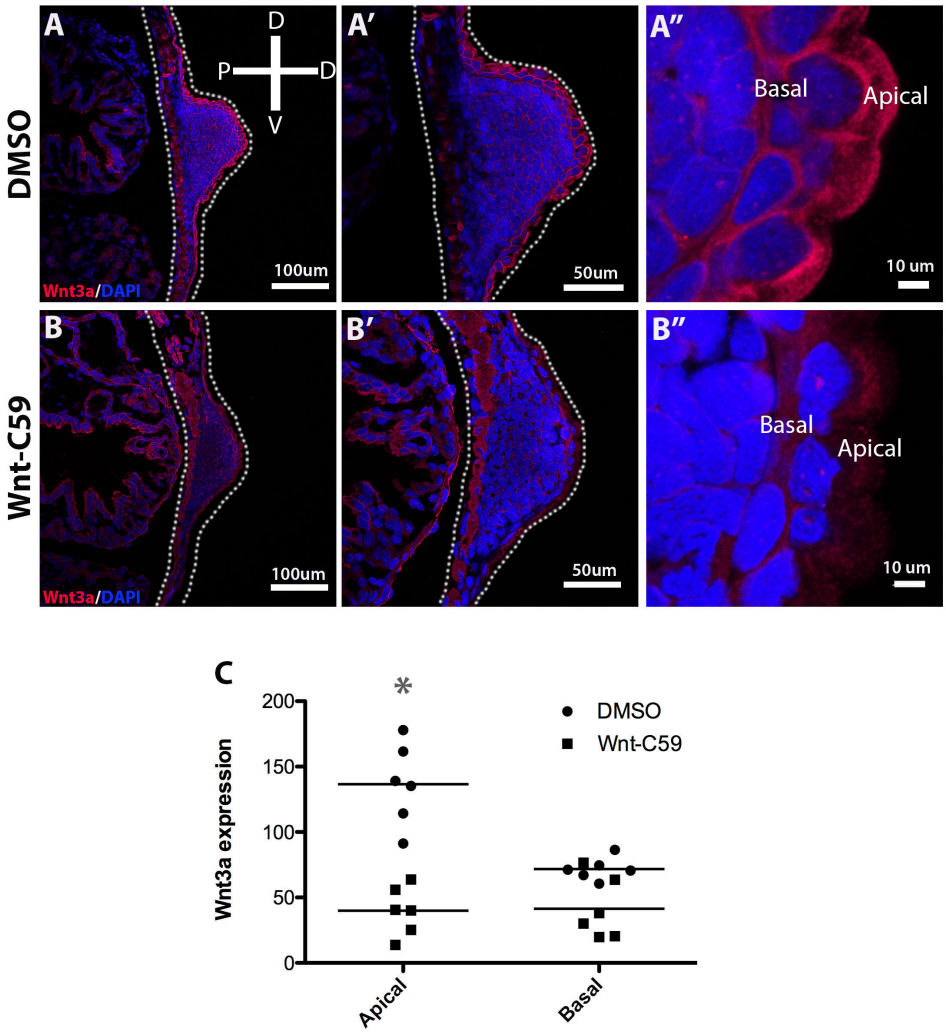

Figure 5.3 Down-regulation of Wnt3a expression by Wnt-C59 treatment is associated with inhibition of forelimb bud development. All the samples were collected at 72 hours after DMSO or Wnt-C59 treatment. The white stippled lines outlined forelimb buds. A-A'') DMSO control forelimb bud stained for Wnt3a in red. Nuclei DNA was labeled by DAPI in blue. B-B'') Forelimb treated with Wnt-C59 and stained for Wnt3a. C) Graph comparing Wnt3a expression between apical and basal sides of DMSO or Wnt-C59 treated forelimb buds, and Wnt3a expression between DMSO or Wnt-C59 treated forelimb buds at apical or basal sides of epidermal cells. *: $p < 0.05$ for the contrast of basal vs apical side of the epidermis in DMSO controls, and DMSO control vs. Wnt-C59 for apical Wnt3a expression. Apical: Apical side of the epidermis. Basal: Basal side of the epidermis.

5.4.4 Polarity of mesodermal cells is disrupted by Wnt-C59 treatment.

The early limb bud is described as an ectodermal bag of randomly arranged and uniformly distributed mesodermal cells (Lu et al. 2008). The elongation of the limb bud along the P-D axis is associated with polarized cellular behaviors (Gao and Yang 2013). The Wnt/PCP pathway regulates oriented cell behaviors, which is very important for directional morphogenesis in developing limbs (Gao and Yang 2013). Zo1 expression is associated with planar cell polarity and is a component of tight junctions (Matter and Balda 2003). To determine if Wnt signaling affects the expression of Zo1, I compared Zo1 expression between DMSO and Wnt-C59 treated embryos. As was observed for Wnt3a, Zo1 expression was higher in apical epidermal regions of DMSO treated embryos, and Zo1 expression was significantly higher in DMSO vs. Wnt-C59 treated embryos (Figure 5.4 A-C, $p < 0.01$, n = 6). The orientation of mesodermal cell nuclei underlying the epidermis appeared to differ between DMSO and Wnt-C59 treated forelimb buds. The orientation of most mesodermal nuclei (relative to the epidermal plane) in DMOS treated embryos was greater than 60 degrees, while most of the nuclei in Wnt-C59 treated embryos were less than 30 degrees (Figure 5.4 A-D, $p < 0.01$, n = 9). Nuclei close to the epidermis of the forelimb bud were elongated and aligned to the epidermis perpendicularly in DMSO treated embryos. Nuclei, located in the center of the limb bud, showed no evidence of elongation and orientation. Mesodermal nuclei density was significantly higher in progress zone 3 compared with progress zones 1 and 2 in DMSO treated embryos (Figure 5.4 E, $p < 0.01$, n = 3). The density of nuclei differed significantly among all three progress zones in Wnt-C59 treated embryos (Figure 5.4 E, $p > 0.01$, n = 3). These results suggest that disruption of Wnt signaling by Wnt-C59 affects cell

orientation and density, and this is associated with a decrease in Zo1 expression in the epidermis.

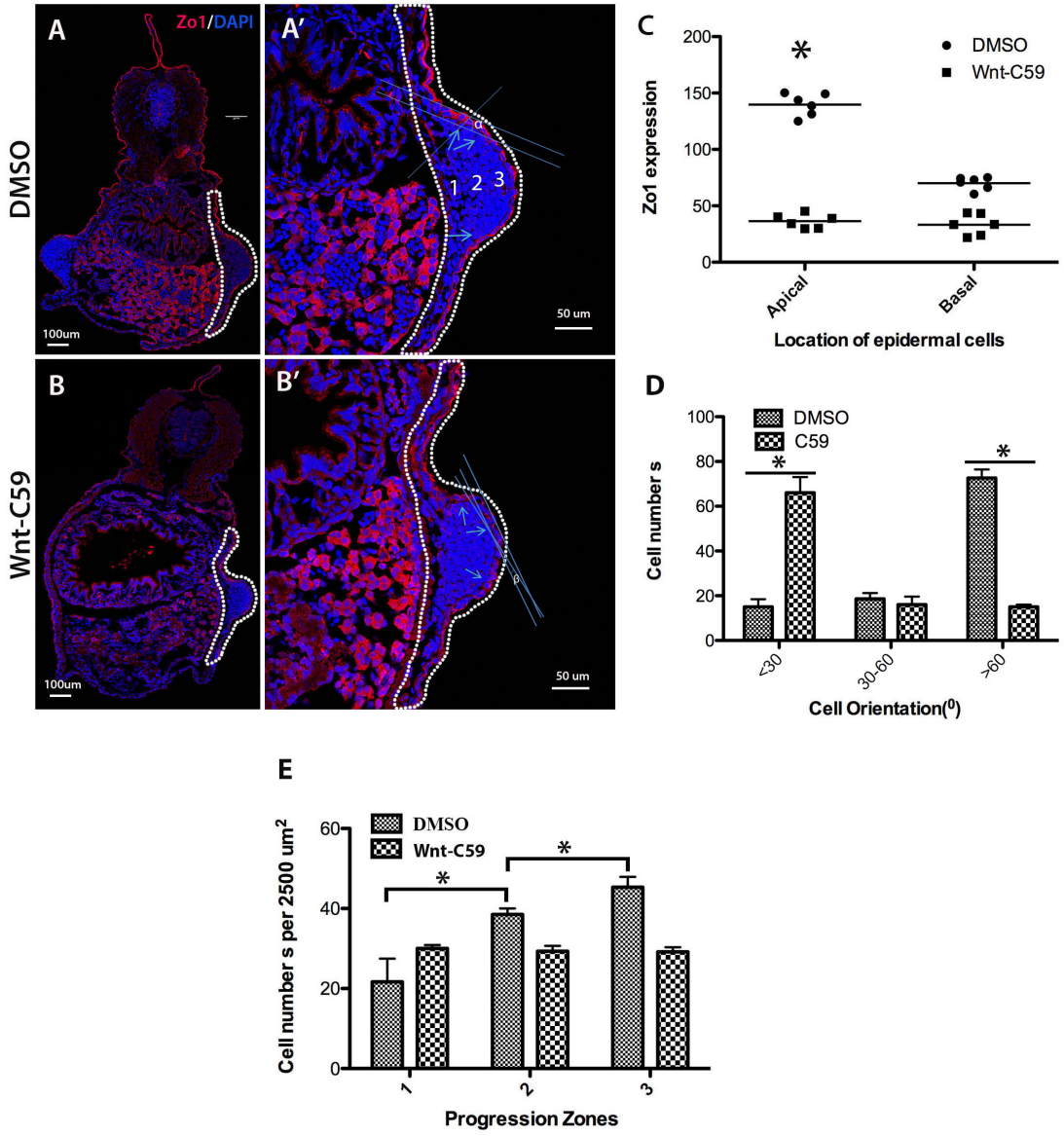

Figure 5.4 Planar cell polarity of forelimb mesodermal cells is disrupted by Wnt-C59. White stippled lines outlined forelimb buds. Cell counts and measures of cell orientation are based on the qualification of DAPI-stained nuclei. A-A') DMSO control forelimb stained with Zo1. Nuclear DNA was labeled with DAPI. B-B') Forelimb treated with Wnt-C59 and Stained with Zo1. C) Zo1 expression in the apical side of the epidermis of forelimb bud. D) Wnt-C59 disrupted the orientation of

mesodermal cell nuclei underlying the epidermis. E) Wnt-C59 altered cell density gradients at the P-D axis. $p > 0.01$). *: $p < 0.05$ for the contrast of basal vs. apical side in DMSO controls, or DMSO control vs. Wnt-C59 for apical Zo1 expression. α and β: representative angles between the longitudinal axis of mesodermal cell nuclei and a parallel line of drawn along the epidermal surface of the forelimb bud in DMSO or Wnt-C59 treated embryos. 1, 2, and 3: progress zone 1, 2, and 3. Blue arrows: representative mesodermal cell nuclei with angles more than 60° in DMSO treated embryos, and angles less than 30° in Wnt-C59 treated embryos.

5.4.5 Wnt and Fgf signaling pathways promote cell progression at M-phase during forelimb bud outgrowth.

Reiter and Solursh (1982) showed that the apical epidermis promotes mitosis of cell-cultured, chick wing mesodermal cells. However, Pengfei Lu et al. (2008) showed that Wnt/β-Catenin signaling promotes survival of AER cells in the mouse limb, but it does not affect cell proliferation and survival of distal mesodermal cells. To determine if Wnt and Fgf signaling pathways affect cell mitosis during axolotl forelimb bud outgrowth, I stained forelimb tissues for a mitotic marker, phosphorylated histone H3. In DMSO control embryos, many mitotic cells were observed (Figure 5.5 A); the mitotic index of DMSO treated embryos was 18.2 ± 2.0% (Figure 5.5 C). Wnt-C59 treatment reduced the mitotic index (9.2 ± 1.0%) significantly (Figure 5.5 A-C, $p < 0.01$, n = 3). To take a closer look at mesodermal cells underlying the apical ectoderm, I performed phosphorylated histone H3 staining using cryo-sections across the forelimb bud at an A-P/P-D plane (Figure 5.5 G and H). The mitotic index in DMSO treated embryos was 5.0 ± 0.9%. Wnt-C59 treated embryos showed a reduced mitotic index 1.1 ± 0.5% ($p < 0.01$, n = 3). There were too few H3 positive cells to

determine if there was a proximal-distal mitotic gradient. H & E staining also showed that Wnt-C59 treatment decreased cell density in the forelimb bud (Figure 5.5 D-F, $p < 0.01$, n = 3).

To further clarify that M-phase cell cycle progression of forelimb mesodermal cells is required for forelimb bud outgrowth, I treated embryos with an Fgf signaling pathway inhibitor because Fgf signaling is required for limb bud outgrowth (REF?). BGJ398 decreased the mitotic index (11.1 ± 1.3%) relative to DMSO controls (18.2 ± 2.0%) (Figure 5.6 A-C, $p < 0.01$, n = 3). I also tested aurora kinase inhibitors that are known to regulate mitotic events (Marumoto et al. 2003). Three aurora kinase inhibitors, CYC116, MK-5108, and Danusertib, significantly inhibited forelimb bud outgrowth (Figure 5.7, $p < 0.01$, n = 4). These results show that Wnt signaling is required for mesodermal cell mitosis during axolotl forelimb bud outgrowth.

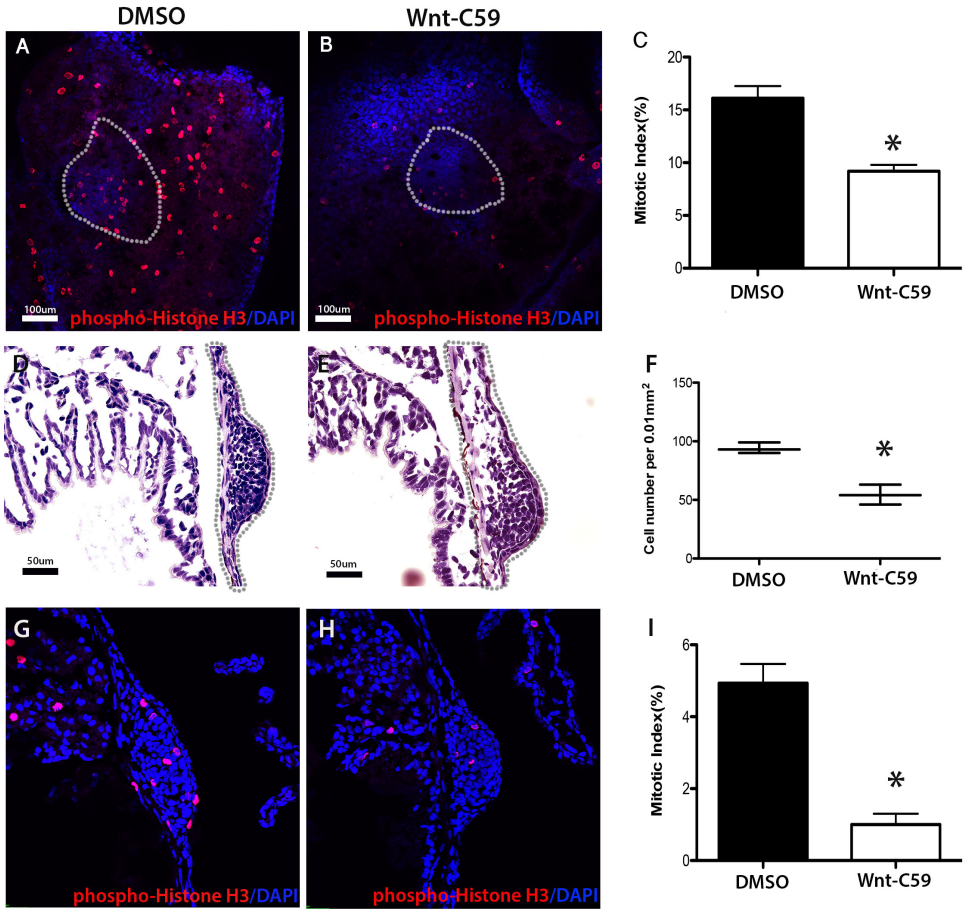

Figure 5.5. Wnt signaling supports the mitosis of forelimb mesodermal cells. A-B) DMSO control or Wnt-C59 treated forelimb field stained with phosphorylated Histone H3 using whole-mount samples. Mitotic cells were stained in red. Total DNA was stained with DAPI in blue. The white stippled line outlines the area within which Histone H3 positive or DAPI stained cells were counted to determine the mitotic index. C) Wnt-C59 treatment reduced the mitotic index of mesodermal cells of the forelimb. D-E) H&E staining of the right forelimb of DMSO or Wnt-C59 treated embryos. F) Wnt-C59 reduced mesodermal cell density in the forelimb buds. G-H) DMSO control or Wnt-C59 treated forelimb field stained with phosphorylated Histone H3 using cryo-sections. I) Wnt-C59 treatment reduced the mitotic index of mesodermal cells in the forelimb. *: $p < 0.05$ for contrast DMSO control vs Wnt-C59.

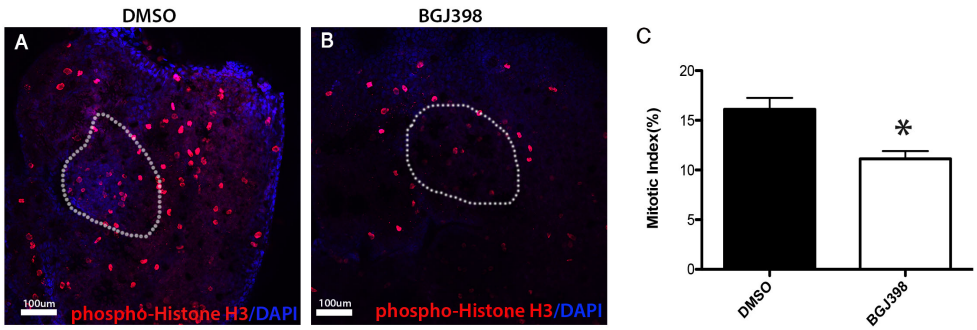

Figure 5.6 Fgf signaling supports the mitosis of forelimb mesodermal cells. A-B) Whole-mount phosphorylated Histone H3 staining for presumptive forelimb fields of DMSO or BGJ398 treated embryos. The images show mitotic cells stained in red. The total DNA was stained with DAPI in blue. The white stippled line areas were used to count phosphorylated Histone H3 positive or DAPI stained cells. C) BGJ398 treatment reduced the mitosis index of the forelimb. *: $p < 0.05$ for contrast DMSO control vs BGJ398.

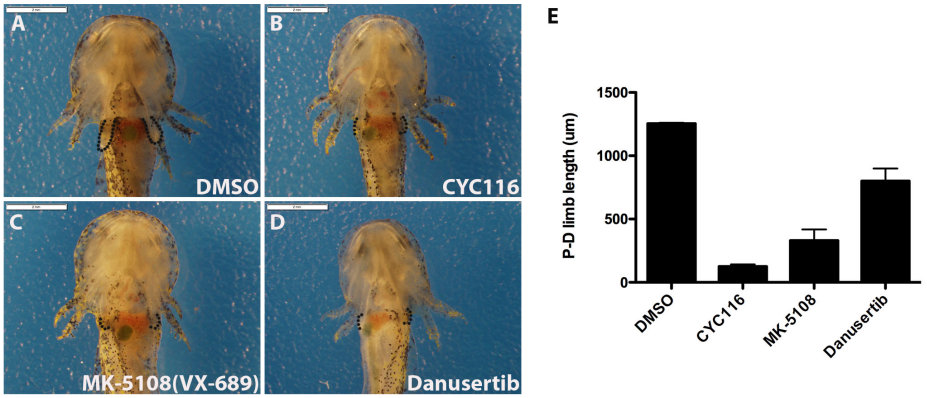

Figure 5.7 Aurora Kinase inhibitors inhibit forelimb bud outgrowth. The black stippled line outlines forelimbs of the embryos. A-D) Representative images showing embryos treated with DMSO, CYC116, MK-5108, and Danusertib. D) CYC116, MK-5108, and Danusertib significantly halted forelimb bud outgrowth. *: $p < 0.01$ for contrasts DMSO control vs CYC116, MK-5108, or Danusertib.

5.4.6 Wnt signaling is critical for mesodermal cell proliferation in the forelimb bud. Cell proliferation is precisely controlled during embryonic development. Vertebrate limb bud morphogenesis depends upon regulated cell proliferation. A prominent hypothesis, the "proliferation gradient" model along the P-D axis, was proposed to explain how proliferation gradients engender limb bud outgrowth (Ede and Law 1969). To test whether there is a proliferation gradient, and whether Wnt signaling plays a role in cell proliferation during forelimb bud outgrowth, cell proliferation was assayed at 72 hours post developmental stage 40 using EdU staining. To label proliferating cells, I delivered EdU at 48 hours post developmental stage 40. Wnt-C59 treatment significantly reduced the cell proliferation index of forelimb bud mesodermal cells; the proliferation index was 52.8 ± 6.2% compared to 68.3 ± 3.8%) for the DMSO control (Figure 5.8 A, A', B, B', and D, $p < 0.01$, n = 6). However, cell proliferation did not differ between proximal and distal mesodermal cell populations. Thus, there does not appear to be a P-D proliferation gradient at this stage of axolotl limb bud development. Fgf signaling inhibitor BGJ398 also significantly decreased the cell proliferation index (BGJ398 vs DMSO control: 48.2 ± 12.2% vs 67.9 ± 3.8%, $p < 0.01$, n = 4) (Figure 5.8 A, A', C, C' and E). The proliferation index of Wnt-C59 treated samples was lower than that of BGJ398 treated samples, but the difference was not statistically significant ($p > 0.05$, n = 4). These results show that Wnt signaling regulates mesodermal cell proliferation.

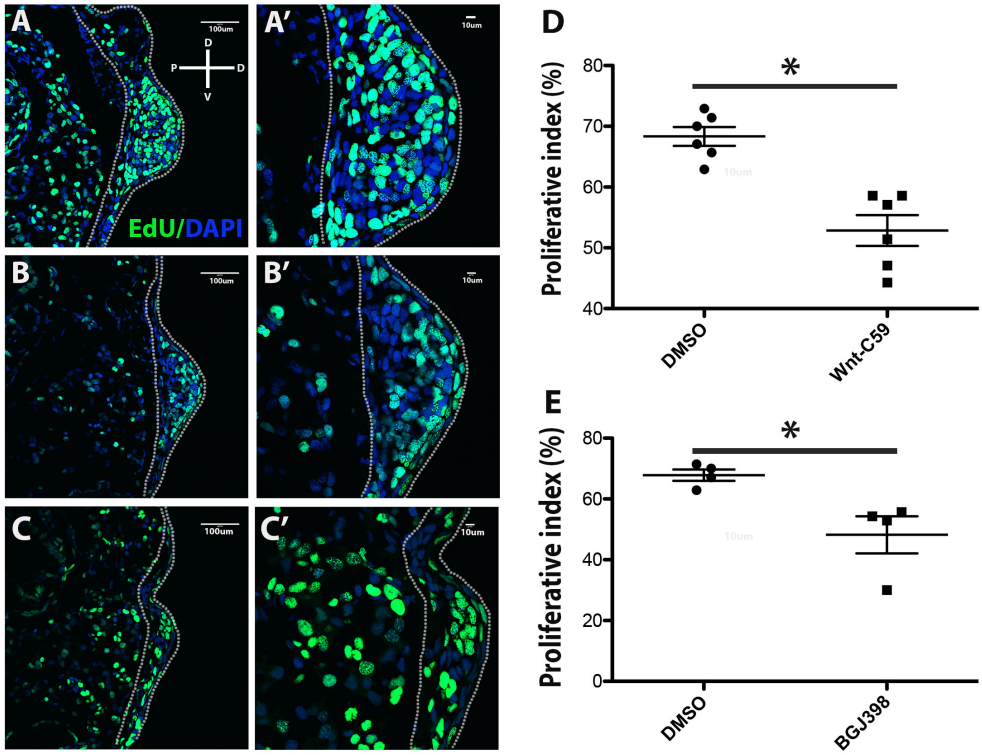

Figure 5.8 Wnt and Fgf signaling pathways regulate cell proliferation of mesodermal cells of the forelimb bud. EdU was injected 48 hours after treatment, and samples were collected 72 hours after treatment. Cryo-sections of D-V/P-D planes at forelimb bud levels were used for EdU staining. A) DMSO control forelimb bud stained with EdU. Proliferating cells were detected by EdU in green. Cell nuclei were labeled with DAPI in blue. A') Detail image of A. B) Forelimb treated with Wnt-C59 and stained with EdU. B') Detail image of B. C) Forelimb treated with BGJ-398 and stained with EdU. C') Detail image of C. D) Wnt-C59 reduced the cell proliferation index relative to the DMSO control. E) BGJ398 reduced the cell proliferation index relative to the DMSO control. *: $p < 0.05$ for contrasts DMSO control vs Wnt-C59 or BGJ398.

5.5 Discussion

In this chapter, I demonstrated the requirement of Wnt signaling pathways during forelimb bud outgrowth. Wnt and Fgf signaling pathways regulated cell proliferation

and mitosis of mesodermal cells during axolotl early forelimb bud outgrowth. Blocking the Wnt and Fgf signaling pathways reduced cell proliferation and mitosis of mesodermal cells, which are required for forelimb bud outgrowth. My results also suggest that cell orientation and cell density of forelimb bud mesodermal cells was disrupted by Wnt-C59 treatment. These differences between Wnt-C59 and control forelimb buds may trace to a disruption of Wnt-mediated patterning during forelimb bud outgrowth.

Wnt3a expression altered by Wnt-C59 is associated with inhibition of forelimb bud outgrowth.

Wnt3a is an early marker for the AER in chick (Kengaku et al. 1998; Kawakami et al. 2001). Although I did not observe AER formation during axolotl forelimb outgrowth, I did observe that Wnt3a was highly expressed in the epidermis of a normally developing forelimb bud. Wnt-C59 altered Wnt3a expression and this was associated with inhibition of forelimb bud development. These results are consistent with ten Berge et al. (2008), who showed that Wnt3a cooperates with Fgf8 to maintain mesodermal cells in an undifferentiated, proliferative state to promote outgrowth of chick limb buds. This is the first study to suggest a role for Wnt3a in axolotl forelimb bud outgrowth.

Reduced cell proliferation and mitosis by Wnt-C59 is associated with inhibition of forelimb bud outgrowth.

Limb bud outgrowth relies on a continuous ectodermal-mesodermal interaction. Epidermal cells are necessary for controlling proliferation and mitosis (Lu et al. 2008), and failure of communication between the ectoderm and mesoderm disrupts

limb development (Fernandez-Teran, Ros, and Mariani 2013). In this study, I found that about 5 percent of cells were mitotic in the forelimb bud in DMSO treated controls. Wnt and Fgf pathway inhibitors significantly reduced cell proliferation and mitosis of mesodermal cells. Ten Berge et al. (2008) reported that Wnt3a alone promotes the growth of chick limb mesenchyme in culture, while Fgf8 alone does not. However, Fgf8 synergistically enhances the proliferative effect of Wnt3a. It would be interesting to titer Fgf and Wnt signaling activities by varying the dosage of chemical inhibitors to determine if these pathways synergistically regulate cell proliferation and mitosis during limb development. It would also be interesting to investigate the aurora kinase inhibitors that were shown to inhibit limb regeneration in this study, as this might link Wnt signaling to a specific mitotic mechanism.

The critical window for forelimb bud outgrowth

I identified a narrow window around developmental stage 40 within which Wnt-C59 blocked forelimb bud outgrowth. This suggests that the requirement for Wnt signaling during limb development has a distinct, offset timing. It seems reasonable to assume that the offset requirement for Wnt signaling coincides with systemic changes in signaling centers that regulate limb bud outgrowth. For example, a regulatory loop consisting of Wnt factors (Wnt3a, Wnt2b, and Wnt8c) and fibroblast growth factors (Fgf8 and Fgf10) regulates AER formation and limb bud outgrowth (Kawakami et al. 2001). Wnt7a expression in non-AER limb ectoderm determines dorsal limb cell identity and dorsal-ventral axis regulation (Riddle et al. 1995). Wnt signaling around developmental stage 40 may coincide with these signaling mechanisms.

Applications for using the axolotl embryo model to identify chemicals that alter limb development and regeneration

The discovery that Wnt-C59 inhibits limb development was serendipitous as it was discovered in a chemical genetic screen using a tail regeneration assay (Ponamareva et al 2015). Many chemicals discovered from this screening project provides tools for investigating mechanisms of tail regeneration (Voss et al 2019). The discovery of Wnt-C59 as an inhibitor of limb development suggests that this same axolotl screening platform can be used to identify chemicals for studies of limb development and regeneration. Additionally, the axolotl embryo assay could provide an efficient and cost-effective tool for screening chemical libraries for toxicity and limb developmental defects.

CHAPTER 6: SUMMARY AND DISCUSSION: SIGNALING PATHWAYS DURING AXOLOTL TAIL REGENERATION AND FORELIMB BUD OUTGROWTH

Signaling pathways and axolotl tail regeneration

Signaling pathways are activated by injury-induced cytokines, growth factors, and local activators during regeneration. The axolotl tail regeneration model provides an excellent tool to investigate signaling pathways during tissue regeneration. The axolotl embryo is capable of regenerating an amputated tail in about seven days. Using this model, Ponomareva et al. (2015) identified three chemicals inhibitors (SB505124, Wnt-C59, and BGJ398) of Tgf-β, Wnt, and Fgf signaling pathways that blocked axolotl tail regeneration. The purpose of my dissertation was to study these chemical inhibitors in more depth as the results might guide progress in understanding mechanisms of regeneration, and ultimately cellular reprogramming and tissue engineering toward repairing complex body parts in mammals.

Disruption of major signaling pathways reduces cell mitosis and cell proliferation.

In my model, axolotl tail regeneration initiates after amputation of 2mm of the distal tail tip. The amputation injury is thought to induce typical innate immune responses, including clotting, immune cell activation, and cell death. Within 1 hour, a simplified epithelium forms over the exposed tail stump. Underneath the epidermis, progenitor cells from different tissues organize in the tail tip and form a regenerating bud. In chapter 2, 3 and 4, I showed that inhibition of Tgf-β, Wnt, or Fgf signaling pathways by SB505124, Wnt-C59, or BGJ398 yielded decreased cell proliferation and mitosis

in several tissue types including spinal cord, dorsal fin, ventral fin, and distal tail tip (Table 6.1). However, the Fgf signaling pathway inhibitor BGJ398 did not significantly affect cell proliferation in the spinal cord. Upon Fgf inhibitor release, the tail regeneration process re-initiated and went to completion. It is thought that Fgfs are morphogens that support progenitor cell proliferation. My results show that signal pathway inhibition can affect tissues differently and a cell proliferation response is not sufficient for regeneration. For example, Naringenin inhibited tail regeneration but not the cell proliferation response (Table 6.1). It seems likely that signaling pathways synergistically and cooperatively control cell proliferation during axolotl tail regeneration. In the future, it will be important to test for synergistic and cooperative effects of inhibitors to determine how pathways interact to regulate cell proliferation and mitosis.

Table 6.1 Inhibitors of cell proliferation and mitosis.

	Target	Signaling pathway	Cell mitosis	Cell proliferation
SB505124	Alk4/5/7	Tgf-β	↓	↓
Naringenin	p-Smad3	Tgf-β	-	NS
Wnt-C59	Porcupine	Wnt	↓	↓
BGJ398	Fgfr1/2/3	Fgf	↓	↓ but not the spinal cord

✓: Expressed; ↑: Increased; ↓: Decreased; NS: Non-significant; -: Not done.

Ligands may induce transcriptional changes that jointly regulate Tgf-β, Wnt, and Fgf signaling.

I found that Tgf-β1 was up-regulated during axolotl tail regeneration. Upregulation of Tgf-β1 was similarly found during tadpole tail regeneration (Denis et al. 2016; Levesque et al. 2007). In my studies, I used Tgf-β pathway inhibitor SB505124, which inhibits Alk5, Alk4, and Alk7 type I receptors. It seems plausible that Tgf-β1 acts through one or more of these receptors to orchestrate axolotl tail regeneration. However, other Tgf-β pathway ligands could be important. For example, *Inhbb* transcripts were decreased at 24hpa upon Wnt pathway inhibition (Ponomareva et al. 2015). *Inhbb* shares a β subunit with *Activin,* and its function is thought to oppose *Activin* (Zhu et al. 2012; Namwanje and Brown 2016).

In contrast to increasing Tgf-β1 levels during regeneration, Wnt3a was decreased at 24 and 72hpa in the regenerating tail. While this suggests down-regulation of some Wnt pathway activities, other Wnt ligands (that were not quantified in my study) may activate Wnt signaling during tail regeneration. For example, Wnt-C59 treatment caused a significant decrease in *Wnt5a* transcription at 24, 48, 72, and 120hpa, suggesting a requirement for Wnt5a during later stages of regeneration, when the rate of tissue outgrowth increases (Ponomareva et al. 2015). Additionally, Wnt-C59 treatment significantly decreased *Fgf9* transcription at 24hpa, and then later between 72-120hpa (Ponomareva et al. 2015). As discussed above, *Inhbb* may function to oppose *Activin* and upregulate Tgf-β signaling. Tgf-β signaling appears to act upstream of Wnt signaling, which in turn up-regulates and positively feeds back on Tgf-β signaling. In future studies, it will be essential to investigate the crucial roles of Wnt5a during axolotl tail regeneration by creating an axolotl *Wnt5a* knock-out

predicted to show decreased expression of *Fgf9* and *Inhbb* at 24 hpa, and inhibited regeneration. This would potentially identify a transcriptional network that jointly regulates Tgf-β, Wnt, and Fgf signaling pathways (Figure 6.1).

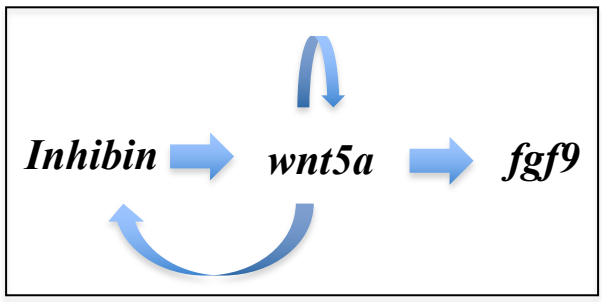

Figure 6.1 Crucial ligands regulate Tgf-β, Wnt, and Fgf signaling pathways.

SB505124 and Naringenin differentially affect early Smad mediated TGF-β signaling.

In chapter 2, I showed that chemical disruption of Tgf-β signaling altered Smad mediated Tgf-β signaling pathway components. In regenerating tails, both Smad2 and Smad3 were activated upon tail amputation as early as 1hpa. p-Smad2 steadily increased afterward at the tested time points while p-Smad3 decreased. Application of SB505124 down-regulated both p-Smad2 and p-Smad3 at all post-amputation time points and blocked tail regeneration. Naringenin also down-regulated p-Smad2 at all post-amputation time points, delayed peak p-Smad3 expression, and completely blocked tail regeneration. However, SB505124 treatment affected p-Smad2 at an earlier time and to a greater degree than p-Smad3, while Naringenin affected p-Smad3 at an earlier time and to a greater degree than p-Smad2 (Table 6.2). The opposing roles played by Smad2 and Smad3 have been studied during both embryo development and tissue regeneration. The differential regulation of p-Smad2 and p-Smad2 may lead to differences in progenitor cell proliferation and mitosis. Further

studies are needed to understand the different requirements for Smad2 and Smad3 signaling and their role in regulating cell proliferation and mitosis during axolotl limb and tail regeneration.

Table 6.2 SB505124 and Naringenin differentially affect Smad-mediated TGF-β signaling.

	DMSO	SB505124 vs DMSO	Naringenin vs DMSO
p-Smad2 at 0hpa	✓		
p-Smad2 at 1hpa	↑	↓↓↓	↓
p-Smad2 at 6hpa	↑	↓	↓
p-Smad2 at 12hpa	↑	↓	↓
P-Smad3 at 0hpa	✓		
p-Smad3 at 1hpa	↑	NS	↓↓↓
p-Smad3 at 6hpa	↓	↓	↑
p-Smad3 at 12hpa	↓	↓	NS

✓: Expressed; ↑: Increased; ↓: Decreased; ↓↓↓: Decreased more than the other chemical; NS: Non-significant.

Inhibition of Tgf-β, Wnt, or Fgf signaling pathways alters phosphorylation of Erk and Akt.

I found that p-Erk and p-Akt responded to tail amputation at an early phase of tail regeneration. P-Erk was expressed at the time of tail amputation, increased at 1hpa and then decreased at 6hpa. P-Akt was expressed at the time of tail amputation; it changed very little at 1hpa and decreased at 6hpa. Overall, increased expression of p-

Erk and decreased expression of p-Akt appear to be important early signaling responses. Furthermore, p-Erk and p-Akt were significantly up-regulated in SB505124-treated tails, but significantly down-regulated in Naringenin-treated tails at 1hpa; thus, p-Erk and p-Akt were affected by disruptions of Tgf-β signaling (Table 6.3). Moreover, Wnt and Fgf signaling pathways regulated phosphorylation of Erk and Akt. In chapter 3, I found that disruption Wnt signaling pathway by Wnt-C59 increased phosphorylation of Erk at 48hpa and phosphorylation of Akt at 48 and 72hpa. In chapter 4, I found that disruption of Fgf signaling by BGJ398 down-regulated p-Erk and p-Akt. Overall, all three signaling pathways affected the phosphorylation of Erk and Akt; pathways are known to regulate cell proliferation, cell survival, and cell fate specification (Table 6.4). Future studies are needed to determine if changes in Erk and Akt phosphorylation affect cell proliferation and mitosis, as well as the regenerative outcome in axolotl embryo model.

Table 6.3 SB505124 and Naringenin differentially affect non-Smad mediated TGF-β signaling.

	DMSO	SB505124 vs DMSO	Naringenin vs DMSO
p-Erk at 0hpa	✓		
p-Erk at 1hpa	↑	↑	↓
p-Erk at 6hpa	↑	↑	NS
p-Erk at 12hpa	↑	↓	NS
p-Akt at 0hpa	✓		
p-Akt at 1hpa	NS	↑	↓
p-Akt at 6hpa	↓	NS	↓
p-Akt at 12hpa	↓	NS	↓

✓: Expressed; ↑: Increased; ↓: Decreased; NS: Non-significant.

Table 6.4 Effects of Wnt-C59 and BGJ398 on Erk and Akt signaling.

	DMSO	Wnt-C59 vs DMSO	BGJ398 vs DMSO
p-Erk at 0hpa	✓		
p-Erk at 24hpa	NS	NS	NS
p-Erk at 48hpa	↓	↑	↓
p-Erk at 72hpa	↑	NS	NS
p-Akt at 0hpa	✓		
p-Akt at 24hpa	↓	NS	NS
p-Akt at 48hpa	NS	↑	↑
p-Akt at 72hpa	NS	↑	↑

✓: Expressed; ↑: Increased; ↓: Decreased; NS: Non-significant.

Inhibition of Wnt or Fgf signaling pathways affects Wnt/β-Catenin signaling.

In chapter 3, I found that β-Catenin was decreased at 48hpa and increased at 72hpa relative to 0hpa during axolotl tail regeneration. Wnt-C59 treatment increased β-Catenin at 48hpa. In chapter 4, I found that BGJ398 treatment increased Wnt3a expression at 48hpa and 72hpa; it also increased β-Catenin at 48hpa (Table 6.5). These data suggest that some Fgf signaling activities are inversely correlated with Wnt/β-Catenin signaling.

Table 6.5 Effects of Wnt-C59 and BGJ398 on Wnt3a and β-Catenin expression.

	DMSO	Wnt-C59 vs. DMSO	BGJ398 vs. DMSO
Wnt3a at 0hpa	✓		
Wnt3a at 24hpa	↓		NS
Wnt3a at 48hpa	NS		↑
Wnt3a at 72hpa	↓		↑
β-Catenin at 0hpa	✓		
β-Catenin at 24hpa	NS	NS	NS
β-Catenin at 48hpa	↓	↑	↑
β-Catenin at 72hpa	↑	NS	NS

✓: Expressed; ↑: Increased; ↓: Decreased; NS: Non-significant.

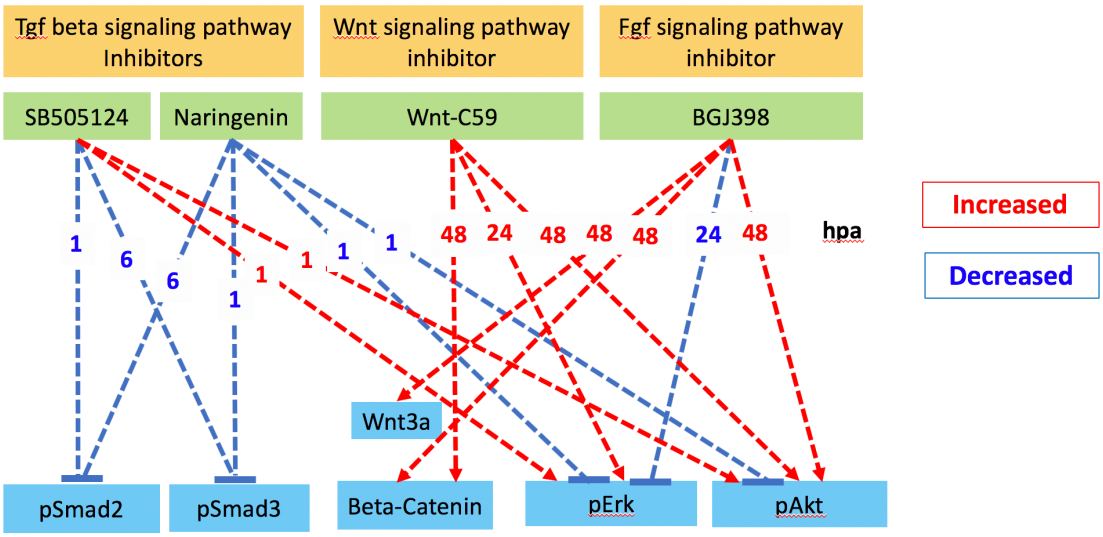

Figure 6.2 Preliminary network for Tgf-β, Wnt, and Fgf signaling pathways during axolotl tail regeneration. Red arrows show how chemicals increased expression of signaling components. Blue arrows show how chemicals decreased expression of signaling components. The numbers report the earliest times (hours post amputation - hpa) at which signaling components were affected.

Wnt3a is an essential ligand for forelimb bud outgrowth.

Wnt3a is known to mediate canonical Wnt/β-Catenin signaling and is an early marker of the AER in amniote vertebrate limbs (Kengaku et al. 1998; Kawakami et al. 2001). In chapter 5, I detected Wnt3a expressed in the epidermis of the developing forelimb bud. Wnt-C59 altered Wnt3a levels and expression patterns in the limb and prevented forelimb bud outgrowth. To my knowledge, this is the first study analyzing Wnt3a ligand in axolotl forelimb bud outgrowth. The Wnt3a expression pattern in the epidermis during axolotl limb development maybe characteristic of non-amniote vertebrate limb development. My results suggest a role for Wnt3a in forelimb bud outgrowth in the axolotl but do not rule out essential roles for other Wnt ligands. For example, Wnt2b-Wnt8c/β-Catenin signaling in the lateral plate mesoderm is vital for

Fgf10 expression in the mesenchyme of the presumptive chick limb bud (Kawakami et al. 2001). Also, Wnt5a regulates limb bud initiation by controlling asymmetric cell behaviors (Gao and Yang 2013; Wyngaarden et al. 2010; Gros et al. 2010).

Planar cell polarity in epidermal cells and underlying mesodermal cells is associated with proximal-distal axis elongation.

In chapter 5, I showed that Wnt signaling pathway inhibition altered the expression of Wnt3a and Zo1 in epidermal cells, appeared to affect the polarity of mesenchymal cells, and blocked forelimb bud outgrowth. The first definitive demonstration of PCP during limb development was established by showing symmetrical localization of Vangl2 in newly formed mesenchymal cells along the proximal-distal limb axis of mice (Gao et al. 2011). In Wnt5a knockout mice, limb elongation is impaired (Gros et al. 2010). Future studies are needed to rigorously document changes in cell polarity that would establish Wnt/PCP signaling in the developing axolotl forelimb.

Wnt and Fgf signaling pathways regulate cell proliferation and mitosis of limb mesodermal cells.

Continuous ectodermal-mesodermal interaction is important for limb bud outgrowth. Epidermal cells of the limb bud are necessary for controlling cell proliferation and mitosis during forelimb outgrowth (Lu et al. 2008). In Chapter 5, the developing axolotl forelimb bud was shown to contain a high number of mitotic cells. Both Wnt-C59 and BGJ398 reduced mesodermal cell proliferation and mitosis. Thus, Wnt and Fgf signals are essential to maintain the function of the apical epidermis as an inducer of cell proliferation and mitosis in underlying mesodermal cells. To further confirm that cell mitosis is necessary for successful forelimb bud outgrowth, I showed that

three different aurora kinase inhibitors CYC116, MK-5108 (VX-689), and Danusertib halted forelimb bud outgrowth, to different degrees. Thus, the proper amount of cell mitosis is required for forelimb bud outgrowth. It would be interesting to find a direct link between Wnt signaling and aurora kinases during axolotl forelimb bud outgrowth. Overall, Wnt and Fgf signaling pathways play essential roles in regulating cell proliferation and mitosis to assure forelimb bud outgrowth.

The critical window for forelimb bud outgrowth

In Chapter 5, a critical narrow window around developmental stage 40 was found during which Wnt-C59 completely blocked forelimb bud outgrowth, thus suggesting a distinct, offset timing for Wnt signaling to regulate limb development. It appears that the offset requirement for Wnt signaling coincides with more systemic changes in signaling centers that regulate forelimb bud outgrowth. For example, a regulatory loop consisting of Wnt factors and the fibroblast growth factors regulates AER formation and limb bud outgrowth (Kawakami et al. 2001). Wnt7a expression in non-AER limb ectoderm determines dorsal limb cell identity and thus dorsal-ventral axis regulation (Riddle et al. 1995). Wnt signaling around developmental stage 40 may relate to systemic signaling changes in signaling centers that regulate forelimb bud outgrowth.

In summary, this dissertation examined the requirements of Tgf-β, Wnt, and Fgf signaling pathways during axolotl tail regeneration and the requirement of Wnt signaling during axolotl forelimb bud outgrowth. Tgf-β, Wnt, and Fgf signaling pathways are required during axolotl tail regeneration. Inhibition of all three pathways affects Erk and Akt signaling pathways, and cell proliferation and mitosis. The Wnt

signaling pathway is required for forelimb bud outgrowth, and failure to develop forelimbs is associated with altered Wnt3a and Zo1 expression and decreased cell proliferation and mitosis. These data enrich understanding of signaling pathway network dynamics that underlie tissue regeneration and vertebrate limb development.

BIBLIOGRAPHY

Akiyama, H., J. P. Lyons, Y. Mori-Akiyama, X. Yang, R. Zhang, Z. Zhang, J. M. Deng, M. M. Taketo, T. Nakamura, R. R. Behringer, P. D. McCrea, and B. de Crombrugghe. 2004. 'Interactions between Sox9 and beta-catenin control chondrocyte differentiation', *Genes Dev*, 18: 1072-87.

Alexandrow, M. G., and H. L. Moses. 1995. 'Transforming growth factor beta 1 inhibits mouse keratinocytes late in G1 independent of effects on gene transcription', *Cancer Res*, 55: 3928-32.

Amamoto, R., V. G. Huerta, E. Takahashi, G. Dai, A. K. Grant, Z. Fu, and P. Arlotta. 2016. 'Adult axolotls can regenerate original neuronal diversity in response to brain injury', *Elife*, 5.

Amano, M., M. Nakayama, and K. Kaibuchi. 2010. 'Rho-kinase/ROCK: A key regulator of the cytoskeleton and cell polarity', *Cytoskeleton (Hoboken)*, 67: 545-54.

Armstrong, L., O. Hughes, S. Yung, L. Hyslop, R. Stewart, I. Wappler, H. Peters, T. Walter, P. Stojkovic, J. Evans, M. Stojkovic, and M. Lako. 2006. 'The role of PI3K/AKT, MAPK/ERK and NFkappabeta signalling in the maintenance of human embryonic stem cell pluripotency and viability highlighted by transcriptional profiling and functional analysis', *Hum Mol Genet*, 15: 1894-913.

Attisano, L., J. Carcamo, F. Ventura, F. M. Weis, J. Massague, and J. L. Wrana. 1993. 'Identification of human activin and TGF beta type I receptors that form heteromeric kinase complexes with type II receptors', *Cell*, 75: 671-80.

Aykul, S., and E. Martinez-Hackert. 2016. 'Transforming Growth Factor-beta Family Ligands Can Function as Antagonists by Competing for Type II Receptor Binding', *J Biol Chem*, 291: 10792-804.

Bakin, A. V., A. K. Tomlinson, N. A. Bhowmick, H. L. Moses, and C. L. Arteaga. 2000. 'Phosphatidylinositol 3-kinase function is required for transforming growth factor beta-mediated epithelial to mesenchymal transition and cell migration', *J Biol Chem*, 275: 36803-10.

Bassat, E., Y. E. Mutlak, A. Genzelinakh, I. Y. Shadrin, K. Baruch Umansky, O. Yifa, D. Kain, D. Rajchman, J. Leach, D. Riabov Bassat, Y. Udi, R. Sarig, I. Sagi, J. F. Martin, N. Bursac, S. Cohen, and E. Tzahor. 2017. 'The extracellular matrix protein agrin promotes heart regeneration in mice', *Nature*, 547: 179-84.

Bikkavilli, R. K., and C. C. Malbon. 2009. 'Mitogen-activated protein kinases and Wnt/beta-catenin signaling: Molecular conversations among signaling pathways', *Commun Integr Biol*, 2: 46-9.

Bosch, T. C. 2007. 'Why polyps regenerate and we don't: towards a cellular and molecular framework for Hydra regeneration', *Dev Biol*, 303: 421-33.

Bryant, S. V., T. Endo, and D. M. Gardiner. 2002. 'Vertebrate limb regeneration and the origin of limb stem cells', *Int J Dev Biol*, 46: 887-96.

Bushdid, P. B., D. M. Brantley, F. E. Yull, G. L. Blaeuer, L. H. Hoffman, L. Niswander, and L. D. Kerr. 1998. 'Inhibition of NF-kappaB activity results in disruption of the apical ectodermal ridge and aberrant limb morphogenesis', *Nature*, 392: 615-8.

Cargnello, M., and P. P. Roux. 2011. 'Activation and function of the MAPKs and their substrates, the MAPK-activated protein kinases', *Microbiol Mol Biol Rev*, 75: 50-83.

Carlson, M. R., S. V. Bryant, and D. M. Gardiner. 1998. 'Expression of Msx-2 during development, regeneration, and wound healing in axolotl limbs', *J Exp Zool*, 282: 715-23.

Carlson, M. R., Y. Komine, S. V. Bryant, and D. M. Gardiner. 2001. 'Expression of Hoxb13 and Hoxc10 in developing and regenerating Axolotl limbs and tails', *Dev Biol*, 229: 396-406.

Cary, G. A., A. Wolff, O. Zueva, J. Pattinato, and V. F. Hinman. 2019. 'Analysis of sea star larval regeneration reveals conserved processes of whole-body regeneration across the metazoa', *BMC Biol*, 17: 16.

Chablais, F., and A. Jazwinska. 2012. 'The regenerative capacity of the zebrafish heart is dependent on TGFbeta signaling', *Development*, 139: 1921-30.
Christen, B., A. M. Rodrigues, M. B. Monasterio, C. F. Roig, and J. C. Izpisua Belmonte. 2012. 'Transient downregulation of Bmp signalling induces extra limbs in vertebrates', *Development*, 139: 2557-65.
Christensen, R. N., and R. A. Tassava. 2000. 'Apical epithelial cap morphology and fibronectin gene expression in regenerating axolotl limbs', *Dev Dyn*, 217: 216-24.
DaCosta Byfield, S., C. Major, N. J. Laping, and A. B. Roberts. 2004. 'SB-505124 is a selective inhibitor of transforming growth factor-beta type I receptors ALK4, ALK5, and ALK7', *Mol Pharmacol*, 65: 744-52.
Denis, J. F., F. Sader, S. Gatien, E. Villiard, A. Philip, and S. Roy. 2016. 'Activation of Smad2 but not Smad3 is required to mediate TGF-beta signaling during axolotl limb regeneration', *Development*, 143: 3481-90.
Derynck, R., and Y. E. Zhang. 2003. 'Smad-dependent and Smad-independent pathways in TGF-beta family signalling', *Nature*, 425: 577-84.
Ding, Q., W. Xia, J. C. Liu, J. Y. Yang, D. F. Lee, J. Xia, G. Bartholomeusz, Y. Li, Y. Pan, Z. Li, R. C. Bargou, J. Qin, C. C. Lai, F. J. Tsai, C. H. Tsai, and M. C. Hung. 2005. 'Erk associates with and primes GSK-3beta for its inactivation resulting in upregulation of beta-catenin', *Mol Cell*, 19: 159-70.
Doellinger, J., M. Grossegesse, A. Nitsche, and P. Lasch. 2018. 'DMSO as a mobile phase additive enhances detection of ubiquitination sites by nano-LC-ESI-MS/MS', *J Mass Spectrom*, 53: 183-87.
Dorey, K., and E. Amaya. 2010. 'FGF signalling: diverse roles during early vertebrate embryogenesis', *Development*, 137: 3731-42.
Duboc, V., and M. P. Logan. 2011. 'Regulation of limb bud initiation and limb-type morphology', *Dev Dyn*, 240: 1017-27.
Dungan, K. M., T. Y. Wei, J. D. Nace, M. L. Poulin, I. M. Chiu, J. C. Lang, and R. A. Tassava. 2002. 'Expression and biological effect of urodele fibroblast growth factor 1: relationship to limb regeneration', *J Exp Zool*, 292: 540-54.
Ede, D. A., and J. T. Law. 1969. 'Computer simulation of vertebrate limb morphogenesis', *Nature*, 221: 244-8.
Edlund, S., S. Y. Lee, S. Grimsby, S. Zhang, P. Aspenstrom, C. H. Heldin, and M. Landstrom. 2005. 'Interaction between Smad7 and beta-catenin: importance for transforming growth factor beta-induced apoptosis', *Mol Cell Biol*, 25: 1475-88.
Fabregat, I., J. Fernando, J. Mainez, and P. Sancho. 2014. 'TGF-beta signaling in cancer treatment', *Curr Pharm Des*, 20: 2934-47.
Fan, Y., B. X. Ho, J. K. S. Pang, N. M. Q. Pek, J. H. Hor, S. Y. Ng, and B. S. Soh. 2018. 'Wnt/beta-catenin-mediated signaling re-activates proliferation of matured cardiomyocytes', *Stem Cell Res Ther*, 9: 338.
Fernandez-Teran, M., M. A. Ros, and F. V. Mariani. 2013. 'Evidence that the limb bud ectoderm is required for survival of the underlying mesoderm', *Dev Biol*, 381: 341-52.
Fields, S., and M. Johnston. 2005. 'Cell biology. Whither model organism research?', *Science*, 307: 1885-6.
Fink, J., A. Andersson-Rolf, and B. K. Koo. 2015. 'Adult stem cell lineage tracing and deep tissue imaging', *BMB Rep*, 48: 655-67.
Franklin, B. M., S. R. Voss, and J. L. Osborn. 2017. 'Ion channel signaling influences cellular proliferation and phagocyte activity during axolotl tail regeneration', *Mech Dev*, 146: 42-54.
Freisinger, C. M., R. A. Fisher, and D. C. Slusarski. 2010. 'Regulator of g protein signaling 3 modulates wnt5b calcium dynamics and somite patterning', *PLoS Genet*, 6: e1001020.
Fukui, L., and J. J. Henry. 2011. 'FGF signaling is required for lens regeneration in Xenopus laevis', *Biol Bull*, 221: 137-45.
Galli, L. M., T. L. Barnes, S. S. Secrest, T. Kadowaki, and L. W. Burrus. 2007. 'Porcupine-mediated lipid-modification regulates the activity and distribution of Wnt proteins in the chick neural tube', *Development*, 134: 3339-48.

Gao, B., H. Song, K. Bishop, G. Elliot, L. Garrett, M. A. English, P. Andre, J. Robinson, R. Sood, Y. Minami, A. N. Economides, and Y. Yang. 2011. 'Wnt signaling gradients establish planar cell polarity by inducing Vangl2 phosphorylation through Ror2', *Dev Cell*, 20: 163-76.
Gao, B., and Y. Yang. 2013. 'Planar cell polarity in vertebrate limb morphogenesis', *Curr Opin Genet Dev*, 23: 438-44.
Gargioli, C., and J. M. Slack. 2004. 'Cell lineage tracing during Xenopus tail regeneration', *Development*, 131: 2669-79.
Georgopoulos, N. T., L. A. Kirkwood, and J. Southgate. 2014. 'A novel bidirectional positive-feedback loop between Wnt-beta-catenin and EGFR-ERK plays a role in context-specific modulation of epithelial tissue regeneration', *J Cell Sci*, 127: 2967-82.
Ghosh, S., S. Roy, C. Seguin, S. V. Bryant, and D. M. Gardiner. 2008. 'Analysis of the expression and function of Wnt-5a and Wnt-5b in developing and regenerating axolotl (Ambystoma mexicanum) limbs', *Dev Growth Differ*, 50: 289-97.
Giarre, M., M. V. Semenov, and A. M. Brown. 1998. 'Wnt signaling stabilizes the dual-function protein beta-catenin in diverse cell types', *Ann N Y Acad Sci*, 857: 43-55.
Gilbert, R. W., M. K. Vickaryous, and A. M. Viloria-Petit. 2013. 'Characterization of TGFbeta signaling during tail regeneration in the leopard Gecko (Eublepharis macularius)', *Dev Dyn*, 242: 886-96.
Gospodarowicz, D. 1976. 'Humoral control of cell proliferation: the role of fibroblast growth factor in regeneration, angiogenesis, wound healing, and neoplastic growth', *Prog Clin Biol Res*, 9: 1-19.
Govindasamy, N., S. Murthy, and Y. Ghanekar. 2014. 'Slow-cycling stem cells in hydra contribute to head regeneration', *Biol Open*, 3: 1236-44.
Grandel, H., and M. Brand. 2011. 'Zebrafish limb development is triggered by a retinoic acid signal during gastrulation', *Dev Dyn*, 240: 1116-26.
Gros, J., J. K. Hu, C. Vinegoni, P. F. Feruglio, R. Weissleder, and C. J. Tabin. 2010. 'WNT5A/JNK and FGF/MAPK pathways regulate the cellular events shaping the vertebrate limb bud', *Curr Biol*, 20: 1993-2002.
Guagnano, V., P. Furet, C. Spanka, V. Bordas, M. Le Douget, C. Stamm, J. Brueggen, M. R. Jensen, C. Schnell, H. Schmid, M. Wartmann, J. Berghausen, P. Drueckes, A. Zimmerlin, D. Bussiere, J. Murray, and D. Graus Porta. 2011. 'Discovery of 3-(2,6-dichloro-3,5-dimethoxy-phenyl)-1-{6-[4-(4-ethyl-piperazin-1-yl)-phenylamin o]-pyrimidin-4-yl}-1-methyl-urea (NVP-BGJ398), a potent and selective inhibitor of the fibroblast growth factor receptor family of receptor tyrosine kinase', *J Med Chem*, 54: 7066-83.
Guengerich, F. P., and D. H. Kim. 1990. 'In vitro inhibition of dihydropyridine oxidation and aflatoxin B1 activation in human liver microsomes by naringenin and other flavonoids', *Carcinogenesis*, 11: 2275-9.
Gurley, K. A., J. C. Rink, and A. Sanchez Alvarado. 2008. 'Beta-catenin defines head versus tail identity during planarian regeneration and homeostasis', *Science*, 319: 323-7.
Habas, R., and I. B. Dawid. 2005. 'Dishevelled and Wnt signaling: is the nucleus the final frontier?', *J Biol*, 4: 2.
Hadari, Y. R., N. Gotoh, H. Kouhara, I. Lax, and J. Schlessinger. 2001. 'Critical role for the docking-protein FRS2 alpha in FGF receptor-mediated signal transduction pathways', *Proc Natl Acad Sci U S A*, 98: 8578-83.
Hamburger, V., and H. L. Hamilton. 1992. 'A series of normal stages in the development of the chick embryo. 1951', *Dev Dyn*, 195: 231-72.
Hamilton, P. W., Y. Sun, and J. J. Henry. 2016. 'Lens regeneration from the cornea requires suppression of Wnt/beta-catenin signaling', *Exp Eye Res*, 145: 206-15.
Han, M. J., J. Y. An, and W. S. Kim. 2001. 'Expression patterns of Fgf-8 during development and limb regeneration of the axolotl', *Dev Dyn*, 220: 40-8.
Harris, T. J., and M. Peifer. 2005. 'Decisions, decisions: beta-catenin chooses between adhesion and transcription', *Trends Cell Biol*, 15: 234-7.

Hayashi, T., N. Mizuno, R. Takada, S. Takada, and H. Kondoh. 2006. 'Determinative role of Wnt signals in dorsal iris-derived lens regeneration in newt eye', *Mech Dev*, 123: 793-800.
Heldin, C. H., K. Miyazono, and P. ten Dijke. 1997. 'TGF-beta signalling from cell membrane to nucleus through SMAD proteins', *Nature*, 390: 465-71.
Herman, P. E., A. Papatheodorou, S. A. Bryant, C. K. M. Waterbury, J. R. Herdy, A. A. Arcese, J. D. Buxbaum, J. J. Smith, J. R. Morgan, and O. Bloom. 2018. 'Highly conserved molecular pathways, including Wnt signaling, promote functional recovery from spinal cord injury in lampreys', *Sci Rep*, 8: 742.
Hill, T. P., M. M. Taketo, W. Birchmeier, and C. Hartmann. 2006. 'Multiple roles of mesenchymal beta-catenin during murine limb patterning', *Development*, 133: 1219-29.
Hino, S., T. Michiue, M. Asashima, and A. Kikuchi. 2003. 'Casein kinase I epsilon enhances the binding of Dvl-1 to Frat-1 and is essential for Wnt-3a-induced accumulation of beta-catenin', *J Biol Chem*, 278: 14066-73.
Ho, D. M., and M. Whitman. 2008. 'TGF-beta signaling is required for multiple processes during Xenopus tail regeneration', *Dev Biol*, 315: 203-16.
Hobmayer, B., F. Rentzsch, K. Kuhn, C. M. Happel, C. C. von Laue, P. Snyder, U. Rothbacher, and T. W. Holstein. 2000. 'WNT signalling molecules act in axis formation in the diploblastic metazoan Hydra', *Nature*, 407: 186-9.
Jazwinska, A., R. Badakov, and M. T. Keating. 2007. 'Activin-betaA signaling is required for zebrafish fin regeneration', *Curr Biol*, 17: 1390-5.
Jhamb, D., N. Rao, D. J. Milner, F. Song, J. A. Cameron, D. L. Stocum, and M. J. Palakal. 2011. 'Network based transcription factor analysis of regenerating axolotl limbs', *BMC Bioinformatics*, 12: 80.
Julien, C., F. Marcouiller, A. Bretteville, N. B. El Khoury, J. Baillargeon, S. S. Hebert, and E. Planel. 2012. 'Dimethyl sulfoxide induces both direct and indirect tau hyperphosphorylation', *PLoS One*, 7: e40020.
Kanegae, Y., A. T. Tavares, J. C. Izpisua Belmonte, and I. M. Verma. 1998. 'Role of Rel/NF-kappaB transcription factors during the outgrowth of the vertebrate limb', *Nature*, 392: 611-4.
Kawakami, Y., J. Capdevila, D. Buscher, T. Itoh, C. Rodriguez Esteban, and J. C. Izpisua Belmonte. 2001. 'WNT signals control FGF-dependent limb initiation and AER induction in the chick embryo', *Cell*, 104: 891-900.
Kawakami, Y., C. Rodriguez Esteban, M. Raya, H. Kawakami, M. Marti, I. Dubova, and J. C. Izpisua Belmonte. 2006. 'Wnt/beta-catenin signaling regulates vertebrate limb regeneration', *Genes Dev*, 20: 3232-7.
Kengaku, M., J. Capdevila, C. Rodriguez-Esteban, J. De La Pena, R. L. Johnson, J. C. Izpisua Belmonte, and C. J. Tabin. 1998. 'Distinct WNT pathways regulating AER formation and dorsoventral polarity in the chick limb bud', *Science*, 280: 1274-7.
Kim, D., O. Rath, W. Kolch, and K. H. Cho. 2007. 'A hidden oncogenic positive feedback loop caused by crosstalk between Wnt and ERK pathways', *Oncogene*, 26: 4571-9.
Kolodziej, H., O. Kayser, A. F. Kiderlen, H. Ito, T. Hatano, T. Yoshida, and L. Y. Foo. 2001. 'Proanthocyanidins and related compounds: antileishmanial activity and modulatory effects on nitric oxide and tumor necrosis factor-alpha-release in the murine macrophage-like cell line RAW 264.7', *Biol Pharm Bull*, 24: 1016-21.
Komiya, Y., and R. Habas. 2008. 'Wnt signal transduction pathways', *Organogenesis*, 4: 68-75.
Kragl, M., D. Knapp, E. Nacu, S. Khattak, M. Maden, H. H. Epperlein, and E. M. Tanaka. 2009. 'Cells keep a memory of their tissue origin during axolotl limb regeneration', *Nature*, 460: 60-5.
Kumar, A., J. W. Godwin, P. B. Gates, A. A. Garza-Garcia, and J. P. Brockes. 2007. 'Molecular basis for the nerve dependence of limb regeneration in an adult vertebrate', *Science*, 318: 772-7.

Kurayoshi, M., H. Yamamoto, S. Izumi, and A. Kikuchi. 2007. 'Post-translational palmitoylation and glycosylation of Wnt-5a are necessary for its signalling', *Biochem J*, 402: 515-23.
Levesque, M., S. Gatien, K. Finnson, S. Desmeules, E. Villiard, M. Pilote, A. Philip, and S. Roy. 2007. 'Transforming growth factor: beta signaling is essential for limb regeneration in axolotls', *PLoS One*, 2: e1227.
Li, G., Y. Y. Li, J. E. Sun, W. H. Lin, and R. X. Zhou. 2016. 'ILK-PI3K/AKT pathway participates in cutaneous wound contraction by regulating fibroblast migration and differentiation to myofibroblast', *Lab Invest*, 96: 741-51.
Li, J., S. Zhang, X. Soto, S. Woolner, and E. Amaya. 2013. 'ERK and phosphoinositide 3-kinase temporally coordinate different modes of actin-based motility during embryonic wound healing', *J Cell Sci*, 126: 5005-17.
Lin, G., and J. M. Slack. 2008. 'Requirement for Wnt and FGF signaling in Xenopus tadpole tail regeneration', *Dev Biol*, 316: 323-35.
Lin, S., L. M. Baye, T. A. Westfall, and D. C. Slusarski. 2010. 'Wnt5b-Ryk pathway provides directional signals to regulate gastrulation movement', *J Cell Biol*, 190: 263-78.
Loomis, C. A., E. Harris, J. Michaud, W. Wurst, M. Hanks, and A. L. Joyner. 1996. 'The mouse Engrailed-1 gene and ventral limb patterning', *Nature*, 382: 360-3.
Love, N. R., Y. Chen, S. Ishibashi, P. Kritsiligkou, R. Lea, Y. Koh, J. L. Gallop, K. Dorey, and E. Amaya. 2013. 'Amputation-induced reactive oxygen species are required for successful Xenopus tadpole tail regeneration', *Nat Cell Biol*, 15: 222-8.
Lu, P., Y. Yu, Y. Perdue, and Z. Werb. 2008. 'The apical ectodermal ridge is a timer for generating distal limb progenitors', *Development*, 135: 1395-405.
MacDonald, B. T., and X. He. 2012. 'Frizzled and LRP5/6 receptors for Wnt/beta-catenin signaling', *Cold Spring Harb Perspect Biol*, 4.
MacDonald, B. T., K. Tamai, and X. He. 2009. 'Wnt/beta-catenin signaling: components, mechanisms, and diseases', *Dev Cell*, 17: 9-26.
Majdi, S., N. Najafinobar, J. Dunevall, J. Lovric, and A. G. Ewing. 2017. 'DMSO Chemically Alters Cell Membranes to Slow Exocytosis and Increase the Fraction of Partial Transmitter Released', *Chembiochem*, 18: 1898-902.
Makanae, A., A. Hirata, Y. Honjo, K. Mitogawa, and A. Satoh. 2013. 'Nerve independent limb induction in axolotls', *Dev Biol*, 381: 213-26.
Makanae, A., K. Mitogawa, and A. Satoh. 2014. 'Co-operative Bmp- and Fgf-signaling inputs convert skin wound healing to limb formation in urodele amphibians', *Dev Biol*, 396: 57-66.
———. 2016. 'Cooperative inputs of Bmp and Fgf signaling induce tail regeneration in urodele amphibians', *Dev Biol*, 410: 45-55.
Mariani, F. V., C. P. Ahn, and G. R. Martin. 2008. 'Genetic evidence that FGFs have an instructive role in limb proximal-distal patterning', *Nature*, 453: 401-5.
Marumoto, T., S. Honda, T. Hara, M. Nitta, T. Hirota, E. Kohmura, and H. Saya. 2003. 'Aurora-A kinase maintains the fidelity of early and late mitotic events in HeLa cells', *J Biol Chem*, 278: 51786-95.
Matter, K., and M. S. Balda. 2003. 'Signalling to and from tight junctions', *Nat Rev Mol Cell Biol*, 4: 225-36.
McCusker, C., S. V. Bryant, and D. M. Gardiner. 2015. 'The axolotl limb blastema: cellular and molecular mechanisms driving blastema formation and limb regeneration in tetrapods', *Regeneration (Oxf)*, 2: 54-71.
Medina, L. S., G. A. Taylor, and M. Donovan. 1997. 'Radiologic-pathologic conference of Children's Hospital Boston: liver nodules after heart transplantation', *Pediatr Radiol*, 27: 95-7.
Minde, D. P., Z. Anvarian, S. G. Rudiger, and M. M. Maurice. 2011. 'Messing up disorder: how do missense mutations in the tumor suppressor protein APC lead to cancer?', *Mol Cancer*, 10: 101.

Minde, D. P., M. Radli, F. Forneris, M. M. Maurice, and S. G. Rudiger. 2013. 'Large extent of disorder in Adenomatous Polyposis Coli offers a strategy to guard Wnt signalling against point mutations', *PLoS One*, 8: e77257.
Mochii, M., Y. Taniguchi, and I. Shikata. 2007. 'Tail regeneration in the Xenopus tadpole', *Dev Growth Differ*, 49: 155-61.
Moses, H. L. 1992. 'TGF-beta regulation of epithelial cell proliferation', *Mol Reprod Dev*, 32: 179-84.
Mukerjee, A. B. 1947. 'Coronaries; coronary arteriosclerosis with special reference to its etiology and pathogenesis; experimental studies', *Calcutta Med J*, 44: 33-41.
Mullen, L. M., S. V. Bryant, M. A. Torok, B. Blumberg, and D. M. Gardiner. 1996. 'Nerve dependency of regeneration: the role of Distal-less and FGF signaling in amphibian limb regeneration', *Development*, 122: 3487-97.
Nacu, E., E. Gromberg, C. R. Oliveira, D. Drechsel, and E. M. Tanaka. 2016. 'FGF8 and SHH substitute for anterior-posterior tissue interactions to induce limb regeneration', *Nature*, 533: 407-10.
Nakamura, R., K. Koshiba-Takeuchi, M. Tsuchiya, M. Kojima, A. Miyazawa, K. Ito, H. Ogawa, and J. K. Takeuchi. 2016. 'Expression analysis of Baf60c during heart regeneration in axolotls and neonatal mice', *Dev Growth Differ*, 58: 367-82.
Nakamura, Y., C. D. Tsiairis, S. Ozbek, and T. W. Holstein. 2011. 'Autoregulatory and repressive inputs localize Hydra Wnt3 to the head organizer', *Proc Natl Acad Sci U S A*, 108: 9137-42.
Namwanje, M., and C. W. Brown. 2016. 'Activins and Inhibins: Roles in Development, Physiology, and Disease', *Cold Spring Harb Perspect Biol*, 8.
Niswander, L., and G. R. Martin. 1993. 'FGF-4 and BMP-2 have opposite effects on limb growth', *Nature*, 361: 68-71.
Nusse, R. 2005. 'Wnt signaling in disease and in development', *Cell Res*, 15: 28-32.
Nye, H. L., J. A. Cameron, E. A. Chernoff, and D. L. Stocum. 2003. 'Regeneration of the urodele limb: a review', *Dev Dyn*, 226: 280-94.
Ogura, T., I. S. Alvarez, A. Vogel, C. Rodriguez, R. M. Evans, and J. C. Izpisua Belmonte. 1996. 'Evidence that Shh cooperates with a retinoic acid inducible co-factor to establish ZPA-like activity', *Development*, 122: 537-42.
Ornitz, D. M., and P. J. Marie. 2015. 'Fibroblast growth factor signaling in skeletal development and disease', *Genes Dev*, 29: 1463-86.
Ortiz-Andrade, R. R., J. C. Sanchez-Salgado, G. Navarrete-Vazquez, S. P. Webster, M. Binnie, S. Garcia-Jimenez, I. Leon-Rivera, P. Cigarroa-Vazquez, R. Villalobos-Molina, and S. Estrada-Soto. 2008. 'Antidiabetic and toxicological evaluations of naringenin in normoglycaemic and NIDDM rat models and its implications on extra-pancreatic glucose regulation', *Diabetes Obes Metab*, 10: 1097-104.
Peiris, T. H., D. Ramirez, P. G. Barghouth, and N. J. Oviedo. 2016. 'The Akt signaling pathway is required for tissue maintenance and regeneration in planarians', *BMC Dev Biol*, 16: 7.
Petersen, C. P., and P. W. Reddien. 2008. 'Smed-betacatenin-1 is required for anteroposterior blastema polarity in planarian regeneration', *Science*, 319: 327-30.
Pfefferli, C., and A. Jazwinska. 2017. 'The careg element reveals a common regulation of regeneration in the zebrafish myocardium and fin', *Nat Commun*, 8: 15151.
Plotnikov, A. N., J. Schlessinger, S. R. Hubbard, and M. Mohammadi. 1999. 'Structural basis for FGF receptor dimerization and activation', *Cell*, 98: 641-50.
Ponomareva, L. V., A. Athippozhy, J. S. Thorson, and S. R. Voss. 2015. 'Using Ambystoma mexicanum (Mexican axolotl) embryos, chemical genetics, and microarray analysis to identify signaling pathways associated with tissue regeneration', *Comp Biochem Physiol C Toxicol Pharmacol*, 178: 128-35.
Poss, K. D., J. Shen, A. Nechiporuk, G. McMahon, B. Thisse, C. Thisse, and M. T. Keating. 2000. 'Roles for Fgf signaling during zebrafish fin regeneration', *Dev Biol*, 222: 347-58.

Qian, D., C. Jones, A. Rzadzinska, S. Mark, X. Zhang, K. P. Steel, X. Dai, and P. Chen. 2007. 'Wnt5a functions in planar cell polarity regulation in mice', *Dev Biol*, 306: 121-33.
Qiu, Q., Y. Su, Y. Zheng, H. Cai, S. Wu, W. Lu, W. Zheng, X. O. Shu, and Q. Cai. 2015. 'Increased pSmad2 expression and cytoplasmic predominant presence of TGF-betaRII in breast cancer tissue are associated with poor prognosis: results from the Shanghai Breast Cancer Study', *Breast Cancer Res Treat*, 149: 467-77.
Reiter, R. S., and M. Solursh. 1982. 'Mitogenic property of the apical ectodermal ridge', *Dev Biol*, 93: 28-35.
Riddle, R. D., M. Ensini, C. Nelson, T. Tsuchida, T. M. Jessell, and C. Tabin. 1995. 'Induction of the LIM homeobox gene Lmx1 by WNT7a establishes dorsoventral pattern in the vertebrate limb', *Cell*, 83: 631-40.
Sader, F., J. F. Denis, H. Laref, and S. Roy. 2019. 'Epithelial to mesenchymal transition is mediated by both TGF-beta canonical and non-canonical signaling during axolotl limb regeneration', *Sci Rep*, 9: 1144.
Saera-Vila, A., P. E. Kish, and A. Kahana. 2016. 'Fgf regulates dedifferentiation during skeletal muscle regeneration in adult zebrafish', *Cell Signal*, 28: 1196-204.
Sato, K., Y. Umesono, and M. Mochii. 2018. 'A transgenic reporter under control of an es1 promoter/enhancer marks wound epidermis and apical epithelial cap during tail regeneration in Xenopus laevis tadpole', *Dev Biol*, 433: 404-15.
Satoh, A., S. V. Bryant, and D. M. Gardiner. 2012. 'Nerve signaling regulates basal keratinocyte proliferation in the blastema apical epithelial cap in the axolotl (Ambystoma mexicanum)', *Dev Biol*, 366: 374-81.
Satoh, A., G. M. Graham, S. V. Bryant, and D. M. Gardiner. 2008. 'Neurotrophic regulation of epidermal dedifferentiation during wound healing and limb regeneration in the axolotl (Ambystoma mexicanum)', *Dev Biol*, 319: 321-35.
Satoh, A., A. makanae, A. Hirata, and Y. Satou. 2011. 'Blastema induction in aneurogenic state and Prrx-1 regulation by MMPs and FGFs in Ambystoma mexicanum limb regeneration', *Dev Biol*, 355: 263-74.
Saunders, J. W., Jr. 1998. 'The proximo-distal sequence of origin of the parts of the chick wing and the role of the ectoderm. 1948', *J Exp Zool*, 282: 628-68.
Schlessinger, J. 2000. 'Cell signaling by receptor tyrosine kinases', *Cell*, 103: 211-25.
Scimone, M. L., K. M. Kravarik, S. W. Lapan, and P. W. Reddien. 2014. 'Neoblast specialization in regeneration of the planarian Schmidtea mediterranea', *Stem Cell Reports*, 3: 339-52.
Shah, J. M., E. Omar, D. R. Pai, and S. Sood. 2012. 'Cellular events and biomarkers of wound healing', *Indian J Plast Surg*, 45: 220-8.
Shapiro, P. 2002. 'Ras-MAP kinase signaling pathways and control of cell proliferation: relevance to cancer therapy', *Crit Rev Clin Lab Sci*, 39: 285-330.
Shaul, Y. D., and R. Seger. 2007. 'The MEK/ERK cascade: from signaling specificity to diverse functions', *Biochim Biophys Acta*, 1773: 1213-26.
Shibata, E., Y. Yokota, N. Horita, A. Kudo, G. Abe, K. Kawakami, and A. Kawakami. 2016. 'Fgf signalling controls diverse aspects of fin regeneration', *Development*, 143: 2920-9.
Shimokawa, T., S. Yasutaka, R. Kominami, and H. Shinohara. 2013. 'Lmx-1b and Wnt-7a expression in axolotl limb during development and regeneration', *Okajimas Folia Anat Jpn*, 89: 119-24.
Singh, B. N., C. V. Weaver, M. G. Garry, and D. J. Garry. 2018. 'Hedgehog and Wnt Signaling Pathways Regulate Tail Regeneration', *Stem Cells Dev*, 27: 1426-37.
Spiering, D., and L. Hodgson. 2011. 'Dynamics of the Rho-family small GTPases in actin regulation and motility', *Cell Adh Migr*, 5: 170-80.
Stoick-Cooper, C. L., G. Weidinger, K. J. Riehle, C. Hubbert, M. B. Major, N. Fausto, and R. T. Moon. 2007. 'Distinct Wnt signaling pathways have opposing roles in appendage regeneration', *Development*, 134: 479-89.

Suetsugu-Maki, R., N. Maki, K. Nakamura, S. Sumanas, J. Zhu, K. Del Rio-Tsonis, and P. A. Tsonis. 2012. 'Lens regeneration in axolotl: new evidence of developmental plasticity', *BMC Biol*, 10: 103.
Sugiura, T., A. Tazaki, N. Ueno, K. Watanabe, and M. Mochii. 2009. 'Xenopus Wnt-5a induces an ectopic larval tail at injured site, suggesting a crucial role for noncanonical Wnt signal in tail regeneration', *Mech Dev*, 126: 56-67.
Sugiura, T., H. Wang, R. Barsacchi, A. Simon, and E. M. Tanaka. 2016. 'MARCKS-like protein is an initiating molecule in axolotl appendage regeneration', *Nature*, 531: 237-40.
Suzuki, M., A. Satoh, H. Ide, and K. Tamura. 2007. 'Transgenic Xenopus with prx1 limb enhancer reveals crucial contribution of MEK/ERK and PI3K/AKT pathways in blastema formation during limb regeneration', *Dev Biol*, 304: 675-86.
Syed, M., C. Skonberg, and S. H. Hansen. 2013. 'Effect of some organic solvents on oxidative phosphorylation in rat liver mitochondria: Choice of organic solvents', *Toxicol In Vitro*, 27: 2135-41.
Tanaka, E. M., and P. W. Reddien. 2011. 'The cellular basis for animal regeneration', *Dev Cell*, 21: 172-85.
Tang, Y., Z. Liu, L. Zhao, T. L. Clemens, and X. Cao. 2008. 'Smad7 stabilizes beta-catenin binding to E-cadherin complex and promotes cell-cell adhesion', *J Biol Chem*, 283: 23956-63.
Tappeiner, C., E. Maurer, P. Sallin, T. Bise, V. Enzmann, and M. Tschopp. 2016. 'Inhibition of the TGFbeta Pathway Enhances Retinal Regeneration in Adult Zebrafish', *PLoS One*, 11: e0167073.
Tazaki, A., E. M. Tanaka, and J. F. Fei. 2017. 'Salamander spinal cord regeneration: The ultimate positive control in vertebrate spinal cord regeneration', *Dev Biol*, 432: 63-71.
ten Berge, D., S. A. Brugmann, J. A. Helms, and R. Nusse. 2008. 'Wnt and FGF signals interact to coordinate growth with cell fate specification during limb development', *Development*, 135: 3247-57.
Ten Dijke, P., M. J. Goumans, F. Itoh, and S. Itoh. 2002. 'Regulation of cell proliferation by Smad proteins', *J Cell Physiol*, 191: 1-16.
Thakur, D. P., J. B. Tian, J. Jeon, J. Xiong, Y. Huang, V. Flockerzi, and M. X. Zhu. 2016. 'Critical roles of Gi/o proteins and phospholipase C-delta1 in the activation of receptor-operated TRPC4 channels', *Proc Natl Acad Sci U S A*, 113: 1092-7.
Tickle, C. 2015. 'How the embryo makes a limb: determination, polarity and identity', *J Anat*, 227: 418-30.
Topol, L., X. Jiang, H. Choi, L. Garrett-Beal, P. J. Carolan, and Y. Yang. 2003. 'Wnt-5a inhibits the canonical Wnt pathway by promoting GSK-3-independent beta-catenin degradation', *J Cell Biol*, 162: 899-908.
Torok, M. A., D. M. Gardiner, J. C. Izpisua-Belmonte, and S. V. Bryant. 1999. 'Sonic hedgehog (shh) expression in developing and regenerating axolotl limbs', *J Exp Zool*, 284: 197-206.
Towers, M., and C. Tickle. 2009. 'Growing models of vertebrate limb development', *Development*, 136: 179-90.
Voss, S. R., H. H. Epperlein, and E. M. Tanaka. 2009. 'Ambystoma mexicanum, the axolotl: a versatile amphibian model for regeneration, development, and evolution studies', *Cold Spring Harb Protoc*, 2009: pdb emo128.
Wagner, D. E., I. E. Wang, and P. W. Reddien. 2011. 'Clonogenic neoblasts are pluripotent adult stem cells that underlie planarian regeneration', *Science*, 332: 811-6.
Whitehead, G. G., S. Makino, C. L. Lien, and M. T. Keating. 2005. 'fgf20 is essential for initiating zebrafish fin regeneration', *Science*, 310: 1957-60.
Willert, K., and R. Nusse. 2012. 'Wnt proteins', *Cold Spring Harb Perspect Biol*, 4: a007864.
Wischin, S., C. Castaneda-Patlan, M. Robles-Flores, and J. Chimal-Monroy. 2017. 'Chemical activation of Wnt/beta-catenin signalling inhibits innervation and causes skeletal tissue malformations during axolotl limb regeneration', *Mech Dev*, 144: 182-90.

Wong, H. C., A. Bourdelas, A. Krauss, H. J. Lee, Y. Shao, D. Wu, M. Mlodzik, D. L. Shi, and J. Zheng. 2003. 'Direct binding of the PDZ domain of Dishevelled to a conserved internal sequence in the C-terminal region of Frizzled', *Mol Cell*, 12: 1251-60.
Wrana, J. L., L. Attisano, J. Carcamo, A. Zentella, J. Doody, M. Laiho, X. F. Wang, and J. Massague. 1992. 'TGF beta signals through a heteromeric protein kinase receptor complex', *Cell*, 71: 1003-14.
Wyngaarden, L. A., K. M. Vogeli, B. G. Ciruna, M. Wells, A. K. Hadjantonakis, and S. Hopyan. 2010. 'Oriented cell motility and division underlie early limb bud morphogenesis', *Development*, 137: 2551-8.
Yang, Y. 2003. 'Wnts and wing: Wnt signaling in vertebrate limb development and musculoskeletal morphogenesis', *Birth Defects Res C Embryo Today*, 69: 305-17.
Yokoyama, H., T. Maruoka, H. Ochi, A. Aruga, S. Ohgo, H. Ogino, and K. Tamura. 2011. 'Different requirement for Wnt/beta-catenin signaling in limb regeneration of larval and adult Xenopus', *PLoS One*, 6: e21721.
Yokoyama, H., H. Ogino, C. L. Stoick-Cooper, R. M. Grainger, and R. T. Moon. 2007. 'Wnt/beta-catenin signaling has an essential role in the initiation of limb regeneration', *Dev Biol*, 306: 170-8.
Young, H. E., C. F. Bailey, and B. K. Dalley. 1983. 'Gross morphological analysis of limb regeneration in postmetamorphic adult Ambystoma', *Anat Rec*, 206: 295-306.
Yu, J. S., and W. Cui. 2016. 'Proliferation, survival and metabolism: the role of PI3K/AKT/mTOR signalling in pluripotency and cell fate determination', *Development*, 143: 3050-60.
Zhai, L., D. Chaturvedi, and S. Cumberledge. 2004. 'Drosophila wnt-1 undergoes a hydrophobic modification and is targeted to lipid rafts, a process that requires porcupine', *J Biol Chem*, 279: 33220-7.
Zhang, Y. E. 2009. 'Non-Smad pathways in TGF-beta signaling', *Cell Res*, 19: 128-39.
Zhang, Y., X. Feng, R. We, and R. Derynck. 1996. 'Receptor-associated Mad homologues synergize as effectors of the TGF-beta response', *Nature*, 383: 168-72.
Zhang, Y., T. Pizzute, and M. Pei. 2014. 'A review of crosstalk between MAPK and Wnt signals and its impact on cartilage regeneration', *Cell Tissue Res*, 358: 633-49.
Zhao, L., Y. Jin, K. Donahue, M. Tsui, M. Fish, C. Y. Logan, B. Wang, and R. Nusse. 2019. 'Tissue repair in the mouse liver following acute carbon tetrachloride depends on injury-induced Wnt/beta-catenin signaling', *Hepatology*.
Zhu, J., S. J. Lin, C. Zou, Y. Makanji, T. S. Jardetzky, and T. K. Woodruff. 2012. 'Inhibin alpha-subunit N terminus interacts with activin type IB receptor to disrupt activin signaling', *J Biol Chem*, 287: 8060-70.

VITA

Author's name: Qingchao Qiu

Place of birth: Hunan, P. R. China

Permanent resident of U.S.A.

Education and trainings

2014-2019 Ph.D. in Neuroscience, Department of Neuroscience, University of Kentucky, KY, U.S.A.

2004-2007 M. S. in Pathology and Physiopathology, School of Medicine, University of South China, P. R. China

2001-2003 Resident in Department of gynecology and obstetrics, Jinhua Guangfu Hospital, Zhejiang Province, P. R. China

1996-2001 M. D. in Clinical Medicine, Xiang-Ya School of Medicine, Central South University, P.R. China

Professional position

2008-2014 Research Fellow in Genetic Medicine and Epidemiology, Vanderbilt University, TN, U.S.A.

2007-2008 Instructor in the Department of Anatomy, School of medicine, University of South China, P. R. China

Scholastic Honors

2014-2016 Ribble Mini-grant, Department of Biology, University of Kentucky

2008 Outstanding Teacher Award, School of Medicine, University of South China, P. R. China

2006-2007 Outstanding Graduate Student Award, School of Medicine, University of South China, P. R. China

Publications

1. Voss SR, Ponomareva LV, Dwarka VB, Pardue KE, Baddar NW, Rodgers AK, Woodcock MR, **Qiu Q**, Crowner A, Blichmann D, Khatri S, Thorson JS. 2019. HDAC regulates transcription at the outset of axolotl tail regeneration. *Scientific Reports*, 2019, 9: 6751.
2. Wang S, Beeghly-Fadiel A, Cai Q, Cai H, Guo X, Shi L, Wu J, Ye F, **Qiu Q**, Zheng Y, Zheng W, Bao PP, Shu XO. Gene expression in triple-negative breast cancer in relation to survival. Breast Cancer Res Treat. 2018, 171(1): 199-207
3. Wang X, Zhang Y, Ponomareva LV, **Qiu Q**, Woodcock R, Elshahawi SI, Chen X, Zhou Z, Hatcher BE, Hower JC, Zhan CG, Parkin S, Kharel MK, Voss SR, Shaaban KA, Thorson JS. Mccrearamycins A-D, Geldanamycin-Derived Cyclopentenone Macrolactams from an Eastern Kentucky Abandoned Coal Mine Microbe. Angew Chem Int Ed Engl. 2017, 56(11): 2994-2998.
4. Su Y, Cai H, Zheng Y, **Qiu Q**, Lu W, Shu XO, Cai Q. Associations of the Transforming Growth Factor β/Smad Pathway, Body Mass Index, and Physical Activity With Breast Cancer Outcomes: Results From the Shanghai Breast Cancer Study. Am J Epidemiol. 2016 Oct 1;184(7):501-509.
5. **Qingchao Qiu**, Yinghao Su, Ying Zheng, Hui Cai, Shenghui Wu, Wei Lu, Wei Zheng, Xiao-ou Shu, Qiuyin Cai. Increased pSmad2 expression and cytoplasmic predominant presence of TGF-βRII in breast cancer tissue are associated with poor prognosis: results from the Shanghai Breast Cancer Study. Breast Cancer Res Treat, 2015, 149(2): 467-477.

6. Yuzhu Xiang, **Qingchao Qiu (Co-first-author)**, Ming Jiang, Renjie Jin, Brian D. Lehmann, Douglas W. Strand, Bojana Jovanovic, David J. DeGraff, Yi Zheng, Dina A. Yousif, Thomas C. Case, Jia Yi, Justin M. Cates, John Virostko, Xiusheng He, Xunbo Jin, Simon W. Hayward, Robert J. Matusik, Alfred L. George Jr, Yajun Yi. SPARCL1 suppresses metastasis in prostate cancer. Molecular Oncology, 2013, 7(6): 1019-1030.
7. **Qingchao Qiu**, Pengcheng Lu, Yuzhu Xiang, Yu Shyr, Xi Chen, Alfred L George, Jr and Yajun Yi. Meta-analysis of Transcriptional Biomarkers in Breast Cancer. PLoS ONE, 2013, 8(1): e54979.
8. **Qingchao Qiu**, Bo Hu, Zhuchu Chen, Xiusheng He. Sexual dimorphism of STGC3 gene's tumor suppressor role in nasopharyngeal carcinoma cell line CNE2. Genet Mol Res, 2012, Oct 9; 11(4): 4585-4597.
9. **Qingchao Qiu**, Bo Hu, Xiupei He, Qiao Luo, Guohua Tang, Zhifeng Long, Zhuchu Chen, Xiusheng He. STGC3 inhibits xenograft tumor growth of nasopharyngeal carcinoma cells by altering the expression of proteins associated with apoptosis. Genetic and Molecular Biology, 2012, 35(1): 18-26.
10. Zhao Qihui, **Qiu Qingchao**, Hu Bo. Effect of Lycopene Induced Cell Apoptosis in Human Colon Cancer SW480 Cells. Cancer Research on Prevention and Treatment, 2012, 39(11): 1306-1310.
11. Bo Hu, Xiusheng He, Ao Li, **Qingchao Qiu**, Cunxi Li, Dan Liang, Ping Zhao, Jie Ma, Robert J. Coffey, Qimin Zhan, Guanqing Wu. Cystogenesis of ARPKD results from increased apoptosis in collecting duct epithelial cells of *Pkhd1* mutant kidneys. Experimental Cell Research, 2011, 317(2): 173-187.
12. Jianzhong Xiao, Xiusheng He, **Qingchao Qiu**, Min Deng, Qiao Luo. Establishment and identifition of Daudi cell line over-expressed STGC3 gene. Journal of Medical Science in Central South China, 2011, 39(4): 367-371.

13. Ming Jiang, Douglas W. Strand, Suzanne Fernandez, Yue He, Yajun Yi, Andreas Birbach, **Qingchao Qiu**, Johannes Schmid, Dean G. Tang, Simon W. Hayward. Functional remodeling of benign human prostatic tissues in vivo by spontaneously immortalized progenitor and intermediate cells. Stem Cells, 2010, 28(2): 344-56.
14. Bo Hu, **Qingchao Qiu**, Xiupei He, Qihui Zhao, Bo Hu, Xiusheng He. Diallyl disulfide induced cell cycle arrest in G1 phase bydownregulation of cyclin D1 and CDK4 in human nasopharyngeal carcinoma CNE2 cells. Chinese Pharmacological Bulletin, 2010, 26(9): 981-985.
15. Xiupei He, Bo Hu, **Qingchao Qiu**, Guohua Tang, Hui Ling, Hailin Tang, Xiusheng He, Qi Su. Effect of Histone Acetylation on Proliferation of CNE2 Cells Inhibited by Diallyl Disulfide. Cancer Research on Prevention and Treatment. 2010, 37(3): 255-258.
16. Jun Wu, **Qingchao Qiu (Co-first-author)**, Lu Xie, Joseph Fullerton, Jian Yu, Yu Shyr, Alfred L George, Yajun Yi. Web-based interrogation of gene expression signatures using EXALT. BMC Bioinformatics. 2009, Dec 14; 10: 420.
17. Qihui Zhao, Bo Hu, Xiusheng He, **Qingchao Qiu**, Qiao Luo, Jianshe Quan, Hailun Wang, Qiuyan He, Guohua Tang. Proliferation inhibition effects by DADS in SW480 cell line and identification of CK19 protein. Chin J Cancer Prev Treat. 2009, 16 (6): 419-423.
18. Qihui Zhao, **Qingchao Qiu**, Xiusheng He, Bo Hu, Qiao Luo, Changying Li, Yangchun Liu. Identification of proteins associated with proliferation inhibition effects by DADS in SW480 cell line. Chinese Pharmacological Bulletin, 2009, 2(4): 518-522.
19. Xiupei He, **Qingchao Qiu**, Bo Hu, Xiusheng He, Guohua Tang, Qi Su. Arrest effect of diallyl disulfide on cell cycle in human nasopharyngeal cancer CNE2 cells. Journal of Practical Oncology, 2009, 24(3): 222-226.
20. Qihui Zhao, Hailun Wang, Bo Hu, **Qingchao Qiu**, Jian Su, Xiusheng He. Apoptosis of

Human colon carcinoma cell line SW480 Induced by DADS. Chinese Journal of Ethnomedicine and Ethnopharmacy, 2009, (6): 4-5.

21. **Qingchao Qiu**, Changyin Lu, Zhengsheng Zhou, Ya Se, Qiwei Li. The construction status of China's college counselors and countermeasures. Journal of Hunan Environment-Biological Polytechnic, 2008, 14(4): 86-88.
22. Tao Zhang, **Qingchao Qiu**, Bo Hu. Arrest Effect of Lycopen on Cell Cycle in Human Prostatic Cancer Cell. Journal of Nanhua University (Medical Edition), 2008, 36 (6): 748-751.
23. Bo Hu, **Qingchao Qiu**, Qihui Zhao, Jianshe Quan, Changying Li. Application of Media Mix in Theory Teaching of Pathology Curriculum. Journal of Hunan Environment - Biological Polytechnic, 2008, 14 (3): 60-62.
24. Qihui Zhao, Bo Hu, **Qingchao Qiu**, Hailun Wang. Application of multimedia courseware in the teaching of pathophysiology. Journal of Hunan Environment - Biological Polytechnic, 2008, 14(4): 77-79.
25. **Qingchao Qiu**, Bo Hu, Xiusheng He, Qiao Luo, ZhiFeng Long, GuoHua Tang, YinHua Liao. Tumorigenicity investigation of CNE2 cell line STGC3 expression induced by Tet-on system in nude mice. Progress in Biochemistry and Biophisics, 2007, 34(4): 359-365.
26. Bo Hu, **Qingchao Qiu**, Xiusheng He, Qiao Luo, GuoHua Tang, ZhiFeng Long, YinHua Liao. Effect of estrogen on CNE2 cell line transfected with STGC3 gene. Progress in Biochemistry and Biophisics, 2007, 34(5): 538-545.
27. Jianduan Chen, Angang Zhou, Cheng Yi, Bo Hu, **Qingchao Qiu**. Environmental Engineering Curriculum Reform. Journal of Hunan Environment - Biological Polytechnic, 2007, 13(4): 67-69.
28. Shuai Zhao, Xiusheng He, Qiao Luo, Min Deng, Chao Zeng, **Qingchao Qiu**, Bo Hu.

Effects on proliferation of SW480 cell line with p33ING1b gene transfection. Tumor, 2006, 26(07): 648-651.

Copy right © Qingchao Qiu 2019